Title
Analysis of glutamatergic actions in the outer plexiform layer of the goldfish retina

Author
Nawy, Scott,

Publication Date
1988

Peer reviewed|Thesis/dissertation

Analysis of Glutamatergic Actions in the Outer Plexiform Layer of the Goldfish Retina

Scott Nawy

Division of Neurosciences

UCSF

February, 1988

for *Electra*

Acknowledgements

This thesis is the culmination of nearly eight years of graduate school. I wish to thank my parents Harold and Martha Nawy, my wife Marilyn Brown and my constant compatriot Leland Stone for helping me through those years. I also would like to thank my advisor David Copenhagen for believing in me and in my project throughout. Finally, I wish to thank the other members of the lab, particularly Jack Belgum, Scott Mittman and George Ayoub, for their advice and encouragement.

The first chapter of this thesis is a reprint of the material as it appears in **Nature**. The coauthor listed in this publication directed and supervised the research which forms the basis for the dissertation.

Table of Contents

Section	Page
Introduction	1
Results: chapter 1 APB Unmasks multiple classes of glutamate receptors on depolarizing bipolar cells in the goldfish retina	18
Results: chapter 2 The synaptic actions of glutamate on retinal depolarizing bipolar cells of the goldfish	30
Results: chapter 3 Evidence for selective presynaptic inhibition of photoreceptors by the glutamate analog APB	82
Results: chapter 4 Analysis of voltage fluctuations in the membrane of rod-driven DBCs	131
Conclusions	152
References	156

List of Tables

Table Page

Table 1 Conductance changes produced by light..46

Table 2 Conductance changes produced by APB....67

List of Figures

Figure		Page
Fig 1	Rod transmitter closes channels	19
Fig 2	APB closes channels	23
Fig 3	Glutamate produces no conductance change	26
Fig 4	DBC Response to 3 intensities of light	39
Fig 5	I-V plots before during and after light	41
Fig 6	Reversal of rod-driven light response	44
Fig 7	Cone transmitter increases conductance	48
Fig 8	DBC response to glutamate	51
Fig 9	Glutamate I-V relations	53
Fig 10	Equivalent circuit	56
Fig 11	Effect of Cs^+ on glutamate conductance	59
Fig 12	I-V relations for APB	62
Fig 13	I-V relations for APB+light	65
Fig 14	Effect of APB on cone-driven DBC	69
Fig 15	Effects of kainate and NMDA on DBC	72
Fig 16	Responses of RHC and CHC	91
Fig 17	Action of kainate on RHC and CHC	96
Fig 18	Action of NMDA on RHC and CHC	99
Fig 19	APB has no effect on the RHC	102
Fig 20	APB antagonizes responses of the CHC	104
Fig 21	Co^{2+} and APB have similar actions	107
Fig 22	APB does not block the action of KA	110

Fig 23 Kynurenic acid antagonizes KA.....113

Fig 24 APB can act directly on cones.....116

Fig 25 APB blocks responses in cone-driven DBCs..119

Fig 26 APB blocks response in the IPL.....121

Fig 27 Diagram of the sites of APB action.....127

Fig 28 Voltage noise vs. light intensity.....134

Fig 29 Spectra of pre-and postsynaptic noise.....137

Fig 30 Current restores light-suppressed noise...140

Fig 31 Variance vs. membrane potential.....143

Fig 32 Effects of TEA^+ on flash response.....146

Scott Nawy

Analysis of Glutamatergic Actions in the Outer Plexiform Layer of the Goldfish Retina

Abstract

Studies of synaptic transmission between photoreceptors and second order neurons in the retina have revealed that horizontal cells and depolarizing bipolar cells (DBCs) possess receptor/channel complexes with different pharmacological and conductance properties. Since these studies focused on postsynaptic cell type, paying less attention to the source of the synaptic input (i.e., rod or cone), less is known about the possible differences between synaptic transmission in the rod and cone pathways. In the present study, intracellular recordings from DBCs and horizontal cells were obtained in the isolated retina of the goldfish (*Carassius auratus*), using a dissection protocol which selectively eliminated either rod or cone input. Conductance measurements of DBCs which, under ordinary conditions, receive synaptic input from both rods and cones, demonstrated that the rod transmitter closed channels with an average reversal potential of -0.2 mV (SD: 11.3 mV), while the cone transmitter opened channels with an average reversal potential of -59 mV, (SD: 8.5 mV). The pharmacology of the two synapses differed as well. The glutamate analog 2-amino-4-phosphonobutyrate (APB) mimicked the action of the rod transmitter, closing channels with an average reversal potential of -1.0 mV (SD: 11.1 mV), but was not an

agonist for the cone transmitter. Glutamate, the putative transmitter for both rods and cones, produced no net conductance change, suggesting that it acted at both postsynaptic sites. Evidence for this idea was obtained with cesium, a potassium channel blocker which eliminated the channel-opening component of glutamate's action. With cesium in the microelectrode, glutamate closed channels with the same reversal potential (-0.5 mV, SD 18.5 mV) as the channels which were closed by APB, or the rod transmitter. A difference between the rod and cone synapses onto horizontal cells was detected as well. APB had no effect on rod-driven horizontal cells, but antagonized the cone transmitter on cone-driven horizontal cells. The precise location and mechanism of APB antagonism remains in doubt. APB may act directly on the cones to antagonize transmitter release, or on a part of the postsynaptic receptor that is separate from the agonist binding site. These results demonstrate differences in the pharmacology and conductance mechanisms of the rod and cone synaptic pathways.

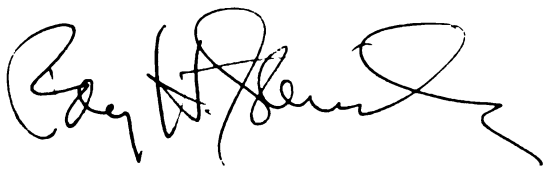

INTRODUCTION

The synapses from rod and cone photoreceptors to horizontal cell, depolarizing bipolar cell (DBC) and hyperpolarizing bipolar cell (HBC) are the first site of communication between neurons in the retina. Even at this early stage of visual processing, the light response of photoreceptors is modified and shaped to produce complex responses in second-order neurons (horizontal cell, DBC and HBC). For example, many properties of the receptive fields of neurons located in higher-order centers of the visual system are created here. These properties include antagonism of the center and surround of the receptive field and, in some animals, antagonism of the wavelength of light in the center and surround as well. Clearly, a detailed understanding of the mechanisms of synaptic transmission from the photoreceptors to second-order neurons is a vital step towards understanding the visual system.

Electrophysiological studies of the synapses between photoreceptors and second-order neurons have revealed a great deal about the synapses. We know a lot about the identity of the transmitter substance which is released by the photoreceptors, the pharmacological properties of the receptors to which the transmitter binds, and the channels which the receptors gate, in order to produce the light response. Unfortunately in many of these studies the identity of the type of photoreceptor that generates the light response has not been specified. In retinas that possess rods and cones, selective

identification and stimulation of one photoreceptor type is difficult. As a result, we know relatively little about the potential differences in synaptic mechanisms underlying the rod and cone pathways.

The central aim of this thesis was to characterize differences in the pharmacology and ionic mechanisms of synaptic transmission from rods and cones to depolarizing bipolar cells (DBCs) in the goldfish retina. Rod and cone input to DBCs can be compared directly, since both types of photoreceptor contact single DBCs. This thesis compliments many of the previous studies of photoreceptor transmitter action, since it compares the action of two photoreceptors that converge onto a single neuron, rather than the action of one photoreceptor that contacts two postsynaptic cells, as in the previous studies. The first two chapters demonstrate that synaptic transmission from rods and cones to DBCs differs in at least two important ways. The rod transmitter closes channels and can be mimicked by the glutamate analog 2-amino-4-phosphonobutyrate (APB), while the cone transmitter opens channels that can be blocked by applying cesium to the inside of the cell. The results suggest that the mechanisms of synaptic transmission from photoreceptors to second-order cells depend upon the source of the synaptic input, as well as its target.

Differences between rod and cone pathways extend beyond the DBC. The third chapter describes results which demonstrate that APB antagonizes the action of the cone, but not the rod, transmitter. The site of the APB-mediated antagonism could not be unequivocally

identified, and appears to be either on cone-driven horizontal cells, or presynaptically, on the cones. Although most of the experiments were performed on cone-driven horizontal cells, the results of experiments on other cone-driven cells, as well as on cones, favor the suggestion that APB acts directly on cones. If photoreceptors, themselves, possess different types of postsynaptic receptors, then the differences between the rod and cone pathways begin even before the first synapse.

The ability functionally to isolate and separate the rod and cone pathways was crucial for the success of this project. Although this can be difficult in many retinas, it is relatively straight-forward in the goldfish retina. Fish photoreceptors elongate and contract, responding to ambient light conditions and to a circadian rhythm. While this phenomenon has been studied most extensively in the green sunfish (*Lepomis cyanellus*; Burnside and Dearry, 1986), it also has been observed in the goldfish (Malchow and Yazulla, 1986). Following dark-adaptation, the cones elongate and the rods shorten, resulting in a loss of the cone outer segments during the isolation procedure, and producing an essentially all rod retina. Conversely, light-adaptation shortens the cones and produces a cone-dominated retina. In agreement with these studies, only rod responses were obtained with retinae which had been dark-adapted for over an hour prior to isolation, while cone responses were obtained from retinae which were dark-adapted for less than 15 minutes. The ability to separate rod and cone input through a physical and essentially irreversible mechanism allowed me to study the rod and cone pathways in complete isolation, and eliminated the need to use

continuous backgrounds or other unreliable manipulations to control the adaptation state of the retina during the experiment.

Also crucial to this study was the ability to measure changes in membrane conductance produced by both native and putative transmitters. While changes in membrane potential and light response alone can be used as a measure of the effects of pharmacological agents, measurements of conductance changes provide a higher degree of resolution and can reveal differences in mechanism of action that would otherwise go undetected. As will be seen, conductance measurements were required to demonstrate a difference in the action of APB and glutamate on DBCs, and to show that APB acted preferentially on the postsynaptic receptor mediating rod input, but not the receptor mediating cone input.

The present results grew out of earlier studies that measured the actions of the "photoreceptor" transmitter on all three types of second order cells. A selected review of this work is presented below. The review emphasizes studies that quantitatively compared the action of the native and putative transmitters, primarily glutamate. Comparisons of power spectra and current-voltage relations obtained with glutamate, glutamate analogs and the native transmitter are stressed. Studies such as these, particularly in DBCs, provide the basis for many of the experiments that I describe in this thesis, particularly the measurements of the actions of glutamate and APB.

Glutamate as a photoreceptor transmitter

Evidence, built upon the standard criteria for neurotransmitter identity, has established that the transmitter released by the photoreceptors is an excitatory amino acid, most likely glutamate. Photoreceptors accumulate radiolabeled glutamate in their terminals (Marc and Lam, 1981). They also release preloaded radiolabeled glutamate when depolarized with a high-potassium solution (Miller and Schwartz, 1983). More recently, isolated cones have been shown to release endogenous glutamate in a Ca^{2+}-dependent fashion (Ayoub et al., in preparation, Copenhagen and Jahr, in preparation). One of the enzymes involved in glutamate production, aspartate aminotransferase, is also present in photoreceptors (Mosinger and Atschuler, 1985), but the ubiquitous role of glutamate in metabolism and as a putative transmitter sheds doubt on the significance of this finding in unequivocally establishing glutamate as a neurotransmitter. Many studies have examined the postsynaptic actions of glutamate and aspartate, comparing them to the action of the native photoreceptor transmitter. Both glutamate and aspartate depolarize horizontal cells (Murakami et al., 1972; Cervetto and MacNichol, 1972), hyperpolarize the DBC and depolarize the HBC (Murakami et al., 1975).

A strict definition of postsynaptic identity of transmitter action requires that the putative transmitter act on the same channel/receptor as the native transmitter. Advances in micro-and patch electrode technology, as well as the increasingly wide-spread use of dissociated cell preparations have made it possible to evaluate the postsynaptic action of glutamate in the retina using more rigorous tests than simple

changes in membrane potential. For example, the conductance changes and kinetics of putative and native transmitter can be compared. Progress towards this goal will be evaluated for each type of second order cell in the retina.

A. Horizontal cells have received the most attention, owing primarily to their large size. They are electrically coupled to one-another, which greatly lowers their input impedance (Yamada and Ishikawa, 1965; Witkowsky and Dowling, 1969). Low input impedance has hindered attempts to measure the reversal potential of the light response, although several attempts have been made (Nelson, 1973; Marshall and Werblin, 1977). Individual horizontal cells, obtained from enzymatically dissociated retinas, have been used to circumvent this problem. Under voltage-clamp, exogenously applied glutamate opens channels that have a reversal potential of about 0 mV (Lasater and Dowling, 1982; Ishida, et al., 1984; Kaneko and Tachibana, 1985; Hals et al., 1986). Unfortunately, measurements of the reversal potential of glutamate and the native transmitter (i.e., the light response) require an intact preparation.

Recently, Murakami and Takahashi (1987) used an elegant technique to estimate reversal potential in the intact retina. Using a solution containing high concentrations of Ca^{2+} and Ba^{2+}, as well as several K^{+} channel blockers, they induced Ca^{2+} "action potentials" in horizontal cells, potentials that lasted up to several minutes and depolarized the entire horizontal cell network above 0 mV. While using this solution to

simultaneously depolarize all of the horizontal cells, including the cell that they were recording from, they applied glutamate and aspartate and found that the amino acids produced a membrane hyperpolarization instead of the predicted depolarization. They also observed a depolarizing response to light. These results suggested that the cell membrane was depolarized beyond the reversal potential for the light and amino acid responses. They estimated the reversal potential of both the light and the glutamate-and aspartate-induced responses to be between -5 and -10 mV, agreeing well with studies on isolated horizontal cells.

As mentioned earlier, very little is known about possible differences between the mechanisms of synaptic transmission in rod and cone pathways. Horizontal cells have been used to address this issue in several retinas. Segregation of rod and cone input is known to occur in horizontal cells of the turtle (Leeper and Copenhagen, 1978) and rabbit (Bloomfield and Miller, 1982; Dachuex and Raviola, 1982). In both cases, the horizontal cell soma receives exclusive synaptic input from cones, while the electrically isolated axon terminal receives input from rods and cones, creating two functional cell types. The pharmacology of the rod and cone input to the rabbit horizontal cell has been compared by Massey and Miller (1987). They found no discernible differences in the pharmacology of the different horizontal cells types, as both were sensitive to kainate and, to a lesser extent, quisqualate, but were completely insensitive to NMDA. On this basis, the authors conclude that the transmitters in both rods and cones are most likely the same, as are the postsynaptic receptors.

B. Hyperpolarizing bipolar cells (HBC) have been the subject of fewer studies, due primarily to their small size. This is unfortunate, since their high input impedance allows for relatively straight forward conductance measurements using single microelectrodes. Conductance measurements of HBCs in the intact retina suggests that the photoreceptor transmitter opens channels with a reversal potential of about 0 mV (Toyoda, 1973; Ashmore and Copenhagen, 1983; but see Saito and Kaneko, 1983).

Recording intracellularly from HBCs of the turtle retina, Ashmore and Copenhagen (1980; 1983) analyzed membrane voltage fluctuations, which were suppressed by light, and found that they could be modeled as the sum of two lorenztian components. They attributed one component to the presynaptic cell (cones) and the other to the action of the cone transmitter, setting an upper limit of 6 msec for the channel lifetime of the cone transmitter-gated conductance. The authors also calculated an elementary event size of 70 μV for the transmitter component of the noise spectrum. Given a resting potential of -45 mV, an average input resistance of 150 MΩ in the dark, and a driving force of about 30 mV for the transmitter-gated conductance (Ashmore and Copenhagen, 1983), the elementary conductance would be about 15 pS. In their model, the elementary event is the result of the action of a quantum of transmitter, rather than a single molecule, suggesting that the single channel conductance might be much smaller.

No study to date has examined the conductance mechanism underlying the action of EAAs on the HBC in the intact retina. However, the action of EAAs has been investigated with the whole-cell patch-clamp using isolated cells of the axolotl (*Ambystoma mexicanum*; Atwell et al., 1987). Glutamate (0.25 mM) activated a current that reversed at about 0 mV, while aspartate (0.50 mM) was without any effect. Glutamate also increased membrane current fluctuations. The noise spectrum could be decomposed into the sum of two lorenztian components, suggesting either the presence of two glutamate receptors, or one receptor with a complex gating scheme. Unfortunately, the authors did not try to activate selectively one noise component with more receptor-specific glutamate analogs in order to distinguish between the two hypotheses. The elementary conductance associated with glutamate was calculated to be 5.4 pS, larger than the estimated conductance for the native transmitter on turtle HBCs, but differences in species, preparations, and recording techniques as well as the inherent errors in such calculations make comparisons difficult.

C. Depolarizing bipolar cells (DBC) have been studied in several retinas. Because of their larger size, particularly in the fish retina, they are easier to study than the HBC. Many of the ideas for the work described in this thesis were derived from these studies. Previous investigators have shown conclusively that the photoreceptor transmitter decreases membrane conductance by closing channels with a reversal potential of about 0 mV (Ashmore and Falk, 1980; Slaughter and Miller, 1981; Shiells et al., 1981). Atwell et al. (1987) measured glutamate-

elicited currents in isolated DBCs and reported a reversal potential of -13 mV, and a conductance decrease, consistent with the action of the endogenous transmitter. Contrary to its actions in the HBC, glutamate produced a decrease in the tonic current noise in isolated DBCs. The events blocked by glutamate had an elementary conductance of about 10.6 pS, twice that of the HBC. In the intact retina, light (transmitter decrease) increased the voltage fluctuations of DBCs in the turtle retina (Ashmore and Copenhagen, 1980), suggesting that transmitter action on DBCs is associated with a noise decrease. An understanding of the origin of the noise may eventually provide clues to the mechanism by which ligand-binding closes synaptic channels.

Bipolar cells of the goldfish retina provide an excellent opportunity to study rod and cone transmitter actions. Anatomical studies have demonstrated that both photoreceptor types contact DBCs (Stell, 1967; Ishida et al., 1980), suggesting that rod and cone signals converge onto the same bipolar cells. Physiological studies have also demonstrated that cone and rod inputs onto individual DBCs can be resolved (Kaneko and Tachibana, 1978). Measurements of conductance and reversal potentials in the goldfish DBC suggested that rods and cones utilize distinct conductance mechanisms (Saito et al., 1978; 1979). In the dark-adapted state, when the light responses are produced by rods, the responses were reversed with depolarizing current, and were associated with a conductance increase. Conversely, in the light-adapted retina, the cone-driven responses were reversed with negative current, and associated with a conductance decrease. On this basis, the

authors concluded that the rod transmitter closes channels with a positive reversal potential, a finding which is consistent with the reported action of the photoreceptor transmitter on DBCs in other species. They also conclude that the cone transmitter acts to open channels with a negative reversal potential. This system provides an excellent opportunity to test the hypothesis that glutamate is the transmitter for both rods and cones. Glutamate should be able to mimic the action of the transmitters at both synaptic sites, simultaneously producing a conductance increase, and a conductance decrease. This model is tested in the present study.

In summary, glutamate mimics the postsynaptic action of the photoreceptor transmitter on all three types of postsynaptic cells. Evidence for aspartate as a transmitter appears much weaker, particularly as judged from experiments on dissociated neurons. Aspartate is ineffective on isolated horizontal cells (Lasater and Dowling, 1982; Ishida, et al., 1984; Kaneko and Tachibana, 1985; Hals et al., 1986; Shiells et al., 1986, using a retinal slice) and both DBCs and HBCs (Atwell et al., 1987). This data appears to conflict with earlier reports that suggested an equal sensitivity to both aspartate and glutamate in the intact retina (Murakami et al., 1972; 1975). It is possible that aspartate-sensitive receptors, present in the intact retina, were lost during the isolation procedure. More likely, the concentration of applied glutamate which is required to elicit a postsynaptic response is elevated by the presence of a high-affinity glutamate uptake system. Ishida and Fain (1981) demonstrated that when

this uptake system is blocked by applying D-aspartate to the retina, glutamate acts at one-half the concentration of aspartate in the intact retina. The present data therefore favor glutamate as a photoreceptor transmitter.

Classification of glutamate receptors on second-order cells

Glutamate receptors can be classified according to the type of EAA analog that activates them. Excluding the retina, three types of receptors have been recognized in the vertebrate CNS, activated by either NMDA, quisqualate or kainate. These receptor/channels have distinct ionic permeabilities and channel conductances as well as pharmacological properties (Fagg and Foster, 1984; Mayer and Westbrook, 1987). This is thought to allow each receptor to perform a specific role in CNS synaptic transmission. For example, NMDA-preferring receptors are permeable to Ca^{2+} (MacDermott et al., 1987), and are thought to produce long-term changes in synaptic excitability in hippocampal neurons as a direct result of this selective Ca^{2+} permeability (Collingridge, 1987).

In the retina, photoreceptors produces two different postsynaptic effects, simultaneously depolarizing the hyperpolarizing bipolar and horizontal cell and hyperpolarizing the depolarizing bipolar cell. Since photoreceptors presumably release the same transmitter onto all three cells, differences in postsynaptic responses must be created through differences in postsynaptic receptors. Indeed, studies of the

effects of EAA analogs in the retina, reviewed below, have demonstrated that synaptic transmission from photoreceptors to second-order cells is mediated via different classes of postsynaptic receptors as well as different conductance mechanisms. The use of subtypes of EAA receptors on second-order cells to mediate postsynaptic responses demonstrates the evolution of receptor/channel complexes to fill the specialized requirements of synaptic transmission, and provides insight into the need for multiple types of glutamate receptors in the CNS. There is some evidence, also reviewed below, that suggests that not only do glutamate receptors on second-order cells differ from each other, but that they also differ from their counterparts in other parts of the nervous system.

A. Horizontal cells are depolarized by kainate (Shiells et al., 1981; Rowe and Ruddock, 1982; Lasater and Dowling, 1982; Slaughter and Miller, 1983; Bloomfield and Dowling, 1985; Hals et al., 1986; Massey and Miller, 1987) and quisqualate (Rowe and Ruddock, 1982; Lasater and Dowling, 1982; Bloomfield and Dowling, 1985; Hals et al., 1986; Massey and Miller, 1987), but not NMDA (Slaughter and Miller, 1983; Bloomfield and Dowling, 1985; Massey and Miller, 1987). The inability of NMDA to depolarize horizontal might be explained by the observation that the normal concentration of Mg^{+} in most Ringers (about 1 mM) blocks NMDA responses in a voltage-dependent manner, but has no effect on kainate or quisqualate responses (Nowak et al., 1984; Mayer and Westbrook, 1985). The presence of Mg^{+} in the bathing solutions may block the action of NMDA on horizontal cells, particularly at the hyperpolarized membrane

potentials associated with horizontal cells at rest. The experiments of Massey and Miller (1987) seem to rule out this possibility, since they failed to see any effects of NMDA in a low-Mg^+ solution.

Both the agonists and glutamate appear to act at the same receptor, since under voltage-clamp in isolated cells they all elicited currents with the same reversal potential (about 0 mV; Ishida and Neyton, 1985; Hals et al., 1986), elementary conductance and channel kinetics, as measured with noise analysis (Ishida and Neyton, 1985).

Relatively few studies have examined the kainate/quisqualate receptor in detail, but those which have suggest that they may differ from EAA receptors found elsewhere in the CNS. The estimate of 2-3 pS for the single channel conductance of the kainate/quisqualate current in horizontal cells (Ishida and Neyton, 1985) is similar to the measured values of 5, 10 or 15 pS in hippocampal neurons (Jahr and Stevens, 1987). However, the current-voltage relations of the non-NMDA channel is quite linear in hippocampal neurons (Mayer and Westbrook, 1984; 1985), but displays a prominent region of negative slope resistance in horizontal cells (Kaneko and Tachibana, 1985a; Hals et al., 1986), a property more reminiscent of the NMDA channel (Mayer and Westbrook, 1984; 1985; Nowak et al., 1984). Unlike the NMDA channel, Cs^+, but not Mg^+ was effective at linearizing the current-voltage relation (Kaneko and Tachibana, 1985a), leading these authors to suggest a second action of glutamate on the anomalous rectifier (1985b). These results also could be explained by postulating a voltage-dependent blockade of the

kainate/quisqualate-gated channel by Cs^+, analogous to the action of Mg^+ on NMDA receptors. Finally, it has been suggested that the kainate/quisqualate-gated channel is permeable to all cations, including Ca^{2+}, whereas this channel is impermeant to Ca^{2+} in other preparations (Hablitz and Langmoen, 1982). What the significance of these differences are, and whether they reflect a different functional role for kainate/quisqualate-preferring receptors in horizontal cells than elsewhere in the CNS remains to be seen.

B. Hyperpolarizing bipolar cells Little is known about the receptor which mediates hyperpolarizing bipolar cell responses. While kainate is known to block HBC light responses and depolarize the membrane (Dvorak, 1984; Bloomfield and Dowling, 1984; Slaughter and Miller, 1985), no attempts to measure conductance changes or reversal potentials have been made. It has been shown that the glutamate analog D-O-phosphoserine blocks light responses in horizontal cells, but not HBCs, suggesting that the 2 receptors are pharmacologically distinct (Slaughter and Miller, 1985). No further data on HBC receptor/channel kinetics or pharmacology are presently available, although a recent study on the action of glutamate on isolated HBCs (Atwell et al., 1987) suggests a course for future study, at least on dissociated neurons.

C. Depolarizing bipolar cells At the synapse between photoreceptors and depolarizing bipolar cells, the polarity of the light response is reversed. This reversal underlies the formation of the "ON" pathway, a pathway which consists of cells that depolarize or produce

action potentials in response to light. The ON pathway is an fundamental principle of retinal organization and appears to be maintained throughout higher-order visual centers. The postsynaptic receptor that mediates this sign-inversion is sensitive to the glutamate analog 2-amino-4-phosphonobutyrate (APB; Slaughter and Miller, 1981; Shiells et al., 1981), first used as a potent antagonist at the locust neuromuscular junction (Cull-Candy et al., 1976). Like the native transmitter, APB has been shown to close channels (Slaughter and Miller, 1981) with a reversal potential near 0 mV (Shiells et al., 1981).

APB Antagonism in the CNS

Although a potent transmitter agonist in the retina, outside of the retina, APB is considered to be a weak EAA antagonist. There is some controversy regarding the location of APB action. Studies reporting the blockade of the effects of exogenous kainate and NMDA (Collingridge et al., 1983; Hori et al., 1982) by D-APB provide evidence for a non-specific postsynaptic antagonism of glutamate receptors. Others have reported that APB blocks the action of the endogenous transmitter, but not applied agonists (Ffrench-Mullen et al., 1986). These authors concluded that APB and the endogenous transmitter both act at a fourth type of receptor, sensitive to APB but not NMDA, kainate or quisqualate. Other studies postulate a presynaptic action of APB (Harris and Cotman, 1983) based upon paired-pulse experiments. Conflicting results on the role of APB in non-retinal regions of the CNS may stem partly from genuine differences in APB receptors. More likely,

they result from the difficulty of recording membrane potential and conductance changes produced by APB and other glutamate analogs.

Chapter 1

APB UNMASKS MULTIPLE CLASSES OF GLUTAMATE RECEPTORS ON DEPOLARIZING BIPOLAR CELLS IN THE GOLDFISH RETINA

Recently it has been shown that cultured central neurons posses multiple subtypes of excitatory amino acid receptors[1]. The significance of this finding depends in part on the assumption that these receptors are present in-vivo as well as in culture, and are involved in synaptic transmission. In the goldfish retina, we have recorded intracellular responses from depolarizing bipolar cells (DBC) known to receive synaptic inputs from rods and cones[2,3,4]. We report here that information from rods and cones is mediated via pharmacologically distinct types of postsynaptic receptors, neither of which has been described previously in the central nervous system. While both types of postsynaptic receptors are sensitive to glutamate, only the postsynaptic receptor which mediates rod signals responds to the glutamate analog 2-amino-4-phosphonobutyrate (APB). These results reveal that rod and cone inputs to DBCs are mediated by pharmacologically distinct glutamate receptors and that multiple types of glutamate receptors existing on single neurons can subserve separate functionally defined synaptic inputs.

We examined the conductance mechanism underlying the rod-driven light response in depolarizing bipolar cells, using a technique described previously[5] to eliminate cone input. Fig 1a shows the maximal response of a bipolar cell to a spot of light. Application of cobalt

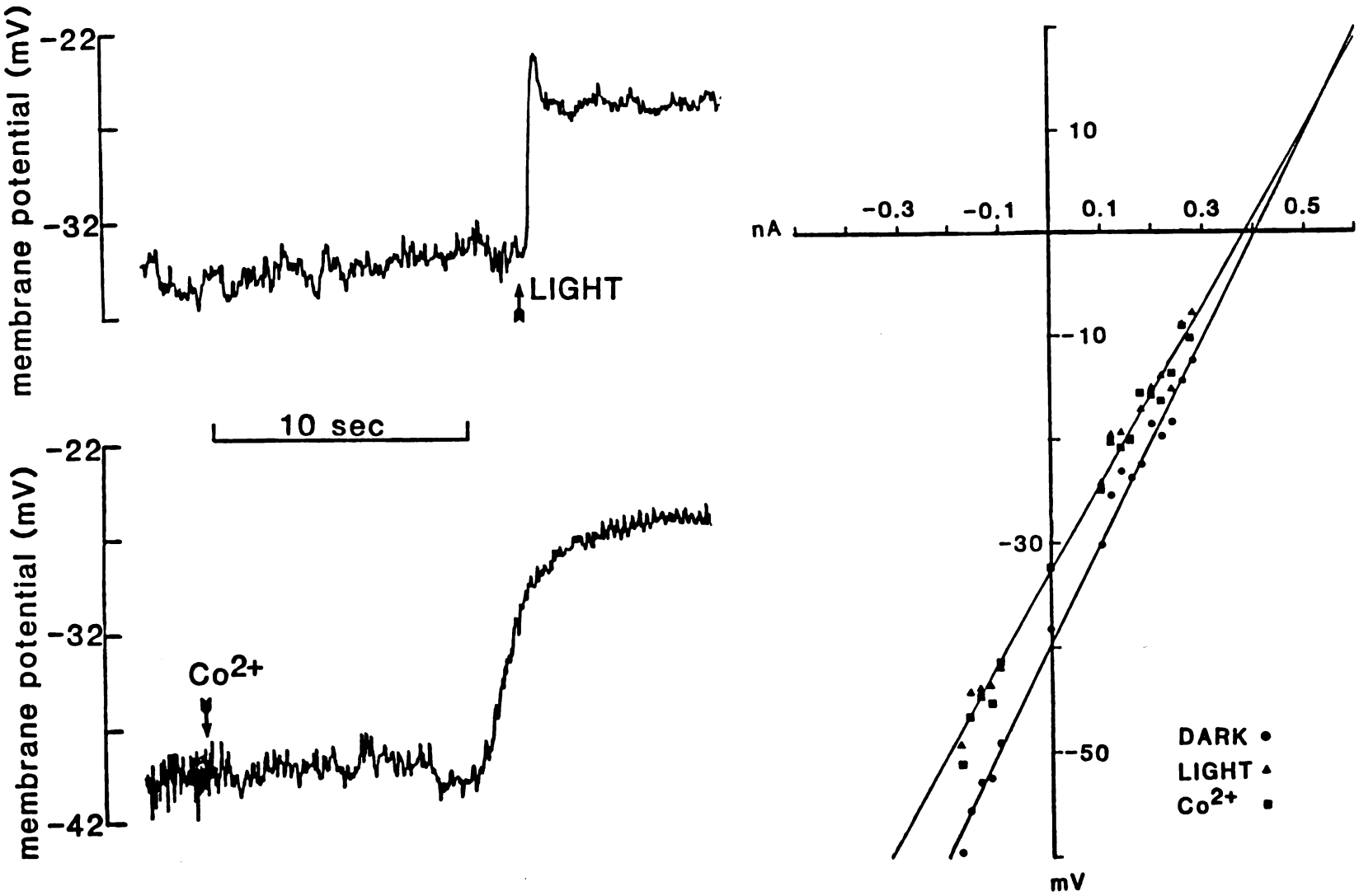
membrane potential (mV)
-22
-32
LIGHT
10 sec
membrane potential (mV)
-22
-32
-42
Co2+
nA
-0.3
-0.1
0.1
0.3
0.5
10
-10
-30
-50
mV
DARK
LIGHT
Co2+

Figure 1: Rod transmitter closes channels.

A: responses of a depolarizing bipolar cell to a light of wavelength 550 nm and intensity of 3.9 photons $sec^{-1}\mu m^{-2}$. B: response of the same cell to 1 mM Co^{2+} added to the normal solution. C: Current-voltage relations for a different cell obtained in the presence of 1 mM Co^{2+} (△), light of 1.96 photons sec^{-1} μm^{-2}(▪), and in darkness (control) (•). These relations were obtained by injecting 500 msec pulses of current and measuring the average resulting steady state voltage deflection across a bridge circuit . The voltage step usually reached its final value within 100 msec. Identical pulses of current were injected into the electrode after pulling out of the cell and the resulting voltage steps were then subtracted from the intracellularly recorded voltage steps in order to obtain the potential drop across the cell membrane. The lines are the best least-squares fit to the data. For the sake of clarity, no line was drawn in this figure for Co^{2+}. Slope of the current-voltage relations in dark, 99 megohms;light, 86 megohms; Co^{2+} (not shown), 87 megohms.

Methods. Current-voltage relations were measured in 24 depolarizing bipolar cells. Retinas from dark-adapted fish that were maintained in an outdoor pond were isolated from the pigment epithelium under infrared light. Fish were kept in darkness 3-6 hours after light onset for at least one hour prior to dissection. We have shown previously that neuronal responses from retinas isolated in this way are nearly exclusively rod driven[5]. Retinas were then incubated in darkness in a 20% solution of Wydase hyaluronidase in superfusion medium for 20-30 minutes at 4 C and then mounted photoreceptor-side up on a doughnut-

Figure 1 (cont.)

doughnut-shaped piece of filter paper in the recording chamber. We found that hyaluronidase effectively dissolved any vitreous remaining on the isolated retina, and allowed better adhesion of the retina to the filter paper. Mounted retinas were superfused continuously with oxygenated superfusion solution at room temperature (20-22^{o}C). This solution was L15 culture medium modified to contain the following composition of salts: NaCl, 120 mM; MgSo4, 1.2 mM; KCl, 2.5 mM; CaCl2, 2.2 mM. The solution also contained 10 mM glucose and was buffered to a ph of 7.8 in 3 mM HEPES. Depolarizing bipolar cells were penetrated with glass micro-electrodes pulled on a Brown-Flaming puller[16] and filled with 2M potassium acetate. Electrode resistances varied from 500 to 800 Megohms.

(Co^{+2}) to the superfusate depolarized the cell to the same potential as light (fig 1b). Previous studies in the fish retina have shown that this concentration of Co^{2+} is able to block transmitter release from photoreceptors[6]. Thus it appears that saturating intensities of light completely suppress transmitter release from rods. To measure membrane conductance, we injected brief pulses of hyperpolarizing and depolarizing current of varying amplitude through the intracellular recording electrode. The resulting voltage change across the membrane was measured and plotted (cf Belgum et. al.[7]). An example of such a current-voltage relation obtained from another bipolar cell during continuous illumination, Co^{2+} and dark is shown in fig 1c. The reduced slope of the light and Co^{2+} plots indicates an increased membrane conductance relative to darkness. The extrapolated reversal of the light and Co^{2+} responses was positive relative to resting potential. These current-voltage relations indicate that the rod transmitter, released continuously in the dark[8] and blocked both by light and Co^{2+}, decreases membrane conductance by closing ionic channels whose reversal potential is more positive than the dark potential. This conductance mechanism has been proposed for the rod transmitter by Saito and his colleagues[4,9], who demonstrated reversal of the rod light response at potentials positive to resting potential.

Conductance changes produced by light and the glutamate analog APB were compared. APB, acting as an agonist, has been shown to block light responses in depolarizing bipolar cells in the all-rod retina of the dogfish[10], and in the mixed rod-cone amphibian retina [11,12].

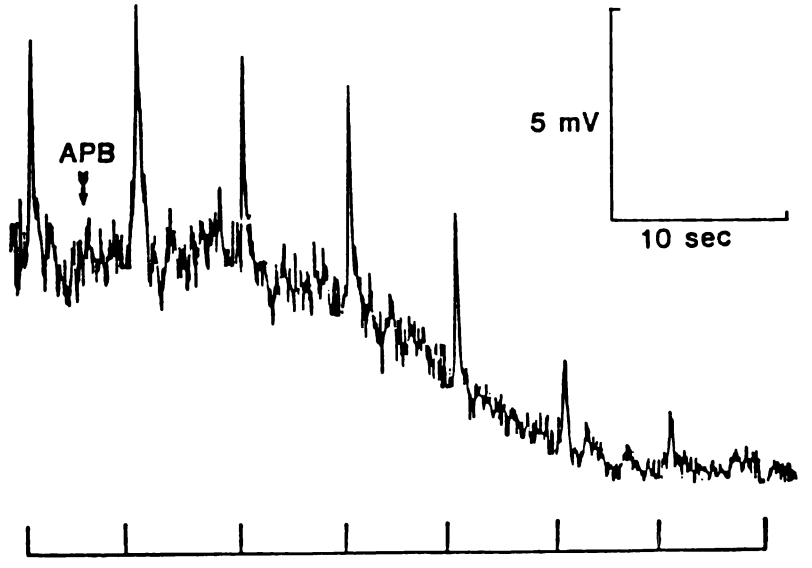
APB
5 mV
10 sec

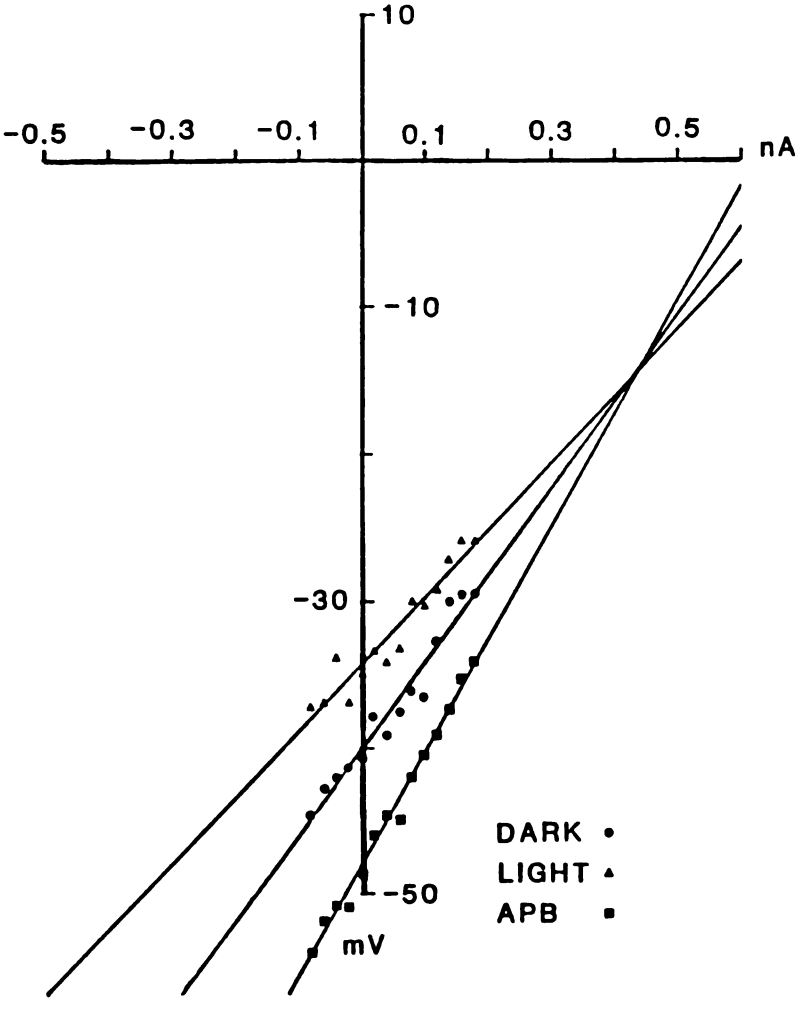
10
-0.5
-0.3
-0.1
0.1
0.3
0.5
nA
-10
-30
-50
mV
DARK
LIGHT
APB

Figure 2: <u>APB and the rod transmitter close ionic channels with the same reversal potential.</u>

A: Response of a bipolar cell to APB. At the arrow, the normal solution was switched to one containing 2 μM APB (D,L-APB obtained from Sigma Co.). The responses shown are to 10 msec flashes of light of 9.8 X 10^{-3} photons.flash$^{-1}\cdot\mu m^{-2}$. The timing of the flashes is shown below. B: Current-voltage relations obtained from the same cell in darkness(•), during a steady background of 9.8 photons $sec^{-1}\cdot\mu m^{-2}$ (▪) and during superfusion of APB (△). The extrapolated reversal potentials of both light and APB are nearly identical. Slope in darkness, 59 megohms; light, 45 megohms; APB, 77 megohms.

Fig 2a shows the response of a bipolar cell to the superfusion of 2 μM APB. The membrane was hyperpolarized and the light responses were blocked. Current-voltage relations for this cell were measured in darkness, during continuous illumination and during superfusion of APB and are shown in fig 2b. The extrapolation of the current-voltage relations obtained in APB crosses the dark current-voltage plot at almost exactly the same potential as the plot obtained in light . These findings support the conclusion that APB is closing the same channels that are closed by the native rod transmitter. They demonstrate an action similar to that found in dogfish retina and dispute the observation that APB has no effect on bipolar cells in the teleost retina[13].

The conductance change underlying the action of glutamate, by contrast, was very different than the action of either the native rod transmitter or APB. In fig 3a, current-voltage relations obtained during separate superfusion of 10 μM APB, 2 mM glutamate and control solution are shown in the same cell. All measurements were made in darkness. Once again, APB produced a hyperpolarization and a decrease in membrane conductance. Glutamate blocked the light response and produced an even larger hyperpolarization of the membrane than APB. But there is little or no apparent conductance change associated with the action of glutamate.

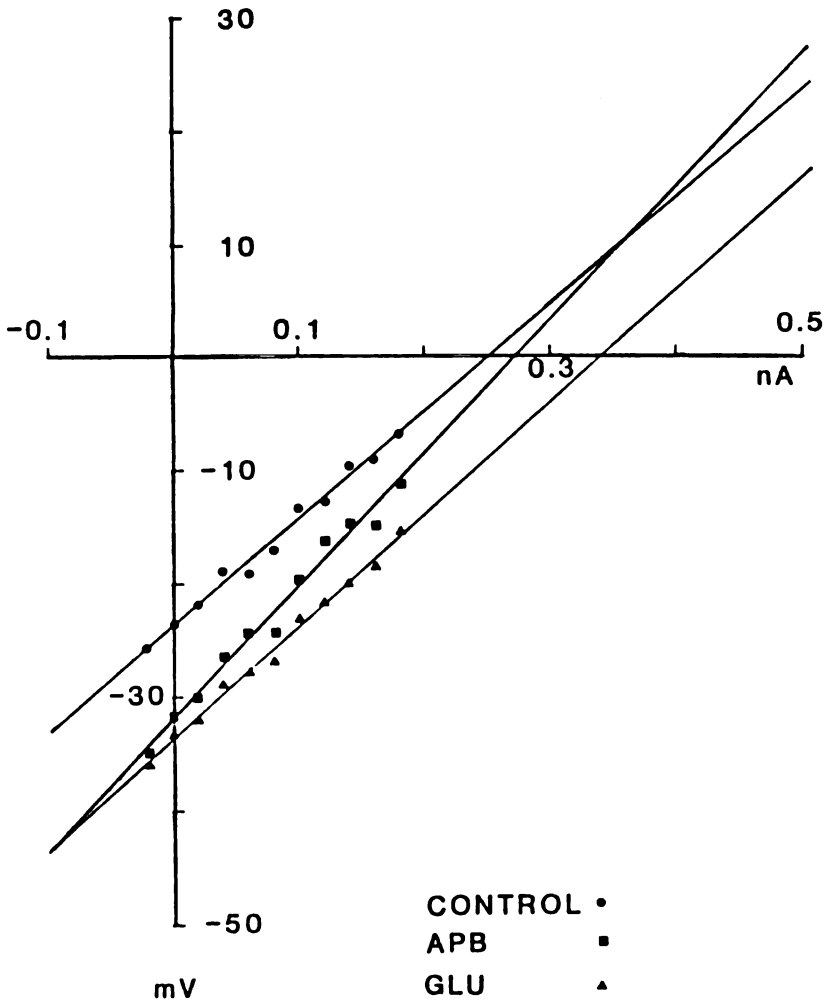
30
10
-10
-30
-50
-0.1
0.1
0.3
0.5
nA
mV
CONTROL
APB
GLU

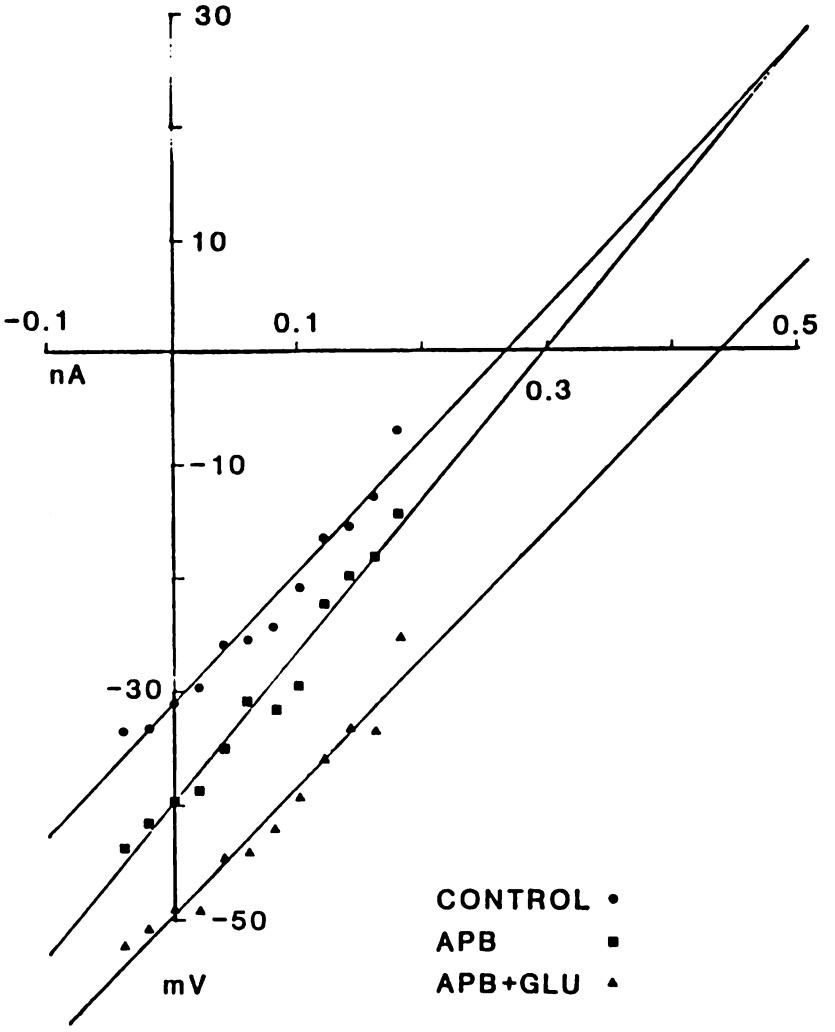
30
10
-10
-30
-50
-0.1
0.1
0.3
0.5
nA
mV
CONTROL
APB
APB+GLU

Figure 3: APB and glutamate act via different conductance mechanisms. A: Current-voltage relations obtained as described above in control solution (•),10 μM APB (▪) and 2 mM glutamate (Sigma Co) (△). Superfusion of APB produced a hyperpolarization of the membrane and an increase in slope. The reversal potential of the APB effect was positive to the dark potential.Superfusion of the cell with 2 mM glutamate also produced a hyperpolarization of the membrane, but a much smaller conductance change. Slope in the dark was 94 megohms; in APB, 117 megohms; in glutamate, 99 megohms. b, Current-voltage relations for a different cell during superfusion of control medium (•), 10 μM APB (▪), and 10 μM APB+2mM glutamate (△). Slope in darkness was 116 megohms; in APB, 134 megohms; in APB+GLU, 113 megohms

The discrepancy between the current-voltage relations in APB and glutamate can be explained most easily if glutamate is acting at both the APB-sensitive site and an additional type of site. Fig 3b illustrates an experiment in which 10 μM APB was first perfused onto the retina. This concentration of APB was five-fold higher than necessary to block the light response. In the presence of APB, the retina was then superfused with 2 mM glutamate (GLU+APB). The slope of the current-voltage relation in GLU+APB was decreased relative to APB alone demonstrating that, in the presence of APB, the ability of glutamate to open channels with a negative reversal potential is unmasked. We therefore postulate that the apparent lack of a conductance change produced by glutamate is due to the summation of two simultaneous actions: The closing of APB-sensitive channels, and the opening of APB-insensitive channels. Both actions of glutamate differ from those found at other excitatory amino acid receptors in the CNS[1,14,15] which open channels with a reversal potential of about 0 mV.

Our results provide strong evidence that the rod and cone pathways utilize pharmacologically distinct receptors on the bipolar cell membrane, One receptor, mediating rod signals, is similar to the DBC receptor described elsewhere[10,11,12]: it is sensitive to APB and acts by closing ionic channels. The second receptor is pharmacologically distinct from the first since it is insensitive to APB. Unlike the first receptor, it opens ionic channels. The reversal potential of ion flow in these channels is similar to the reversal potential of the cone light response, as determined in previous studies[4,8]. Thus, this receptor

most likely mediates cone signals. These findings demonstrate an example of a single neuron which possesses two types of glutamate receptor, each type receiving synaptic input from separate and distinctly identifiable presynaptic sources.

CHAPTER 2

THE SYNAPTIC ACTIONS OF GLUTAMATE ON THE RETINAL DEPOLARIZING BIPOLAR CELLS OF GOLDFISH

Introduction

Studies of glutamatergic synaptic transmission have suggested that there are at least 3 classes of glutamate receptor in the CNS. These receptors can be distinguished by the actions of different glutamate agonists (Watkins and Evans, 1981; Mayer and Westbrook, 1987), and by the ion selectivity and voltage-dependence of the channels which these agonists gate (Mayer et. al., 1984; Nowak et. al., 1984; MacDermott et. al., 1986; Jahr and Stevens, 1987). An unresolved issue involving glutamatergic transmission in the nervous system is the spatial specificity and organization of receptors on single neurons. While experiments have demonstrated that glutamate can activate more than one class of receptor on a single cell (Mayer and Westbrook, 1984; 1985; Cull-Candy and Usowicz, 1987; Jahr and Stevens, 1987), it is not clear if glutamate receptors are organized on the postsynaptic membrane so that a single specific type of synaptic input activates a single class of receptor or if a single input activates several classes of receptor.

In some neural systems it is possible to selectively stimulate identified, glutamatergic presynaptic neurons, and compare the

postsynaptic responses to the actions of applied agonists and antagonists (e.g., Dale and Roberts, 1985; Dale and Grillner, 1986). The goldfish retina provides an example of such a neural system. A variety of studies using morphological, pharmacological and physiological techniques have suggested that photoreceptors release glutamate as a transmitter onto the second order neurons, including horizontal cells, hyperpolarizing bipolar cells (HBCs) and depolarizing bipolar cells (DBCs; see Massey and Redburn, 1987 for review). Both rods and red-sensitive cones make synapses onto individual DBCs (Stell, 1967; Ishida, Stell and Lightfoot, 1980), providing a good model for studying the convergence of multiple glutamatergic inputs onto a single postsynaptic cell. By manipulating the adaptation state of the retina, it is feasible to isolate one pathway from the other, making it possible to investigate and compare the pharmacology of either the rod or cone input onto the DBC, and to correlate the class of postsynaptic receptor associated with each input.

Utilizing the dark-adapted retina, in which only the rod pathway is active, a previous study has shown that the rod transmitter keeps the DBC membrane relatively hyperpolarized by closing channels with a reversal potential of about 0 mV (Nawy and Copenhagen, 1987). In that study, it was also demonstrated that APB, a glutamate analog which acts specifically at DBCs (Slaughter and Miller, 1981), can block the rod-driven light response and mimic the conductance change produced by the rod transmitter. Furthermore, it was suggested that glutamate itself

acts at the APB site, and also at least one additional channel-opening site.

The present study quantifies the rod input to DBCs, dissects the dual action of glutamate, and tests the hypothesis that the second, non-APB-sensitive conductance mediates the cone-elicited light response in DBCs. Current-voltage (I-V) relations presented here demonstrate that the cone transmitter opens channels with a negative reversal potential. The conductance-decreasing effect of APB in dark-adapted retinas is contrary to the action of the cone transmitter, suggesting that APB has a low affinity for the postsynaptic receptor mediating synaptic transmission from cones. To confirm this hypothesis, we measured the conductance change produced by applying APB to cone-driven DBCs recorded from the light-adapted retina. The results demonstrate that the mechanisms of cone transmitter and APB action are quite different.

In an attempt to confirm the hypothesis that glutamate simultaneously increases one conductance and decreases another, we tried to block one conductance pharmacologically. Experiments using Cs^+-loaded electrodes show that one component of the dual glutamate action was blocked, and that this component has a similar reversal potential to the cone light response. The remaining cesium-resistant conductance has the same reversal potential as the rod transmitter and APB. These results provide further confirmatory evidence for the hypothesis that DBCs in the goldfish retina possess two classes of glutamate receptor, distinguished by their sensitivity to Cs^+-blockade and APB. The results

are also consistent with the idea that the two classes of receptor are functionally segregated so as to mediate synaptic transmission from two separate, identified inputs: rods and cones.

Materials and methods

Preparation of the dark-adapted retina

Goldfish (*Carassius auratus*) (4-6 inches in length) were obtained from Grassyforks fisheries (Martinsville, IN), housed in an outdoor pond, exposed to a natural light-dark cycle and fed twice weekly. Fish were placed in complete darkness for at least 1.5 hours prior to sacrifice by decapitation. The eyes were enucleated and hemisected, and then the retina was isolated from the pigment epithelium and placed into a 20% solution of hyaluronidase (Wydase, Wyeth Labs) for 20-30 minutes at 4^{0} C in order to degrade the vitreous humor. The entire isolated retina was then mounted on an annular-shaped piece of #2 filter paper with the receptor-side up and placed in the superfusion chamber. Stimulating light used for intracellular recordings was focused onto the retina from below through the hole in the filter paper. The microelectrode was lowered to a position just above the retina and centered in the spot of light. To ensure that the retina remained completely dark-adapted, the entire procedure, including the dissection, was performed under infra-red illumination using an image converter (Varoscope).

Preparation of the light-adapted retina

Goldfish were placed in complete darkness for no longer than 10 minutes prior to sacrifice. The 10 minutes of dark-adaptation decreased the amount of pigment epithelium which stuck to the retina following

isolation. The dissection was performed using a standard dissecting microscope illuminator, the beam of which was covered by three layers of red acetate paper. Although varying slightly from experiment to experiment, the light intensity was about 150 $\mu W/cm^2$, as measured with a Minolta LS-100 luminance meter. Complete spectral irradiance measurements were not made, but we do know that from spectrophotometric measurements, the acetate paper acted as a high-pass filter with 10 percent transmission at about 610 nm, and 90 percent transmission at about 676 nm. Retinas were exposed to this illuminator for about 10 minutes, the duration of a typical isolation procedure. Following 20 minutes in complete darkness, the isolated retina was transferred to the filter paper under the same red light. There were no differences in the light- and dark-adaptation dissections other than the differences in illumination. Light responses in light-adapted retinas were shown by several criteria to originate from cones. The details, based upon spectral and flash sensitivities of the light-elicited responses, will be published elsewhere.

Superfusion and recording

The recording chamber was continuously superfused with oxygenated L-15 culture medium (Gibco) modified to contain the following concentration of ions (in mM): NaCl, 120; $MgSO_4$, 1.2; KCl, 2.5; $CaCl_2$, 2.2; glucose, 10.0; and was buffered to a pH of 7.8 with 3 mM HEPES. All amino acid analogs as well as Co^{2+} were added without substitution to this solution. Gravity-fed control and test solutions were

alternately connected to the recording chamber through a series of valves (Hamilton) following the design of Belgum, Dvorak and McReynolds (1982). The volume of the chamber was about 0.3 ml. We typically obtained full physiological responses to different test solutions within 45 seconds after switching the valves.

Microelectrodes formed from standard omega-dot tubing were pulled on a Brown-Flaming puller to a resistance of 750-1000 MΩ and filled with 2M potassium acetate except where noted otherwise. Electrodes were advanced through the retina in small steps (1-10 microns) until a cell was penetrated. Depolarizing bipolar cells were identified on the basis of their light responses and position in the retina. Current-voltage (I-V) relations were measured by injecting current pulses of 500 msec duration through the recording microelectrode and then recording the voltage change across the previously balanced bridge circuit. The charging time constant of the microelectrode was typically less than 4 msec. The data were recorded and stored on FM tape (Racal) for later analysis on a PDP 11-23. The voltage changes to each current pulse were digitized and individually displayed on a monitor. The position of an horizontal cursor on the monitor was moved to give the best fit to the last 200-400 msecs of the 500 msec voltage response. The cursor amplitude was taken to be the value of the steady state voltage response. After withdrawing the microelectrode from the cell, the I-V relations of the microelectrode alone was then measured.

Light Stimulation

Light was projected onto the retina from an optical bench mounted beside the light-tight Faraday recording cage. Neutral density and interference filters (10 nm halfwidth) were used to attenuate the light and adjust its color. The unattenuated photon flux (550 nm) at the plane of the retina was 1.9×10^6 photons μm^{-2} sec^{-1}.

Results

Conductance changes produced by the rod and cone transmitter

Figure 4 shows the intracellular voltage responses of a typical rod-driven DBC to three different intensities of steady illumination. The dimmest stimulus evoked a sustained depolarization at light-on and a slight undershoot at off (trace a), while higher intensities increased the amplitude of both the sustained and transient responses, and at light-off, decreased the rate at which the undershoot decayed back toward the dark resting potential.

To measure the conductance change elicited by the rod transmitter, we compared steady-state current-voltage (I-V) relations obtained in darkness, when the rate of transmitter release from the photoreceptors is highest (Dowling and Ripps, 1972), to those obtained in light, when release is suppressed. We also measured I-V relations during the slower afterhyperpolarizing phase of the response following light-off. Figure 5 shows the curves obtained from another cell under all three conditions. The figure inset shows records of the voltage response to current injections used to construct the curves. The bottom record of the inset shows voltage records obtained after the microelectrode was withdrawn from the cell. The potential drop across the electrode was subtracted from the raw records. Lines through each set of data points are best fits obtained by a linear least squares routine. The upper I-V relation (light) has a shallower slope than the middle I-V relation

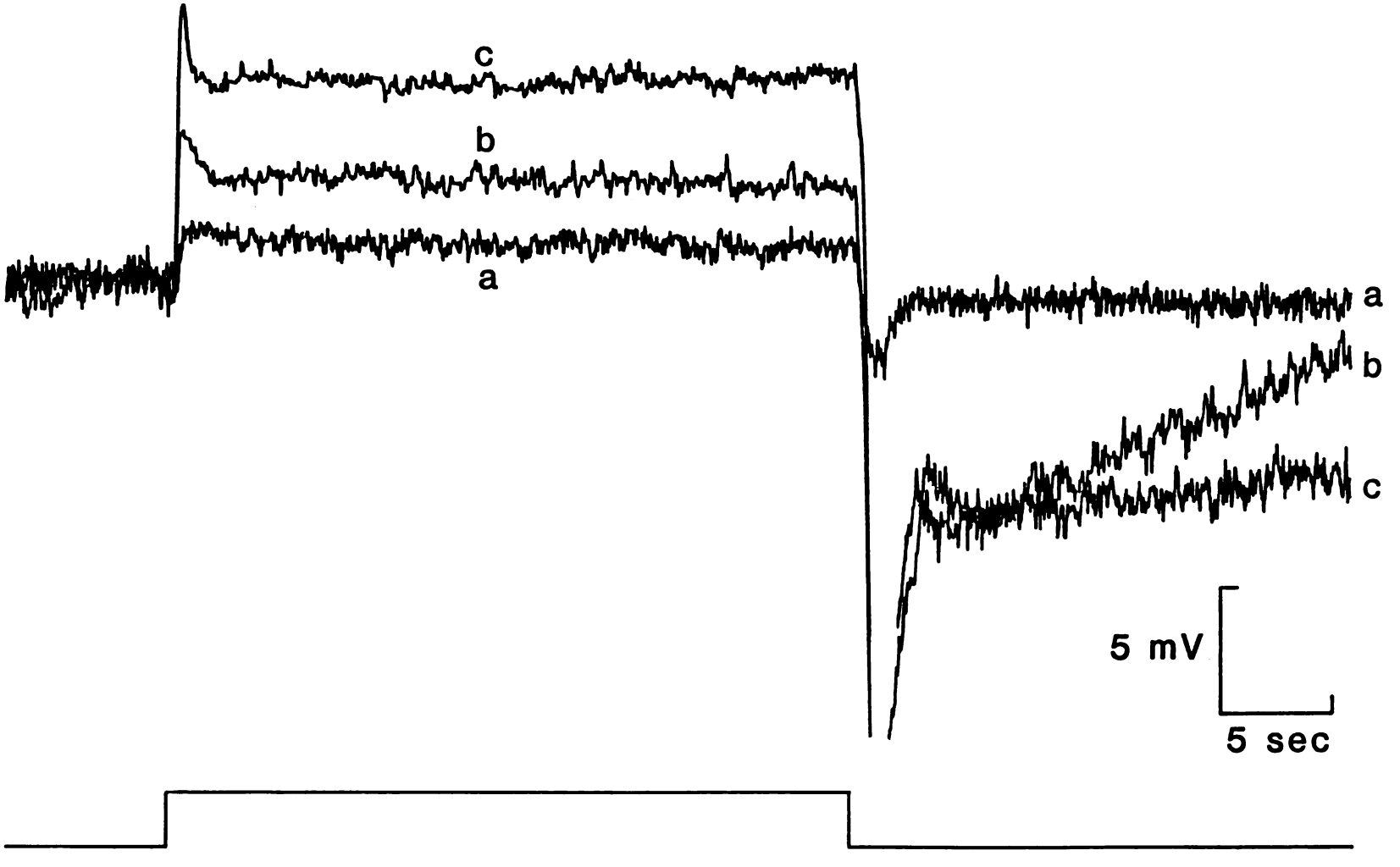
c
b
a
a
b
c
5 mV
5 sec

Figure 4: Responses to three intensities of light

The responses of a depolarizing bipolar cell (DBC) to 550 nm light at intensities of 0.2 (a), 0.97 (b) and 3.9 photons·μm $^{-2}$ sec^{-1} (c) are superimposed. The timing of the stimulus is indicated beneath the records. The fast component of the off response to the brightest stimulus is truncated. Maximum response amplitude of the steady-state light response was 13 mV (at 9.8 photons·μm^{-2} sec^{-1}). The membrane potential in the dark ranged between -31 and -33mV.

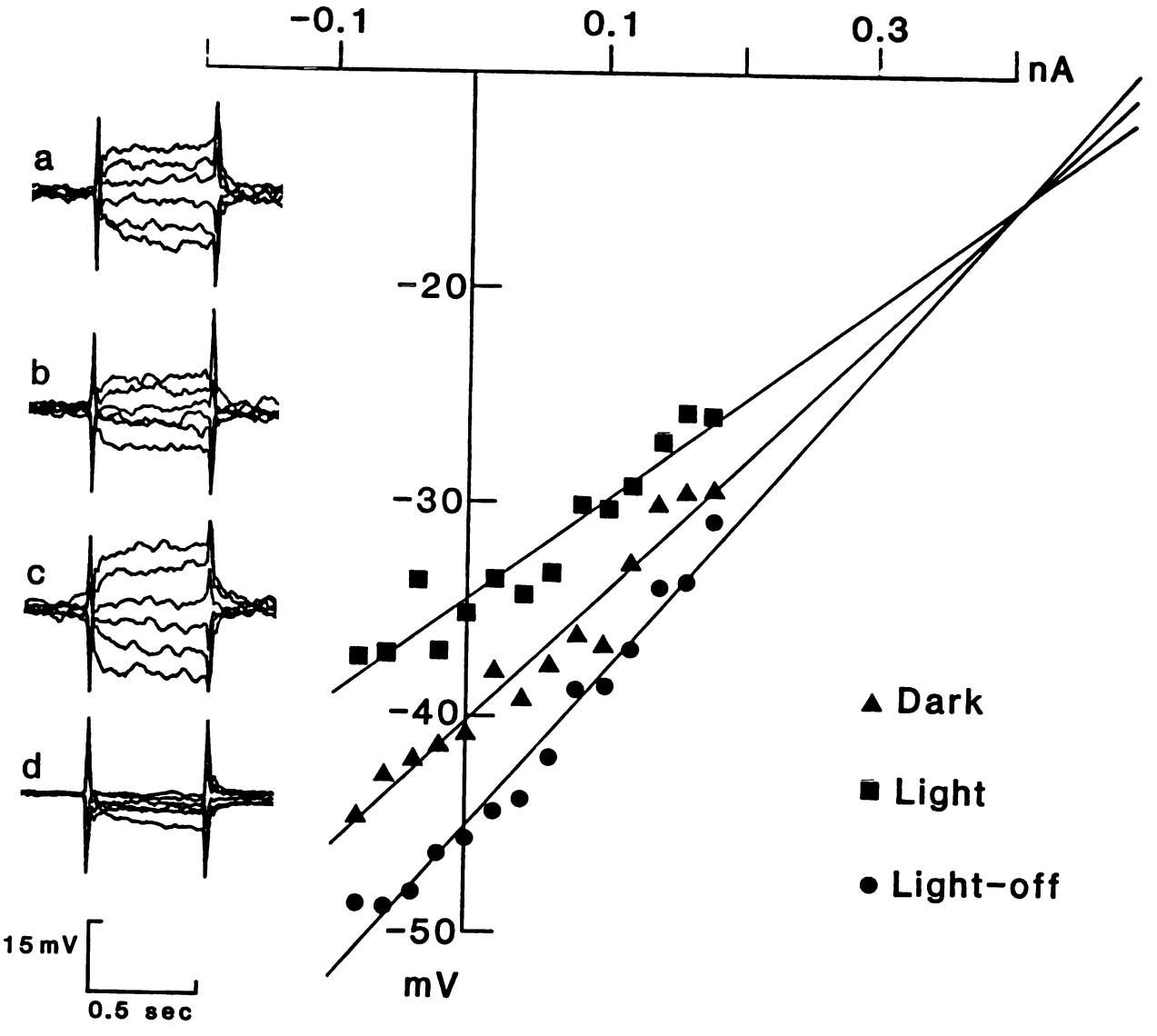
-0.1
0.1
0.3
nA
a
b
c
d
-20
-30
-40
-50
mV
▲ Dark
■ Light
● Light-off
15 mV
0.5 sec

Figure 5: Current-voltage relations before, during and after light stimulation

I-V plots from another DBC measured in darkness (triangles), light (9.8 photons·μm^{-2} sec^{-1}, squares) and immediately following the cessation of light (circles). The continuous lines were fitted using a least squares routine. The slopes of the lines were 59 MΩ, 45 MΩ, and 71 MΩ, respectively. Data points were obtained by injecting 500 msec pulses of positive and negative current in 0.02 nA increments into the cell and recording the resulting voltage response. Responses obtained from the electrode alone were subtracted from the raw cell records. The steady-state voltages were then plotted as a function of the injected current.

Inset: Intracellular voltage response to injection of current pulses of +/- 0.02, 0.06, 0.08 nA in darkness (a), light (b), and during the afterhyperpolarization (c). The voltage response of the microelectrode (d) was obtained after removing the electrode from the DBC. As mentioned in Methods, the mean amplitude of the last 200-400 msec of the voltage response was taken as the steady-state value. In those voltage responses where there was some sag the application of longer duration current pulses revealed only minimal sag after initial 300 msecs. For the most part, the sag could be accounted for by time-varying conductances in the microelectrode itself. Note that several of the responses to depolarizing current are downward in (d) due to a slight overbalance adjustment of the bridge circuit.

An estimate of the reversal potential of the light response was made by extrapolating the I-V plots to their crossing points. The extrapolated I-V curves for light and the afterhyperpolarization intersect the dark curve at nearly the same membrane potential, consistent with the idea that both the depolarizing and later hyperpolarizing phases of the response to continuous illumination share a common reversal potential. Complete I-V relations for light and dark were obtained in a total of 14 cells. Table I lists each cell and the estimated reversal potential as well as the conductance change. The average reversal potential of the light response was -0.2 mV (S.D.=14 mV), similar to that estimated for the action of the rod transmitter on DBCs in the dogfish retina (Ashmore and Falk, 1980; Shiells, Falk and Naghshineh, 1981), but slightly more negative than previously reported in the carp retina (Saito et. al, 1978; 1979). The mean conductance increase was 3.6 nS.

In some of the recordings from DBCs the reversal potential of the light response was directly obtained by applying brief flashes in the presence of steady hyperpolarizing or depolarizing currents. The middle trace in figure 6 illustrates the response of a cell to a flash in the absence of any applied current. The bottom trace shows the response of the cell to the same stimulus during injection of -0.3 nA of steady current which hyperpolarized the cell to -32 mV. The peak amplitude of

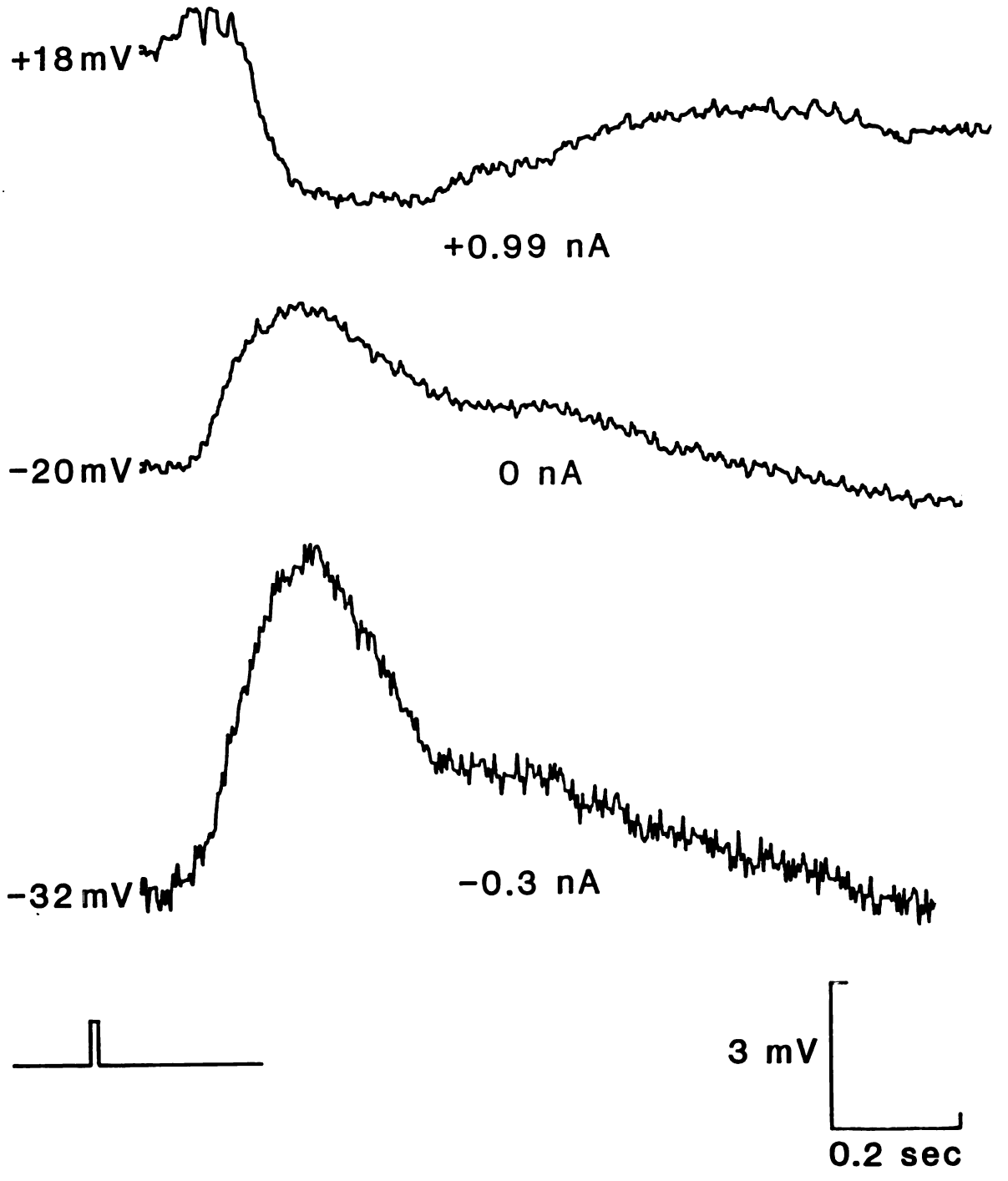
+18 mV
+0.99 nA
-20 mV
0 nA
-32 mV
-0.3 nA
3 mV
0.2 sec

Figure 6: Effects of extrinsic current on the flash response

The traces show averaged responses to brief flashes (10 msec) of light delivering 0.096 photons μm^{-2} $flash^{-1}$. The timing of the flashes is shown at the bottom and the membrane potentials are indicated to the left of each trace. Top trace is the average of 5 responses during injection of +0.99 nA of steady current. The middle trace is the average of 3 responses in the absence of current.and the bottom trace is the average of 3 responses during injection of -0.3 nA of current. Noise in the bottom record originated from the electrode, as it was still present when the same current was passed after withdrawal from the cell.

TABLE I

Current-voltage relations for light/dark

CELL	G_d	G_l	G_{l-d}	REV POT
1	12.5	21.7	9.2	-15 mV
2	14.5	16.2	1.7	-15 mV
3	11.1	12.8	1.7	+10 mV
4	12.2	16.1	3.9	+6 mV
5	8.1	10.6	2.5	+1 mV
6	16.9	22.2	5.3	-15 mV
7	10.0	14.7	4.7	-1 mV
8	14.1	20.0	5.9	-7 mV
9	5.3	6.5	1.2	+15 mV
10	14.9	20.8	5.9	-12 mV
11	11.2	16.1	4.9	+6 mV
12	8.9	10.0	1.1	+19 mV
13	8.1	10.4	2.3	0 mV
14	6.9	7.5	0.6	+5 mV
mean	11.1	14.7	3.6	-0.2 mV
SD	3.4	5.2	2.5	11.3 mV

I-V relations for 14 cells in darkness and steady illumination. Only cells with a light-induced depolarization of at least 5 mV were used. The reversal was estimated from the intersection of the extrapolated light and dark relations. G_d: conductance in darkness. G_l: conductance during steady illumination. G_{l-d}: Increase in conductance produced by light.

the flash response increased to 7 mV, compared to 3 mV for the control response. The upper trace shows the cell's response during injection of +0.99 nA of current, which depolarized the cell to +18 mV. The light response was reversed in polarity, having a peak amplitude of about 4 mV. Although this procedure was done on only a few cells, the results were in good agreement with estimates of the reversal potential obtained from the current-voltage relations.

Cone-driven responses in DBCs were obtained from light-adapted retinas, prepared as described in the methods section, and were smaller and more rectangular in appearance than the rod-driven responses, with a smaller undershoot at light-off. Saito et al. (1978; 1979) estimated the reversal potential of the cone-driven light response in carp retina to be around -60 mV. Figure 7, which plots the I-V characteristics of a cone-driven DBC in the goldfish retina, reveals an extrapolated reversal potential of -65 mV, in good agreement with the results of Saito et al.

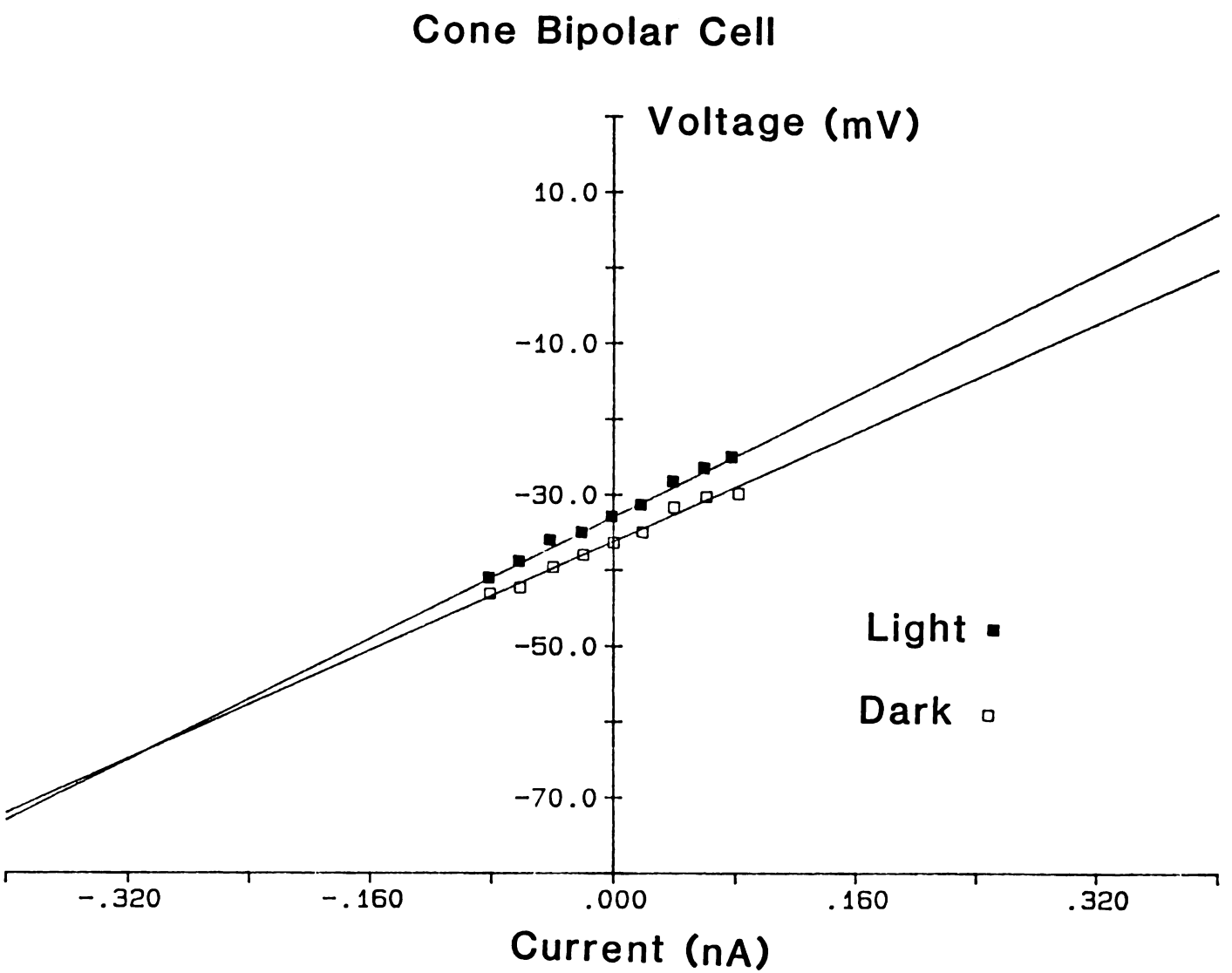
Cone Bipolar Cell
Voltage (mV)
10.0
-10.0
-30.0
-50.0
-70.0
-.320
-.160
.000
.160
.320
Current (nA)
Light
Dark

Figure 7: The cone transmitter increases conductance.

I-V relation for a cone-driven DBC in darkness ( ) and during steady illumination ( ). Background illumination was 650 nM and $1.70X10^4$ photons/$sec^1 \cdot \mu m^2$. Light decreases a conductance with a negative reversal potential. Slope in darkness was 90 MΩ, and in light was 101 MΩ.

Synaptic effects of glutamate

Since glutamate is the leading candidate for both the rod and cone photoreceptor transmitter (see Massey and Redburn, 1987) we examined the effects of glutamate on DBCs. Superfusion of 2 mM glutamate reversibly hyperpolarized the membrane and blocked the rod-driven light response as illustrated in figure 8. The actions of glutamate suggest that it is an agonist at the postsynaptic receptor mediating rod input, since it blocked the light responses from rods and hyperpolarized the membrane as expected. If glutamate acted solely on the rod pathway, then it ought to produce the same conductance change as the native rod transmitter. The I-V relations illustrated in figure 9 show that this is not the case. Instead of the predicted conductance decrease, glutamate produced essentially no conductance change, despite the large shift in membrane potential. This result was obtained even when 1 mM Co^{2+} was added to ensure that glutamate was acting only on the DBC and was not exerting its action through the presynaptic neurons or interneurons.

The apparent lack of a glutamate-elicited conductance can be explained by postulating that glutamate simultaneously acts to increase one conductance and decrease another (Nawy and Copenhagen, 1987). The glutamate-gated conductances, along with a fixed leak conductance, are modeled using an equivalent circuit of the DBC membrane (figure 10). The membrane capacitance of the DBC is ignored in the equivalent circuit since only the steady-state conductances are being considered.

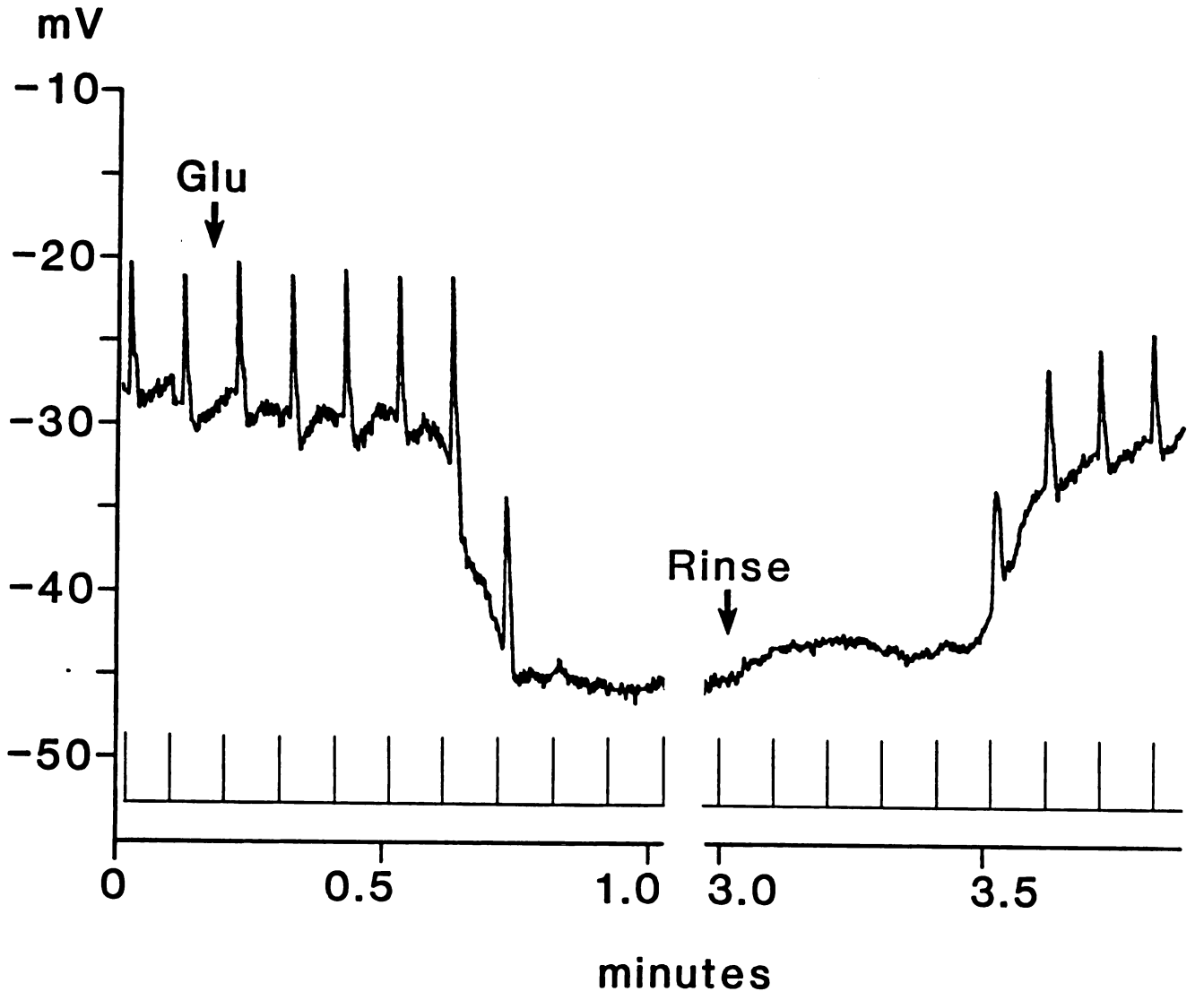
mV
-10
-20
-30
-40
-50
Glu
Rinse
0
0.5
1.0
3.0
3.5
minutes

Figure 8: Response to glutamate

Response of a cell to superfusion of 2 mM glutamate (L-glutamate, Sigma Co.) applied at a time shown by the arrow. The light stimulus was a 10 msec flash producing 0.97 photons·μm^{-2} $flash^{-1}$. Second arrow shows when glutamate was rinsed out. The lines through the record represent a break of approximately two minutes. The membrane potential remained constant throughout this interval.

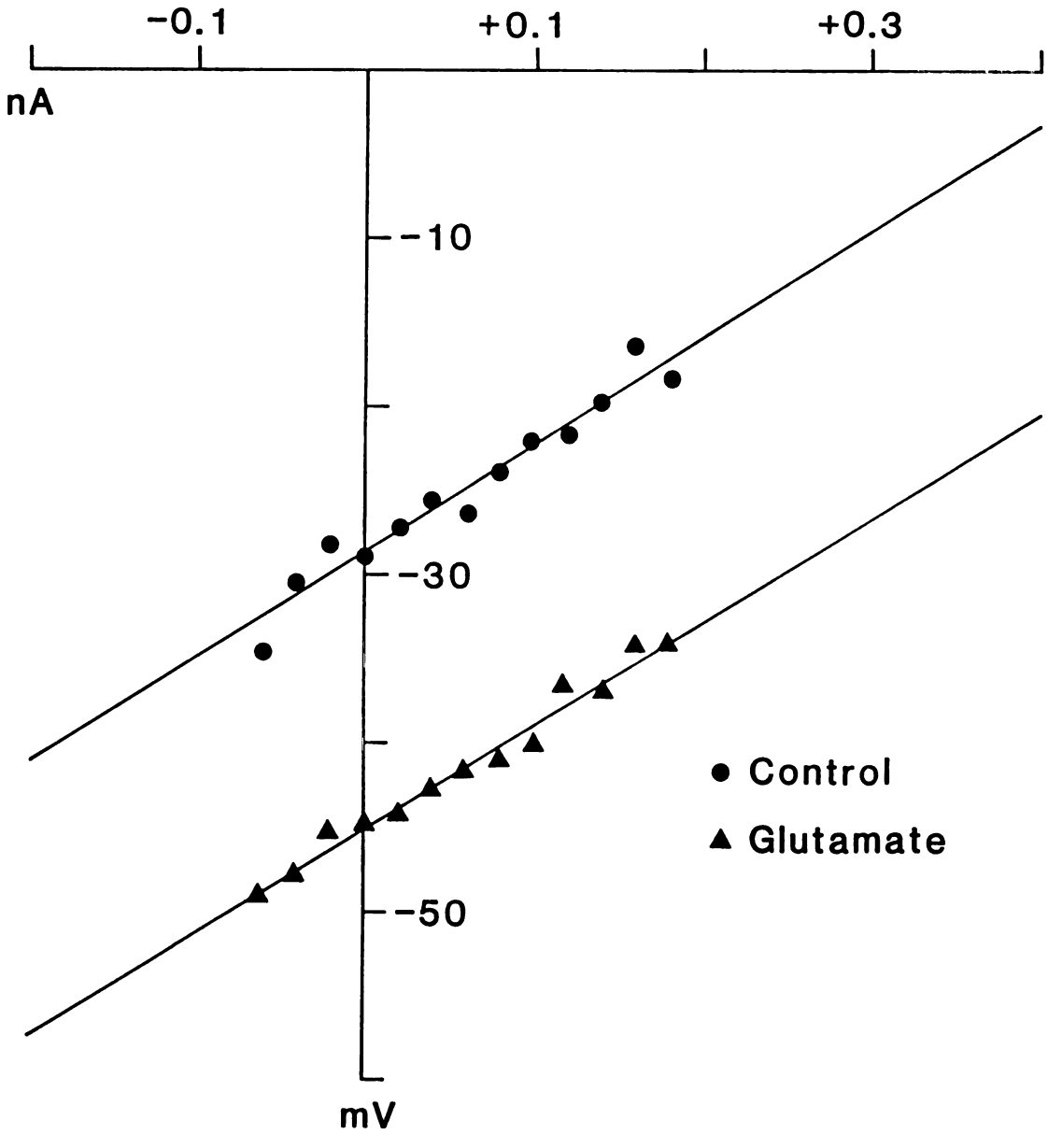
-0.1
+0.1
+0.3
nA
-10
-30
-50
mV
Control
Glutamate

Figure 9: Action of glutamate on DBCs

Current-voltage relations for control (circles), and 2 mM glutamate (triangles). The solution of glutamate also contained 1 mM Co^{2+}. The slope of the control curve was 64 MΩ while the slope of the glutamate curve was 62 MΩ.

In figure 10, G_O and G_C are the glutamate-modulated conductances, and G_L is a fixed leak conductances, with E_O, E_C and E_L the reversal potentials of each conductance.

At the reversal potential for glutamate, the current flow through both the channel-opening and channel-closing conductances must be equal and opposite, so:

$$\Delta G_C(E_{rev}-E_C)=-\Delta G_O(E_{rev}-E_O) \quad , \qquad (1)$$

where ΔG_C and ΔG_O are the conductance changes produced by glutamate, and E_{rev} is the glutamate reversal potential. Solving for E_{rev} yields:

$$E_{rev}= \frac{(\Delta G_C/\Delta G_O)E_C+E_O}{(\Delta G_C/\Delta G_O)+1} \qquad (2)$$

If the transmitter-gated conductances are of equal magnitude but of opposite polarity then $\Delta G_C/\Delta G_O$ is -1 and the reversal potential is at infinity. Under these conditions there would be no net change in the membrane conductance evoked by glutamate. Even if the magnitude of ΔG_C and ΔG_O are not equal, as long as the conductances are of opposite polarity, then the reversal potential for glutamate must lie in a voltage range outside that of the reversal potentials of either of the individual conductances.

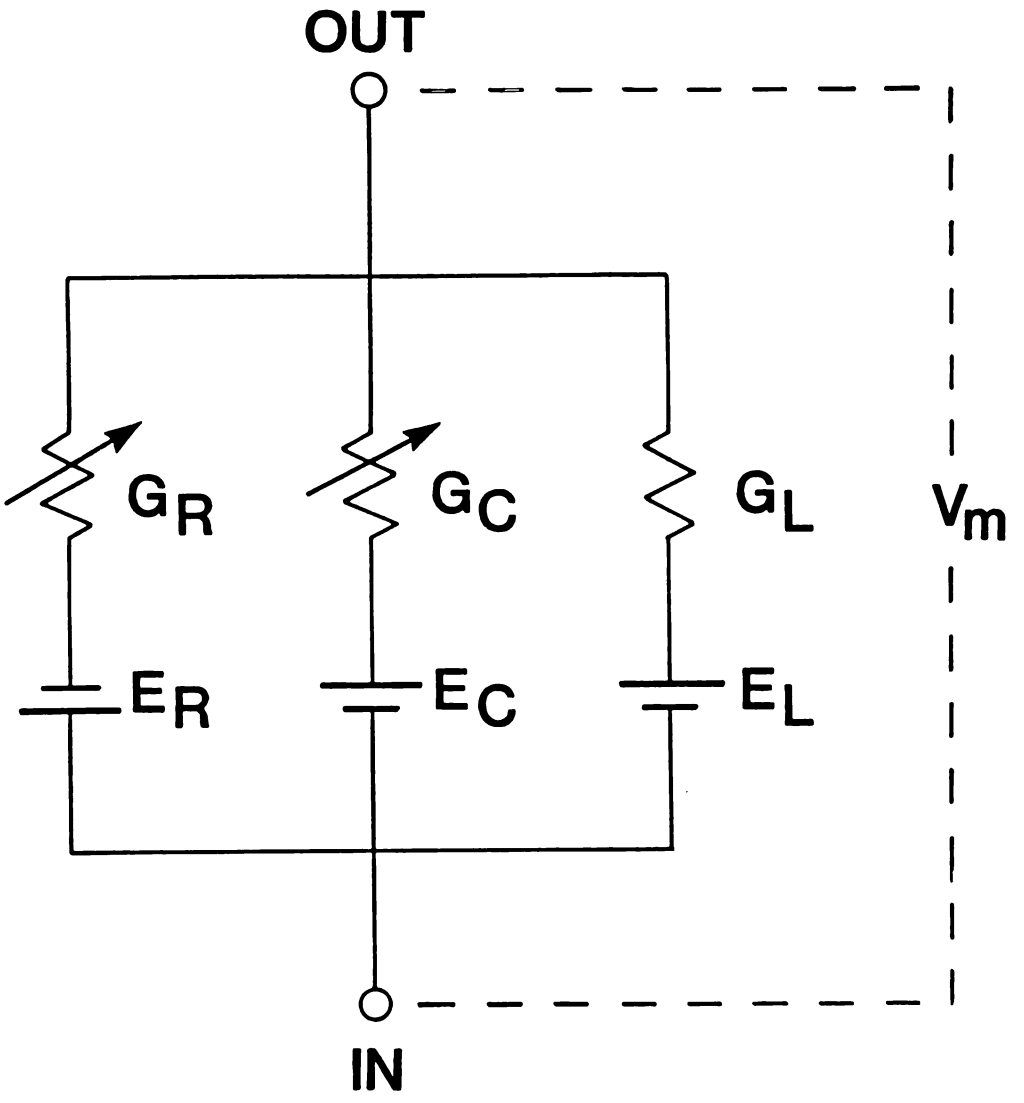
OUT
G_R
G_C
G_L
V_m
E_R
E_C
E_L
IN

Figure 10: Circuit diagram depicting the two synaptic inputs modulated by glutamate. V_m: membrane potential, G_O: the conductance increased by glutamate, E_O: the reversal potential of this conductance, G_C: conductance decreased by glutamate, E_C: the reversal potential of this conductance. The leak conductance is given as G_L and its reversal potential as E_L .

Effects of intracellular cesium

Pharmacological evidence that glutamate modulates two types of channels was obtained with a specific channel blocker. Since one of glutamate's actions is to opens channels with a reversal potential more negative than the resting potential, it seemed reasonable to assume that these channels might be permeable to K^+ ions. It has been shown in a variety of systems (Puil and Werman, 1979; Brown and Johnston, 1983; Crunelli et. al., 1984) that internally applied Cs^+ blocks several types of K^+ conductances. If Cs^+ blocks the channels which are opened by glutamate, than the conductance-decreasing component of glutamate's action would be isolated.

The 2M potassium acetate normally used as the microelectrode electrolyte was replaced with a solution of 2M cesium sulfate. Current-voltage relations for DBCs recorded with Cs^+-filled electrodes were measured in the presence of glutamate and in the control bathing solution. An example of the cesium results is shown in figure 11. Glutamate produced a decrease in conductance along with the hyperpolarization. The reversal potential was about +5.0 mV. In six cells recorded with Cs^+-filled electrodes, the average reversal potential of the glutamate response was -0.5 mV (SD=19.2 mV), the average conductance change was 4.2 nS.

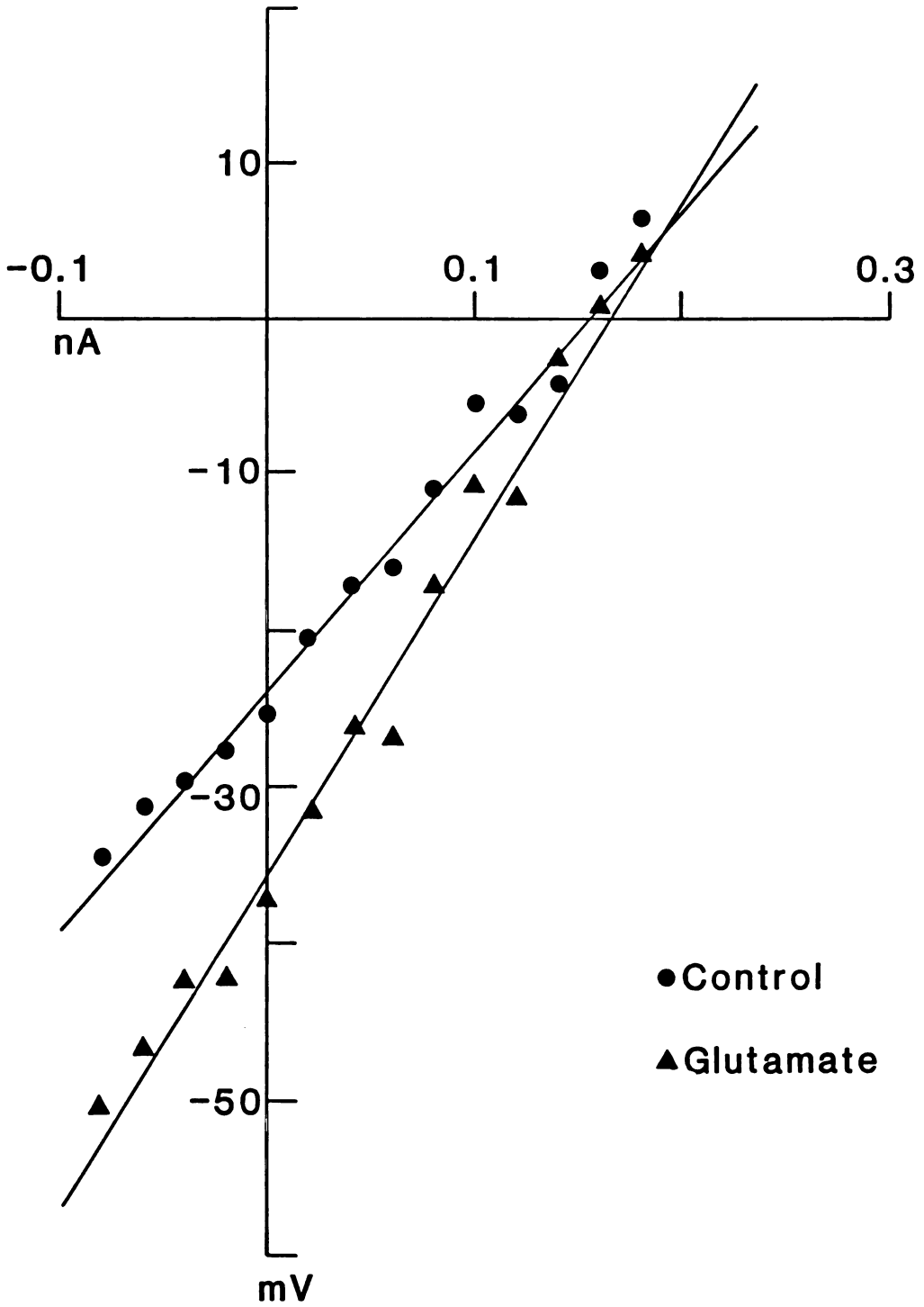
10
-10
-30
-50
-0.1
0.1
0.3
nA
mV
●Control
▲Glutamate

Figure 11: I-V relations of glutamate with Cs^{+}-filled micro-electrode
Current-voltage relations obtained in control (circles) and 2 mM glutamate (triangles) using a microelectrode filled with 2M cesium sulfate. Slope of the best least squares-fitted lines are 155 MΩ and 217 MΩ. The lines intersect at +5 mV.

Synaptic effects of APB on rod-driven DBCs

The glutamate analog 2-amino-4-phosphonobutyrate (APB) blocks the light response of DBCs in a variety of species (mudpuppy: Slaughter and Miller, 1981; 1985, dogfish: Shiells et. al., 1981, rabbit: Bloomfield and Dowling, 1985). In those retinas, the bipolar cells which were studied receive input from only one type of photoreceptor. We therefore examined the effects of APB on DBCs in the goldfish retina to see if it acted preferentially on either the rod or cone pathway or if, similar to glutamate, it acted on both pathways.

APB (2 μM) blocked the rod-driven light response and hyperpolarized the membrane, suggesting that at least part of its action is on the rod pathway. Current-voltage relations in control solution, in APB and after return to control were obtained in 10 cells. An example is shown in figure 12. The upper portion of the figure illustrates the reversible effect of APB on the membrane potential and the light response. The lower part of the figure shows that the APB-evoked hyperpolarization is associated with a clear conductance decrease, as would be expected if the sole action of APB were to close the rod transmitter-gated channels. The conductance change was reversed following the return to control solution. It should be noted that much less APB was required than glutamate to polarize the DBC membrane. This difference can be attributed to very active glutamate uptake in the retina which reduces the effective concentration of glutamate at the synaptic sites (Ishida and Fain, 1981)

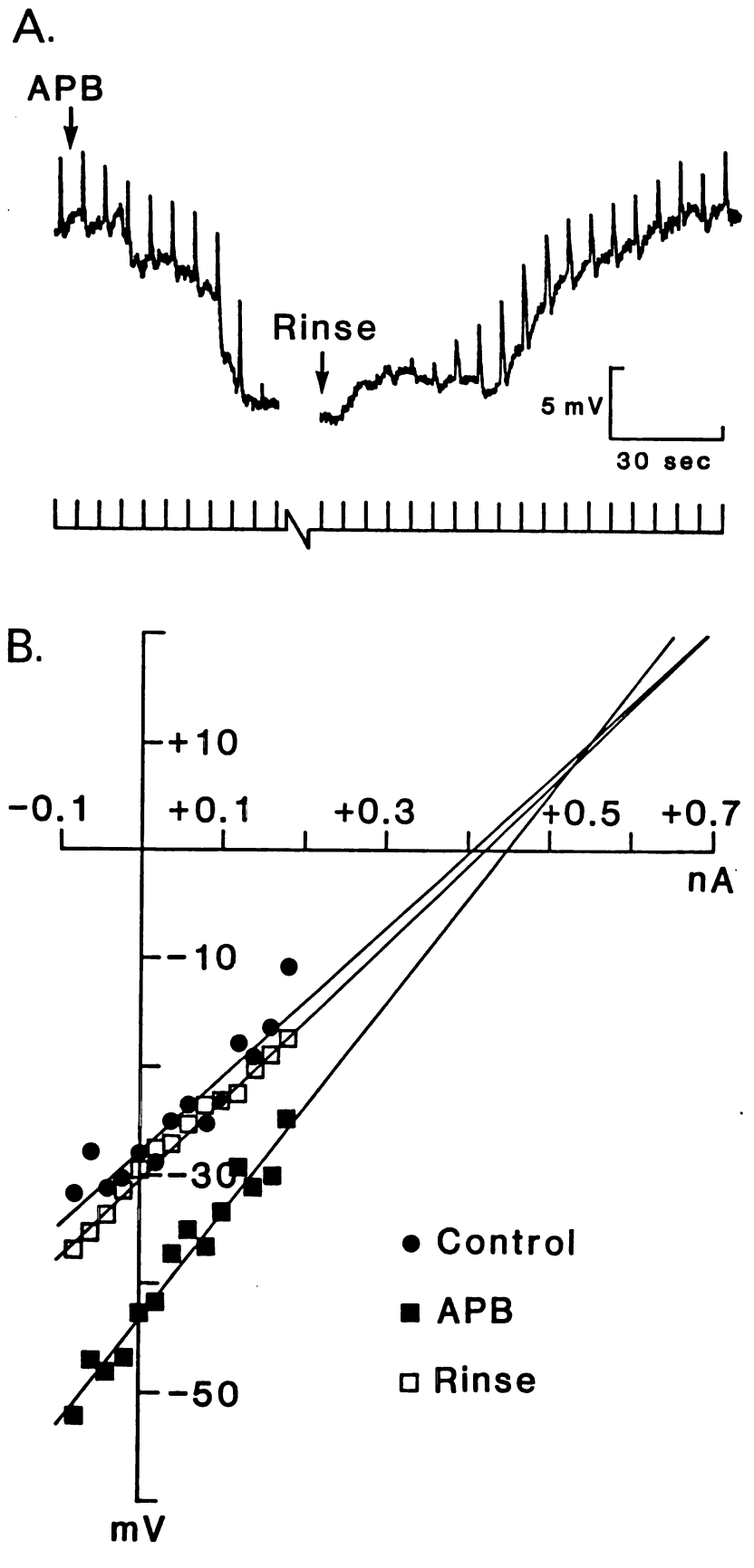
A.
APB
Rinse
5 mV
30 sec
B.
+10
−0.1
+0.1
+0.3
+0.5
+0.7
nA
−10
−30
−50
mV
Control
APB
Rinse

Figure 12: Current-voltage relations for APB

A: Response of a DBC to superfusion of 10 μM APB + 1mM Co^{2+}, and following rinse out. The light stimulus was a 10 msec flash containing 0.12 photons μm^{-2} $flash^{-1}$. The break in the record was approximately 2 minutes. The recording was maintained throughout this period with minimal change in the membrane potential.

B: Current-voltage relations for control (circles), 10 μM APB + Co^{2+}(squares), and after rinse back to control (open squares). Slopes of the lines were 67 MΩ, 92 MΩ and 72 MΩ.

Table II summarizes data obtained from all 10 cells. The average extrapolated reversal potential was -2.8 mV (SD 10.9), very similar to the reversal potential for the light response reported in table I. We have been able to measure complete I-V relations for both the rod transmitter and APB in 4 cells (Cells no. 2, 3, 6 and 14). For these cells, the reversal potential for both the rod transmitter and APB was within a few millivolts.

To further test the ability of APB to mimic the rod transmitter, we attempted to "titrate" the effects of APB against those of the rod transmitter. One μM APB, a concentration which was not sufficient to block the light response, was superfused onto the retina. Following the membrane hyperpolarization, we used a steady background light to depolarize the membrane potential back to its previous control value. This experiment is illustrated in figure 13A. Figure 13B shows the I-V relations for this cell obtained in darkness, APB and APB+light. The relations for darkness and APB+light were nearly identical, indicating that APB was closing the same channels that were closed by the rod transmitter.

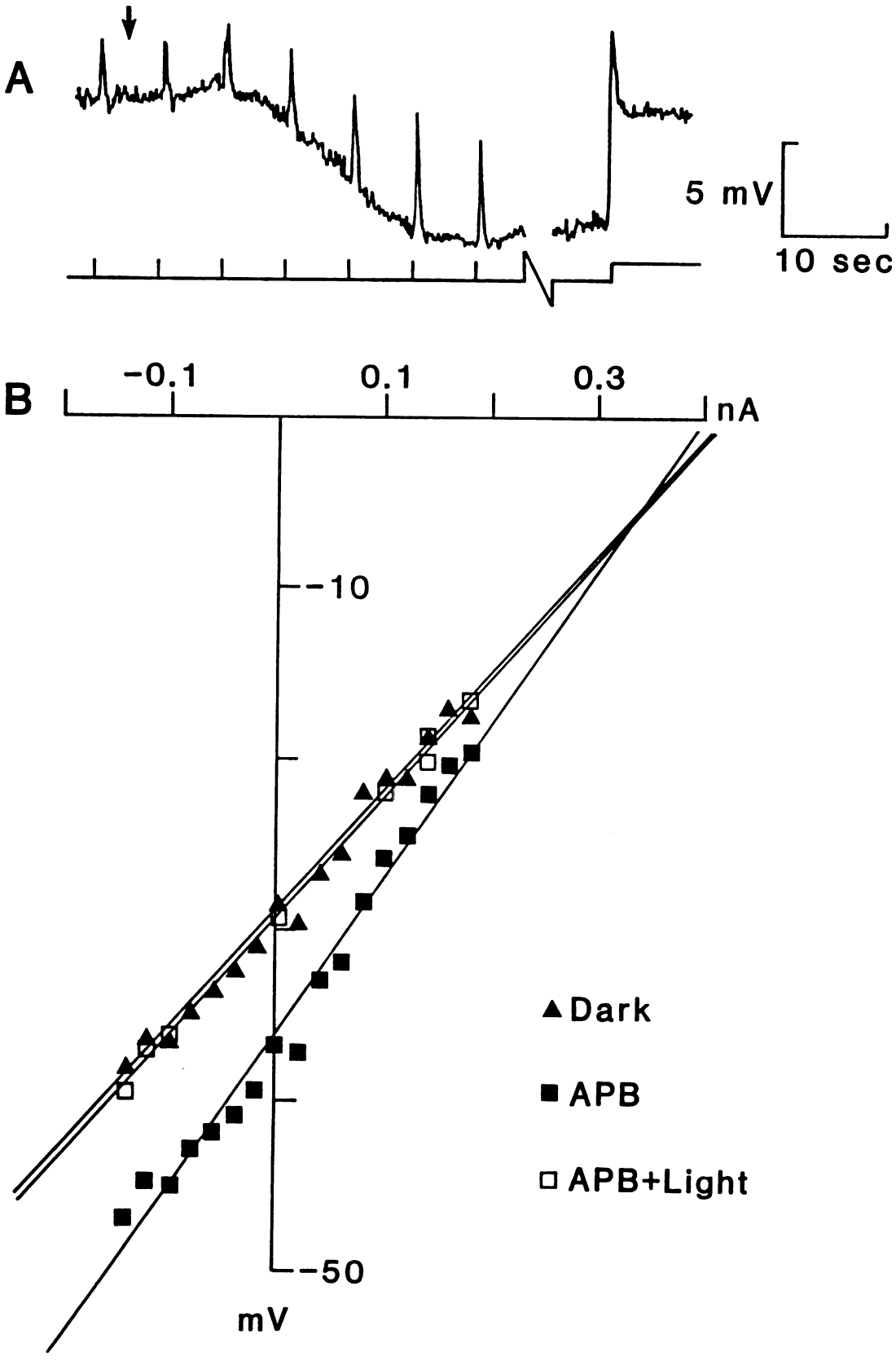
A
5 mV
10 sec
B
-0.1
0.1
0.3
nA
-10
-50
mV
Dark
APB
APB+Light

Figure 13: Current-voltage relations for APB+light

A) Response of a DBC to superfusion of 1 μM APB. After the APB-induced hyperpolarization reached a steady-state level, a continuous stimulus light was turned on which depolarized the cell back to the original dark potential. This steady light projected 9.8 photons$\cdot$ μm^{-2} sec^{-1} onto the retina. The 10 msec flash stimulus contained 0.041 photons$\cdot$ μm^{-2} sec^{-1} .
B: Current-voltage relations for control (triangles), 1 μM APB (squares) and APB + light (open squares). The linear regression lines for all three conditions are shown. Slopes of the lines are 69 MΩ, 91 MΩ and 68 MΩ.

TABLE II

Current-voltage relations for APB/Control

CELL	[APB]	G_C	G_{APB}	G_{C-APB}	REV POT
2	10	14.5	11.1	3.4	-8 mV
3	1	11.1	8.5	2.6	+9 mV
6	1	16.9	13.0	3.9	-15 mV
14	1	6.9	4.5	2.4	-2 mV
15	2	10.6	6.7	3.9	-8 mV
16	2	18.2	11.6	6.6	-7 mV
17	10	11.8	9.2	2.6	+5 mV
18	10	8.5	7.5	1.0	+20 mV
19	10	10.7	6.1	4.6	-12 mV
20	10	13.9	10.3	3.6	+8 mV
mean	--	12.6	9.3	3.5	-1.0
SD	--	2.9	2.3	1.7	10.9

I-V relations for 10 cells in control and 1, 2 or 10 μM APB. Cells 18 and 19 were superfused with 1 mM Co^{2+} as well as APB. The reversal potential was estimated from the intersection of the extrapolated control and APB relations. [APB]: Concentration of APB. G_C: Conductance in control solution. G_{APB}: Conductance in the presence of APB. G_{C-APB}: Conductance decreased by APB.

Effect of APB on cone-driven DBCs

The difference in the observed conductance changes produced by the cone transmitter, and by APB in the rod-dominated retina suggest that APB would be ineffective at the postsynaptic receptor mediating input from cones. It is possible that a more dominant rod input in those cells recorded from in the dark-adapted retina might swamp-out any possible postsynaptic action of APB in the cone pathway. To rule out this possibility, the effects of APB on membrane potential and conductance were examined in cells which clearly received a dominant input from cones in the light-adapted retina.

Application of 10 μM APB produced a large membrane hyperpolarization, shown in figure 14a. While this hyperpolarization resulted in a loss of the cone-driven light response, the I-V relations in figure 14b provide evidence that APB was not acting on the same receptor as the cone transmitter. The hyperpolarization was associated with a conductance decrease, rather than a conductance increase, which would be expected if APB mimicked the action of the cone transmitter. Rather, the I-V relations suggest that even in DBCs where the cone input can be monitored directly, and rod input is absent, APB still acts at the postsynaptic receptor mediating a channel closure.

It is noteworthy that even though APB didn't exert its effect through the channel-opening mechanism used by the cone transmitter, it never-the-less blocked the cone light response. Several mechanisms can account for the absence of a cone light response in the presence of APB.

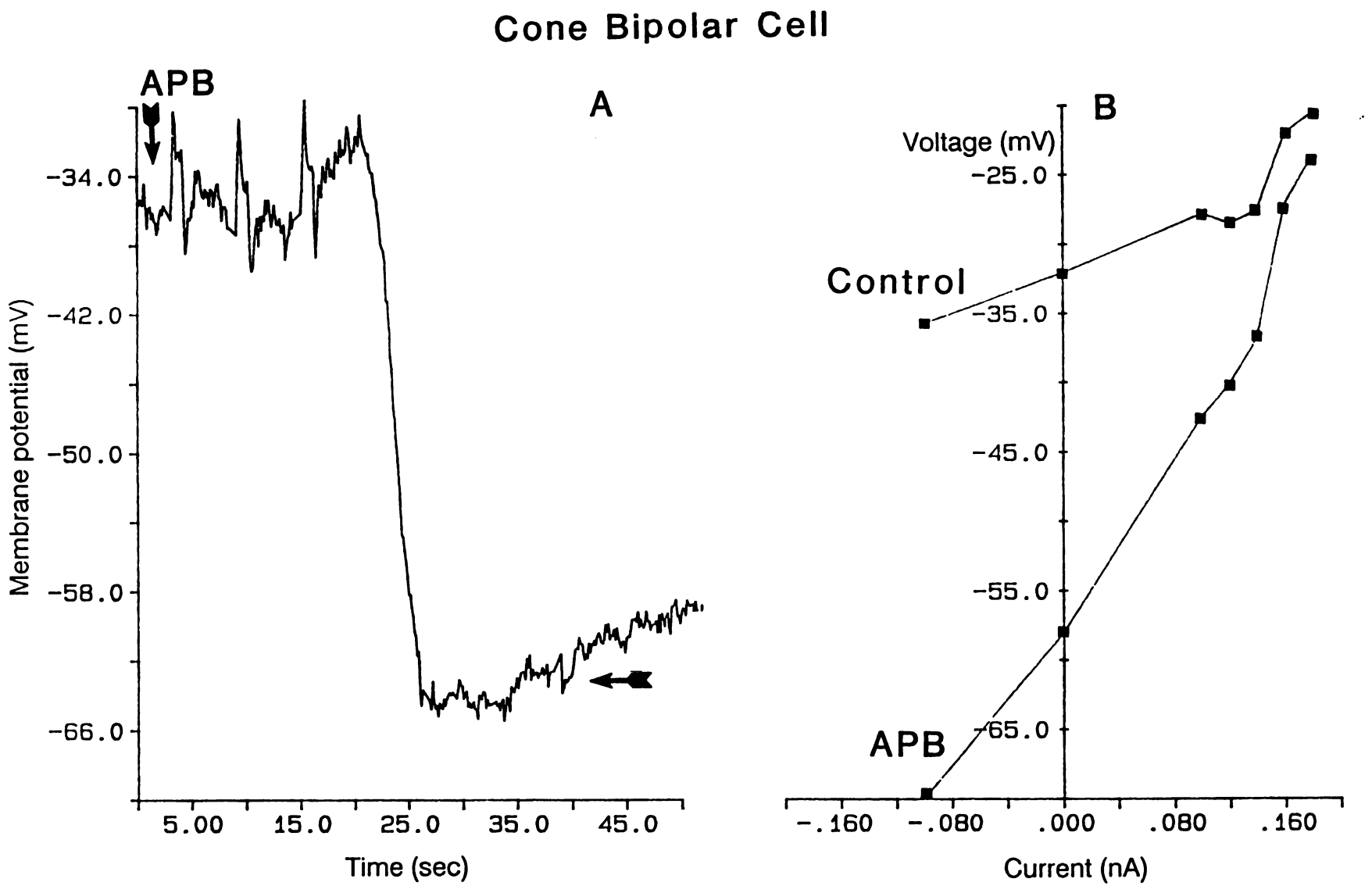
Cone Bipolar Cell
APB
A
-34.0
-42.0
-50.0
-58.0
-66.0
Membrane potential (mV)
5.00
15.0
25.0
35.0
45.0
Time (sec)
B
Voltage (mV)
-25.0
-35.0
-45.0
-55.0
-65.0
Control
APB
-.160
-.080
.000
.080
.160
Current (nA)

Figure 14: APB still produces a conductance decrease under light-adapted conditions.

A: Response of a cone-driven DBC to 4 μM APB. Note the presence of a hyperpolarizing light response indicated by the second arrow. Whether this response is the reversed cone response, or some other input now unmasked by the APB is not clear. Stimulus: 1 second 650 nm at $6.8X10^{3}\cdot \mu m^{-2}$ sec^{-1}. At the second arrow, the stimulus intensity was increased by 1 log unit. B: I-V relations from the same cell for APB and control. Note that APB produces a conductance decrease in the light adapted retina, as it does in the dark-adapted retina. The difference in conductance mechanism associated with the cone transmitter and APB make it highly unlikely that APB is an agonist for the cone postsynaptic receptor.

An APB-induced hyperpolarization of the membrane to a sufficiently negative potential would be expected to remove, or reverse the driving force for the synaptic current generated by the cone transmitter. Close inspection of figure 14A reveals that a small hyperpolarizing light response, possibly the reversed cone light response, was present following treatment with APB, when the light intensity was increased (see second arrow). If the cone response was blocked by the reduction in driving force, then depolarizing the membrane back to the resting potential should restore the cone-driven light response. Unfortunately, attempts to restore the light response in other cells by polarizing the cell back toward the dark potential were unsuccessful, owing primarily to the difficulty of injecting a sufficient amount of depolarizing current into the electrode without losing the recording. An additional mechanism which can't be ruled out is a blockade of the cone response through an interaction of APB and the cone pathway at a site other than on the DBC. Evidence in favor of this possibility will be presented in chapter 3.

Effects of other glutamate analogs

The effects of kainate and NMDA on dark-adapted DBCs were also examined. In light of the suggestion that kainate is more effective at blocking the light response of DBC in other species at lower concentrations than APB (Shiells et al., 1983; Massey and Redburn, 1987), the relative sensitivity of APB, NMDA and kaniate in the dark-adapted goldfish retina was assessed.

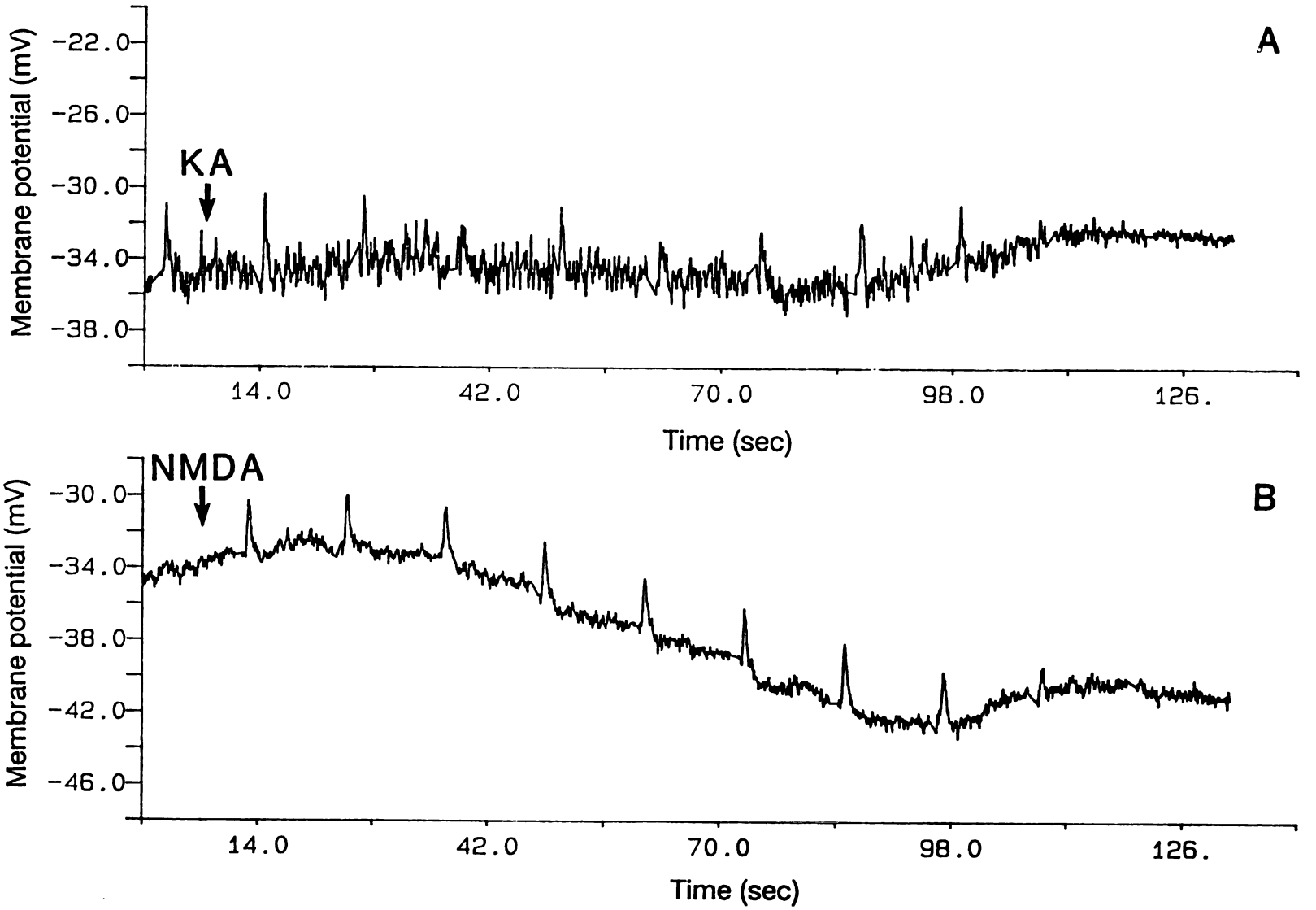
A
KA
Membrane potential (mV)
-22.0
-26.0
-30.0
-34.0
-38.0
14.0
42.0
70.0
98.0
126.
Time (sec)
B
NMDA
Membrane potential (mV)
-30.0
-34.0
-38.0
-42.0
-46.0
14.0
42.0
70.0
98.0
126.
Time (sec)

Figure 15: Effects of kainate and NMDA on DBCs

A: Response of a rod-driven DBC to a solution containing 90 μM kainate and 1 mM Co^{2+}. Note the reduction in noise. Stimulus: 10 msec 550 nm flash containing 0.89 photons$\cdot\mu m^{-2}$ sec^{-1}. Following rinse-out, both the noise and light response returned (not shown). B: Response of another rod-driven DBC to 50 μM NMDA and 1 mM Co^{2+}. The effects were also reversed in this cell. Stimulus: 10 msec 550 nm flash containing 0.09 photons$\cdot\mu m^{-2}$ sec^{-1}.

The effects of kainate on DBCs were variable. At concentrations of 10 and 20 μM, kainate depolarized the membrane and had little effect on the rod-driven light response. Higher concentrations produced a biphasic response, first depolarizing, then hyperpolarizing the membrane, and blocking the light response. The depolarization at low concentrations as well as the biphasic responses at higher concentrations were probably due to polysynaptic actions of kainate (Shiells et al., 1981). In order to eliminate these effects, the action of kainate in the presence of 1 mM Co^{2+} was examined, and is shown in figure 15a. At the time indicated by the arrow, the retina was superfused with a solution containing 100 μM kainate and 1 mM Co^{2+}. The effect of kainate was minimal, the depolarization and blockade of the light response being due to the effect of cobalt. Although effects were often observed at higher concentrations, the rod-mediating receptor appears to be much less sensitive to kainate than APB.

NMDA was tested on 6 DBC's, 3 at a concentration of 50 μM, and 3 others at a concentration of 500 μM. An example of the action of 50 μM on the rod-driven DBC in the presence of 1 mM Co^{2+} is shown in figure 15b. This cell was chosen since the observed hyperpolarization was the largest seen in any cell. Blockade of the light response was due to the effect of Co^{2+} rather than NMDA, since NMDA had no effect on light response when applied alone in this cell. It did not have any substantial effect on the amplitude or kinetics of the light response in any of the cells tested. Similar findings with NMDA have been made in

studies of DBC's in the amphibian (Slaughter and Miller, 1983) and rabbit (Bloomfield and Dowling, 1985) retina.

Discussion

Anatomical studies have demonstrated that a major class of DBCs in the goldfish receives input from both rods and red-sensitive cones (Stell, 1967; Ishida et. al., 1980). Kaneko and Tachibana (1978) showed that the spectral sensitivity of these cells depended upon the adaptation state of the retina, while Saito and his colleagues (Saito et. al., 1978; 1979) found that the reversal potential of the light response also depended upon the adaptation state of the retina. They reported that the rod-dominated light response was reversed at positive membrane potentials, while the cone-dominated light response was reversed at negative membrane potentials.

Measurements of the conductance changes produced by the rod and cone pathways were repeated in the present study for several reasons. Previous workers obtained results from retinas which, judging by the mixed rod and cone inputs, were not fully light- or dark-adapted. As a result, it is more difficult to measure the reversal potential of either the rod or cone pathway in complete isolation. In the present study, care was taken to keep the retina fully light or dark-adapted during both the dissecting and recording procedure, resulting in purer rod and cone responses. Secondly, previous workers estimated reversal by measuring the amplitude of the flash response during current steps. Since I-V relations in the present study measured the conductance changes produced by steady state application of glutamate and APB, consistency required that rod and cone light responses be measured

during the steady state as well. Despite the differences in techniques and preparations, the results obtained in the present study agree reasonably well with the previous results.

Separation of rod and cone pathways with APB

Previous studies have demonstrated that APB can block the light responses of DBCs in mudpuppy (Slaughter and Miller, 1981), dogfish (Shiells et al, 1981) and rabbit (Bloomfield and Dowling, 1985), while having no effect on hyperpolarizing bipolar cells or horizontal cells, the other targets of photoreceptors. The photoreceptor-DBC synapse is an important link in forming the ON pathway which is preserved in the retina and throughout the visual system. The use of APB as a selective blocker of the ON pathway, presumably by pharmacologically blocking this synapse, is well documented (Slaughter and Miller, 1981) (for review see Massey and Redburn, 1987). We therefore used APB to probe for pharmacological differences between the rod and cone pathway in goldfish DBCs.

The results presented here indicate that APB acts selectively at the postsynaptic receptor mediating rod responses. Concentrations of 1 μM or higher closed channels with a reversal potential of about 0 mV, very near the reversal potential of the rod transmitter, but very different than the reversal potential of the cone transmitter. The effects of APB on the cone-driven DBCs were consistent with an action at the receptors mediating the rod inputs.

The blocking effect of cesium on the channel-opening glutamate receptor

Unlike APB, glutamate acts at both the channel-opening and channel-closing receptor, as suggested previously (Nawy and Copenhagen, 1987). In normal superfusion media using potassium acetate-filled microelectrodes, it was not possible to isolate the effect of glutamate on either type of receptor. In the present study, this was accomplished by using microelectrodes filled with 2M cesium sulfate. In cells recorded with these microelectrodes, cesium blocked the conductance produced by the channel-opening receptor.In this case, the action of glutamate became indistinguishable from that of APB.

Based on the model of the dual glutamate action (fig. 10), it appears that cesium is selectively blocking a glutamate-activated potassium conductance. Cesium has been found to block K^+ conductances in other systems, but generally these have been voltage- rather than synaptically-gated ones (Hablitz and Langmoen, 1982; Brown and Johnston, 1983). The potassium conductance activated by glutamate in DBCs is an action that has not yet been reported for glutamatergic receptors in the CNS (Mayer and Westbrook, 1987). Rod-driven light responses in DBCs were unaffected by cesium, suggesting that the channel mediating rod responses is not blocked. This is consistent with the idea that cesium does not effect either sodium or non-selective cationic conductances gated by glutamate (Brown and Johnston, 1983).

We propose that the action of glutamate on the channel-opening conductance is identical to the action of the cone transmitter, as

judged by the similarity of conductance changes and reversal potentials. More rigorous confirmation of this model await the development of a glutamate agonist which is specific for the receptor mediating the channel opening conductance.

Multiple classes of glutamatergic receptor in other neurons

The net result of glutamate's actions on goldfish DBCs is a large change in membrane potential with only a small change in membrane conductance. A similar phenomenon has been observed in studies of different types of spinal cord neurons (Zieglgansberger and Puil, 1973; Altmann, Ten Bruggencate, Pickelmann and Steinberg, 1976; Engberg, Flatman and Lambert, 1979) and hippocampal pyramidal cells (Hablitz and Langmoen, 1982). However, the underlying mechanisms appear to be quite different.

Using voltage clamped cultured spinal cord neurons, Mayer and Westbrook (1984, 1985) compared the effects of glutamate to those of the pure agonists. They found that cultured spinal neurons have both an NMDA-preferring and a non-NMDA-preferring (i.e., quisqualate and kainate) receptor. The NMDA-preferring receptor activated a highly voltage-dependant conductance with a "negative conductance" region, while the non-NMDA receptor activated a conductance which was essentially ohmic. The simultaneous activation of both types of receptors by glutamate therefore resulted in a depolarization of the membrane with little or no change in conductance.

In spinal neurons, glutamate opens both a voltage-dependent and a voltage-independent channel. We have not found any evidence that either of the glutamate-sensitive conductances in goldfish DBCs is voltage-sensitive. While the steady-state I-V plot of the NMDA-induced conductance is highly non-linear from about -80 mV to -40 mV (Mayer and Westbrook, 1987), both the APB and the glutamate steady-state I-V plots are essentially linear over the range of voltages we have tested (approximately -60 mV to 0 mV) (see figs 5,8,9).

Spatial separation of different glutamate receptors on single neurons

Previous studies (Dale and Roberts, 1985; Dale and Grillner, 1986; O'Brien and Fishbach, 1986) have demonstrated that transmitter released from a single presynaptic neuron can simultaneously activate several types of glutamate receptor. This finding would suggest that in some glutamatergic systems several classes of receptor are clustered together at one location on the postsynaptic neuron. Although DBCs also possess at least two classes of receptors, it appears that each type of synaptic input activates only one of these classes. The synaptic inputs to DBCs are spatially segregated since they are presumed to occur at the tips of the individual dendritic processes of the DBC where they contact the synaptic terminals of the rods and cones. If rods and cones both utilize the same neurotransmitter, our findings provide strong evidence that each dendritic process contains only the appropriate type of receptor. It is only in this manner that the rod and cone pathways could be isolated from one another. Thus, these results provide a

possible example of the segregation and transport of different classes of postsynaptic receptor to the site of the appropriate presynaptic input.

Chapter 3

EVIDENCE FOR SELECTIVE PRESYNAPTIC INHIBITION OF PHOTORECEPTORS BY THE GLUTAMATE ANALOG APB

Abstract

Two separate synaptic actions of the glutamate analog 2-amino-4-phosphonobutyric acid (APB) have been reported in the vertebrate CNS. In the retina, APB defines a class of glutamate receptor thought to be found only on depolarizing bipolar cells (DBC). Binding of APB to this receptor produces a hyperpolarization of the DBC membrane, but has no reported effect on horizontal or hyperpolarizing bipolar cells (Slaughter and Miller, 1981; Bloomfield and Dowling, 1985). Elsewhere in the CNS, APB is characterized as a nonspecific antagonist of excitatory amino acid transmission, perhaps acting via a presynaptic mechanism to block transmitter release (Harris and Cotman, 1983). These two actions have been considered separate and unrelated, the agonist action of APB on retinal bipolar cells is considered to be novel. We have previously reported that in the dark-adapted isolated goldfish retina, when the rod pathways were active, APB acted postsynaptically on DBC's as in other species (Nawy and Copenhagen, 1987). In the present paper, we extend our study of APB to the cone pathways. In the light-adapted retina, APB had potent effects on cone-driven horizontal cells (CHCs), hyperpolarizing the membrane and blocking the light response, effects consistent with an antagonist rather than an agonist action.

However, unlike other antagonists, APB was not able to block the actions of exogenously applied agonists such as kainate, suggesting that its action may be mediated presynaptically through the cones. Presynaptic inhibition of cones may well be mediated by the same APB-preferring receptor found on the DBC, reducing transmitter release by hyperpolarizing the cone terminal. This same receptor may also mediate the inhibitory effects of APB described elsewhere in the nervous system, suggesting that the action of APB in the retina and elsewhere may be more consistent than previously thought, and providing a broader role for APB receptors in the CNS.

INTRODUCTION

Three classes of excitatory amino acid receptor have been characterized in the vertebrate CNS based upon the selective actions of the agonist N-methyl-D-aspartate (NMDA), kainate and quisqualate (Watkins and Evans, 1981). Studies of the retina have demonstrated a fourth class of glutamate receptor found on depolarizing bipolar cells (DBC) and selectively activated by the glutamate analog 2-amino-4-phosphonobutyric acid (APB) (Shiells et al., 1981; Slaughter and Miller, 1981; 1985). Inversion of the light response at the DBC requires that the photoreceptor transmitter hyperpolarize the postsynaptic membrane; an unusual action for an excitatory transmitter. Not only does APB produce this hyperpolarization, it also has no effect on the other second order neurons (horizontal and hyperpolarizing bipolar cells) where the photoreceptor transmitter produces a more conventional depolarization. The specific action of APB on DBCs has led to the wide usage of APB as a tool for selectively blocking the "on" pathway while studying higher-order visual centers (e.g., Schiller, 1986).

Utilizing both the dark and light-adapted isolated goldfish retina, APB was shown previously (Nawy and Copenhagen, 1987) to mimic the action of the rod, but not the cone, transmitter on DBCs. In this section, a second, previously uncharacterized role of APB in the retina is demonstrated, this time as an antagonist in the cone pathway. Both APB and NMDA antagonize the action of the cone transmitter on cone

horizontal cells (CHC) by hyperpolarizing the cells and blocking the light responses. While NMDA has been shown previously to act postsynaptically on horizontal cells (Bloomfield and Dowling, 1985), evidence is presented here that is consistent with APB acting presynaptically to reduce the rate of transmitter release from both red- and green-sensitive cones. These results suggest a broader role for an APB-preferring receptor in the retina than previously suspected, and cloud the interpretation of the effects of retinal APB-injection on higher-order pathways.

APB has also been proposed as a presynaptic antagonist of excitatory amino acid-mediated synaptic transmission in other parts of the CNS such as the spinal cord, (Evans et al., 1982) olfactory cortex (Hori et al., 1982) and hippocampus (Harris and Cotman, 1983). This conclusion has been drawn partly from the observation that APB could block transmission via electrical stimulation of presynaptic pathways, but not the effect of applied amino acids (Mayer and Westbrook, 1987 for review). Although the role of APB as presynaptic inhibitor previously has been thought of as fundamentally separate from its actions in the retina, the demonstration of APB-mediated presynaptic inhibition in the retina lessens the gap between this and other regions of the nervous system. Moreover, the action of APB on bipolar cells in the rod-driven retina, on cones in the light-adapted retina, and elsewhere in the nervous system might all be accounted for by a single conductance mechanism. We suggest that the APB-preferring receptor best

characterized in the retina, may also mediate the antagonistic effects of APB found elsewhere in the CNS.

Materials and methods

Preparation of the retina

The procedure for isolating, stimulating and recording from the retina has been described previously for the dark-adapted retina (Nawy and Copenhagen, submitted). In the present study, a relatively light adapted retina was used so that cone-driven responses could be recorded. Briefly, goldfish were placed in complete darkness for no longer than 10 minutes prior to sacrifice. Following enucleation and hemisection of the eye, the retina was isolated from the retina, incubated in a 20% solution of hyaluronidase (Wydase, Wyeth Labs) for 20-30 minutes, and then mounted on an annular-shaped piece of #2 filter paper with the receptor-side up and placed in the superfusion chamber. The 10 minutes of dark-adaptation decreased the amount of pigment epithelium which stuck to the retina following isolation.

The recording chamber was continuously superfused with oxygenated L-15 culture medium (Gibco) modified to contain the following concentration (in mM): NaCl, 120; MgSO4, 1.2; KCl, 2.5; CaCl2, 2.2; glucose, 10.0; and was buffered to a pH of 7.8 with 3 mM HEPES. All amino acid analogs as well as Co2+ were added without substitution to this solution. Gravity-fed control and test solutions were alternately connected to the recording chamber through a series of valves (Hamilton) following the design of Belgum, Dvorak and McReynolds (1982). The volume of the chamber was about 0.3 ml. We typically obtained full

physiological responses to different test solutions within 45 seconds after switching the valves.

The dissection was performed using a standard dissecting microscope illuminator whose beam was filtered by 3 layers of red acetate paper. Although varying slightly from experiment to experiment, the light intensity was about 150 $\mu W/cm^2$. From spectrophotometric measurements, the acetate paper acted as a high-pass filter with 10 percent transmission at about 610 nm, and 90 percent transmission at about 676 nm. The isolation procedure lasted about 10 minutes. Following 20 minutes in complete darkness, the isolated retina was transferred to the filter paper under the same red light. Under these conditions, we repeatedly found cone-dominated retinas with few rod-driven responses, and horizontal cells which responded to APB. On several occasions, when the dissection was performed under brighter lights, we still obtained viable light responses, but the responses to APB appeared to be diminished.

Microelectrodes formed from standard omega-dot tubing were pulled on a Brown-Flaming puller to a resistance of 300-700 megohms and filled with 2M potassium acetate. Electrodes were advanced through the retina in small steps (1-10 microns) until a cell was penetrated. Horizontal cells were identified on the basis of their light responses and position in the retina.

Light Stimulation

The stimulating light was focused onto the retina from below through the hole in the filter paper. The light was projected onto the retina from an optical bench mounted beside the light-tight Faraday recording cage. Neutral density and interference filters (10 nm halfwidth) were used to attenuate the light and adjust its color. Spectral sensitivity measurements of horizontal cells were obtained by adjusting the intensity at each wavelength using 0.1 and 0.2 ND filters so that the response amplitude was 3 mV. The average of 3 responses was used. Wavelengths were presented in random order throughout the experiment, and the wavelength presented at the start was also presented at the end of the experiment to insure that the sensitivity of the cell had not changed.

Results

Properties of H-cell responses

The predominant class of photoreceptor driving the retina can be selected by controlling the retinal dissection and isolation procedures. Figure 16A shows responses of a horizontal cell to 3 intensities of light. This cell was recorded in a dark-adapted isolated retina. A 10 msec flash of green light at 0 sec elicited a response with a time to peak (T) of about 500 msec for the dimmest stimulus, and longer for the brighter stimuli. Values of T in the RHCs ranged from about 400-600 msec. Similar values were found for horizontal cells with rod input in the turtle (Leeper and Copenhagen, 1979) and dogfish (Ashmore and Falk, 1980). The relatively high flash sensitivity of the cells also indicated that they are rod-driven. At a wavelength of 500 nm, the flash sensitivity for responses in the linear range was 29.5 mV/photon$\cdot\mu m^2$ (n=14), similar to the value of 22.8 obtained in rod horizontal cells of the dogfish (Ashmore and Falk, 1980).

Further confirmatory evidence for establishing the rod-driven origin of the light responses came from analysis of the horizontal cell spectral sensitivity. The average spectral sensitivity for 7 cells is plotted in figure 16B. The log of the inverse number of photons in a flash which elicited a 3 mV response is plotted against the inverse wavelength (frequency) of the flash. The continuous line is the nomogram for porphyropsin, the visual pigment found in goldfish rods (Munz and Schwanzara, 1967). There is a reasonable fit between the data

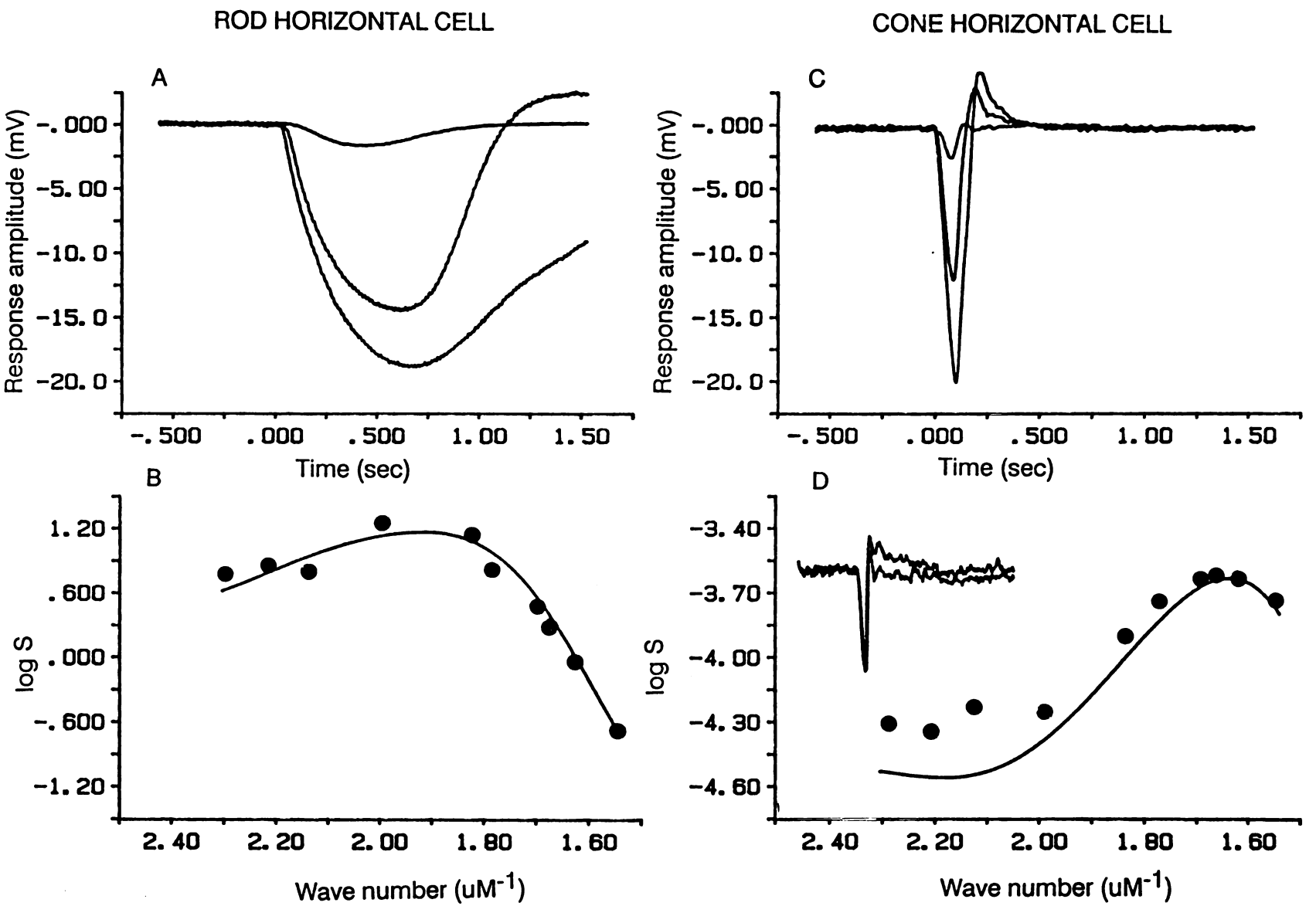
ROD HORIZONTAL CELL
CONE HORIZONTAL CELL
A
C
Response amplitude (mV)
-. 000
-5. 00
-10. 0
-15. 0
-20. 0
-. 500
. 000
. 500
1. 00
1. 50
Time (sec)
B
D
log S
1. 20
. 600
. 000
-. 600
-1. 20
-3. 40
-3. 70
-4. 00
-4. 30
-4. 60
2. 40
2. 20
2. 00
1. 80
1. 60
Wave number (uM-1)

Figure 16: Properties of horizontal cells in light- and dark-adapted retinas.

A: Responses of a horizontal cell recorded in a dark-adapted retina to 10 msec flashes of 550 nm light at intensities of 0.09, 0.90 and 8.97 photons/$\mu m^2 \cdot$flash. In this and all subsequent figures, the light was turned on at 0 seconds.

B: The data points are the average spectral sensitivity for 7 horizontal cells. The log number of photons required to elicit a 3 mV light response is plotted on the y-axis, while the wavenumber (inverse of wavelength) is plotted on the x-axis. The smooth curve is the nomogram for an A_2 with a peak sensitivity at 523 nm. The curve was generated by computer using a polynomial which provided a good fit to the A_2 nomogram (Dawis, 1980). The horizontal cells therefore appear to be rod-driven.

C: Responses of a horizontal cell recorded in a light-adapted retina to 10 msec flashes of 600 nm light at intensities of 62.65, 3140.0 and $3.1X10^4$ photons/$\mu m^2 \cdot$flash.

D: The average sensitivity of 6 horizontal cells as a function of wavelength. The nomogram is a polynomial for an A_2 retinol with a peak sensitivity of 618 nm (Dawis, 1980). Inset: responses to 10 msec flashes of 500 nm and 650 nm light. These cells are most likely driven by red cones.

and the nomogram, consistent with the hypothesis that these horizontal cells are driven by rods. Similar results have been found in the carp retina (Kaneko and Yamada, 1972).

In order to obtain completely rod-driven retinas, it was necessary to keep the animal in complete darkness at least one hour prior to dissection, and to perform the entire dissection under infrared illumination. Once isolated, cone responses were not detected even after prolonged light-adaptation in room light or unattenuated 600 nm light ($1.45X10^6$ photons/μm^2). However, brief exposure to dim red light prior to isolation produced a preparation with mixed rod-cone responses. This type of preparation is probably analogous to the goldfish and carp dark-adapted retinas described in many previous studies (e.g., Saito et al., 1978; Kaneko and Yamada, 1972) where both rod and cone responses were seen.

Cone-dominated retinas were created by dark-adapting the fish for 10 minutes or less and then dissecting under red light. The flash response of a horizontal cell obtained under these conditions is shown in figure 16C. The time to peak and shape of the light response were similar to those found in cone horizontal cells of the turtle (Schnapf and Copenhagen, 1982), about five times faster than the RHC responses. The average flash sensitivity for 11 cells of this type at 618 nm was about 150 $\mu V/photon \cdot \mu m^2$, over 3 log units less sensitive than the RHCs, and similar to the value of 345 μV obtained in the turtle (Schnapf and Copenhagen, 1982). This type of cell was maximally sensitive to red

light, as is shown in figure 16D. The average spectral sensitivity of 6 cells is plotted, along with the nomogram for the A_2 retinols with a peak sensitivity at 623 nm, a value obtained with intracellular recordings from red cones in the carp (Tomita et. at., 1969).

The cause of the deviation of the data from the nomogram at shorter wavelengths is not clear, but might reflect the presence of an additional synaptic input. Additional evidence for this possibility comes from examining the shape of the responses to 2 wavelengths. At 500 nm, a depolarization could be seen at the decay of the light response. No depolarization was evident at 650 nm. Such a lack of univariance strongly indicates that these horizontal cells receive synaptic input from cells other than red cones. This input might come directly from photoreceptors or perhaps from other horizontal cells.

Although several other types of cone-driven horizontal cell were regularly encountered, only one other will be mentioned here, since the effects of APB on this cell type were also documented. These cells were driven primarily by green cones. The kinetics of the light response differed slightly from the red-driven horizontal cell, as can be seen in figure 18A, with a time to peak of about 150 msec. Many of these cells also appeared to have multiple synaptic inputs, with an additional hyperpolarizing component which was maximal for blue light (434-467 nm). Their spectral sensitivity peaked in the green region, and their flash sensitivity was similar to that of the red horizontal cells.

<u>NMDA and kainate in dark and light-adapted retinas</u>

Figure 17 compares the effects of kainic acid on both types of horizontal cell in 2 different retinas. A CHC is shown on the top, while a RHC is shown at the bottom. After the control solution was switched for one containing 10 μM kainate, the cells depolarized to about -10 mV. Light responses for the CHC were too small to be seen clearly in the low-gain figure at the left, and are shown on the right before, during, and after application of kainate. The light response in both cells is reduced in the presence of kainate, consistent with the notion that it may be an agonist for both for the transmitter of both photoreceptors. However, since the reversal potential of the light response is near 0 mV, it is not possible to determine if the absence of a light response is due to a direct action of kainate or is a consequence of the membrane depolarization. These data indicate that kainate has similar effects on rod and cone horizontal cells although, since conductance changes cannot be measured in horizontal cells in the intact retina, a different mechanism of action in each cell cannot be ruled out. Similar results have been obtained for horizontal cells in the rabbit retina (Massey and Miller, 1987).

The only noticeable difference between cell types was the timecourse of depolarization induced by kainate. In most of the cone horizontal cells, the responses to kainate had two components. The first component was a gradual and smooth depolarization towards 0 mV, while the second, more rapid component appeared later, producing peak depolarization and then decaying back to a plateau. This phenomenon has been studied in detail elsewhere (Murakami and Takahashi, 1987) and is

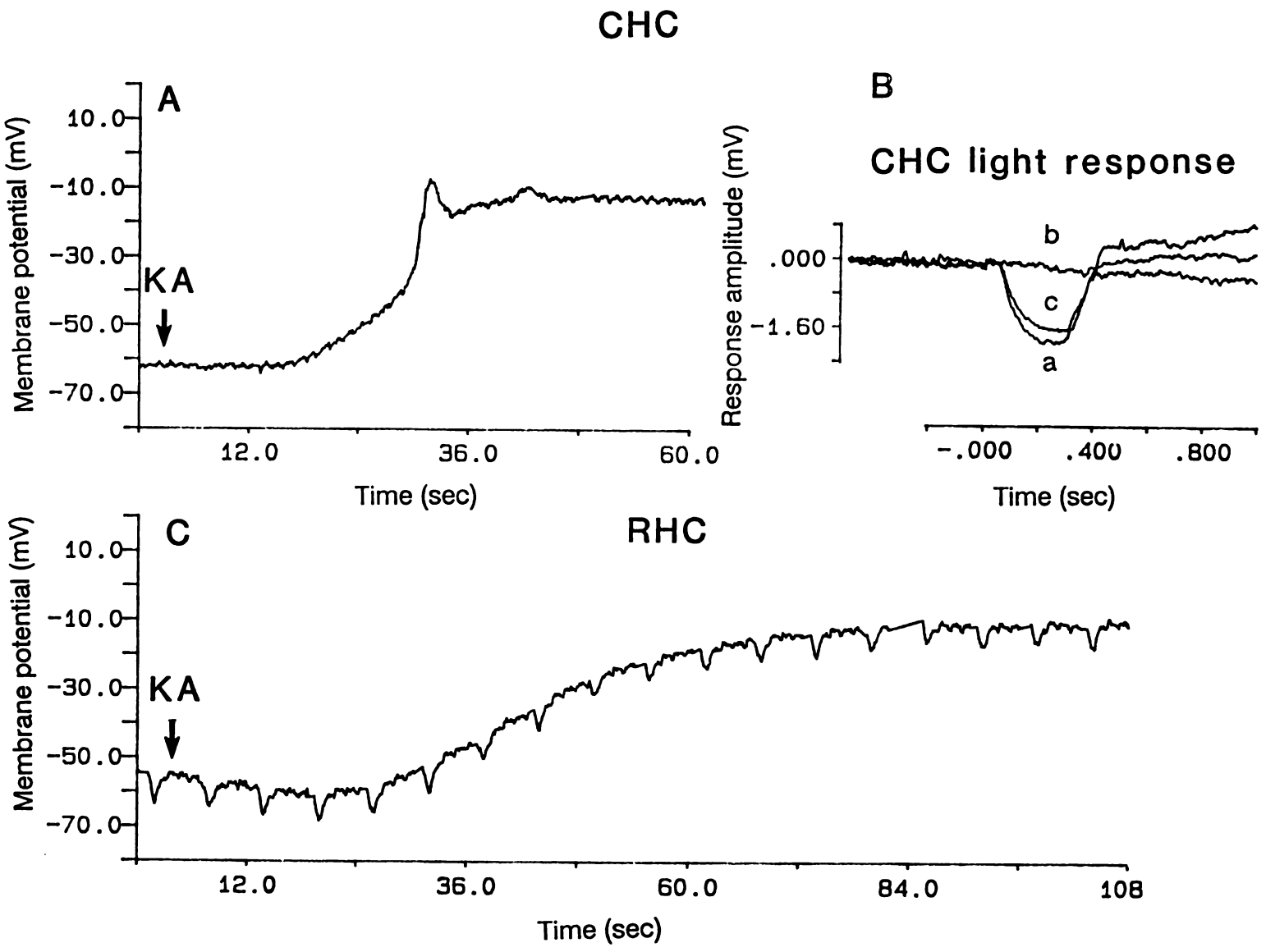
CHC
A
10.0
-10.0
-30.0
-50.0
-70.0
KA
Membrane potential (mV)
12.0
36.0
60.0
Time (sec)
B
CHC light response
Response amplitude (mV)
.000
-1.60
b
c
a
-.000
.400
.800
Time (sec)
C
RHC
10.0
-10.0
-30.0
-50.0
-70.0
KA
Membrane potential (mV)
12.0
36.0
60.0
84.0
108
Time (sec)

Figure 17: Kainate depolarizes rod and cone horizontal cells

A: Response of a CHC to 10 mM kainate, recorded on the low-gain channel of the tape recorder. Following rinse-out, the cell repolarized to its previous potential (not shown). B: Light response of the same cell before (a) during (b) and after (c) the application of kainate. The cell was relatively insensitive, requiring an unusually long and bright stimulus. The 550 nm stimulus, indicated beneath the records, contained $3.93X10^4$ photons/μm^2., and lasted 110 msec. C: Effect of 10 μM kainate on a RHC, recorded on the low-gain channel. The response reversed upon rinse-out (not shown). Stimulus: 10 msec flash of 550 nm containing 0.90 photons/μm^2.

thought to be due to a Ca^{2+} channel, activated by membrane depolarization rather than a specific action of kainate. A dual-component depolarization such as this was not seen in any of the 4 RHCS in which kainate was applied. It is possible that the Ca^{2+} currents described in cone horizontal cells are absent in the rod horizontal cells.

Analogous experiments were performed with NMDA and are illustrated in figure 18. An example of a CHC is at the top, and a RHC at bottom. The RHC light responses are shown at the right at a higher gain, both before, during and after NMDA application. Application of 100 μM NMDA produced a reversible hyperpolarization and an attenuation of the light response in both types of horizontal cells. The size of the hyperpolarization in both rod and cone preparations was substantial, about 30 mV. These results are consistent with those found for NMDA action on the roach (Rowe and Ruddock, 1982) and rabbit retina (Bloomfield and Dowling, 1984). The present results demonstrate for the first time that NMDA is an antagonist for rod horizontal cells as well.

At a lower concentration of NMDA (50 μM), the effects in both rod and cone horizontal cells were reduced in equal proportion. Although complete dose-response curves were not constructed for either type of cell, the minimal effective concentration required for NMDA, as with kainate, is similar for both the rod and cone retinas. If there are differences in the EAA receptors on rod and cone horizontal cells, they

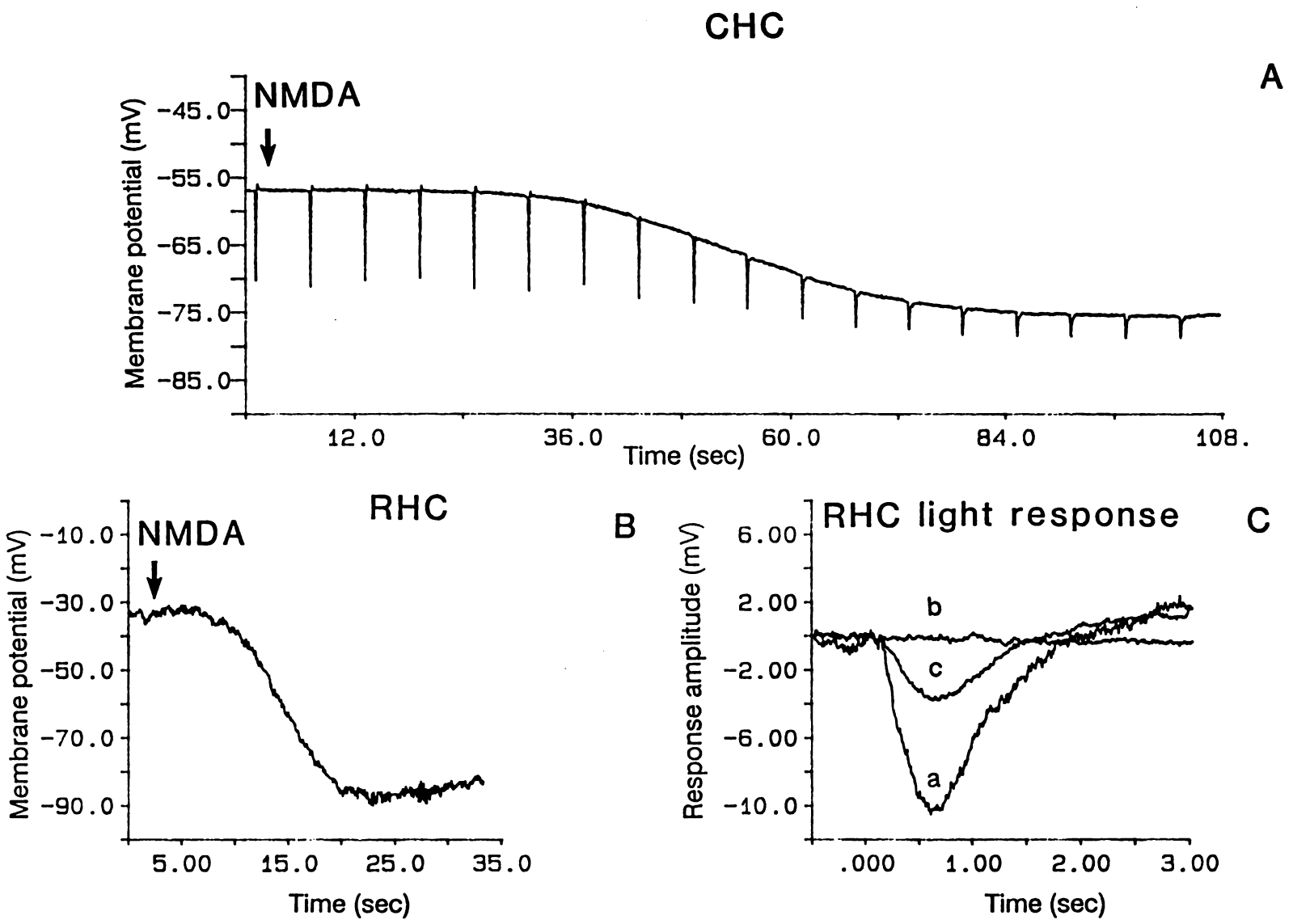
CHC
A
NMDA
Membrane potential (mV)
-45.0
-55.0
-65.0
-75.0
-85.0
12.0
36.0
60.0
84.0
108.
Time (sec)
RHC
B
NMDA
Membrane potential (mV)
-10.0
-30.0
-50.0
-70.0
-90.0
5.00
15.0
25.0
35.0
Time (sec)
RHC light response
C
Response amplitude (mV)
6.00
2.00
-2.00
-6.00
-10.0
b
c
a
.000
1.00
2.00
3.00
Time (sec)

Figure 18: NMDA is an antagonist on RHCs and CHCs

A: Response of a CHC to 100 μM NMDA. The cell was lost before the effect could be reversed. Stimulus: 10 msec flash of 600 nm containing 2893 photons/μm^2. B: Low gain recording of a RHC. Because of the poor signal to noise ratio, the light response was obscured, and is therefore shown in (C). Following rinse-out, the membrane potential returned to the previous control value (not shown). Concentration of NMDA was 100 μM. C: Response to 10 msec flash of 550 nm light containing 0.89 photons/μm^2, shown before (a), during (b) and after (c) application of NMDA.

cannot be resolved with the use of conventional amino acid analogs and the present recording techniques.

Specific action of APB in the light-adapted retina

Previous studies in the amphibian (Slaughter and Miller, 1981; 1983) and dogfish (Shiells et al., 1981) retinae have shown that the glutamate analog 2-amino-4-phosphonobutyric acid (APB) acts specifically on depolarizing bipolar cells, and has no effect on horizontal cells. In order to confirm these results in the goldfish retina, we tested the effects of APB on both rod- and cone-driven horizontal cells.

Figure 19 illustrates the effect of APB on an RHC. At the time indicated by the arrow, the normal superfusate was switched to one containing 10 μM APB. There was no clear change in membrane potential during the application of APB. Figure 19B shows the averaged light responses on an expanded voltage and time scale before and during APB application, and confirm that there was no significant change in response shape or amplitude.

More unexpected were the results obtained with APB in the light-adapted retina. Figure 20 illustrates these effects on a green cone-driven horizontal cell. As in the previous figure, the time at which the superfusate was changed to one containing 10 μM APB is indicated by the first arrow. The cell was hyperpolarized by 25 mV to a potential of about -60 mV. Following a return to the original superfusate, the cell depolarized back to its original membrane potential. Figure 20B shows

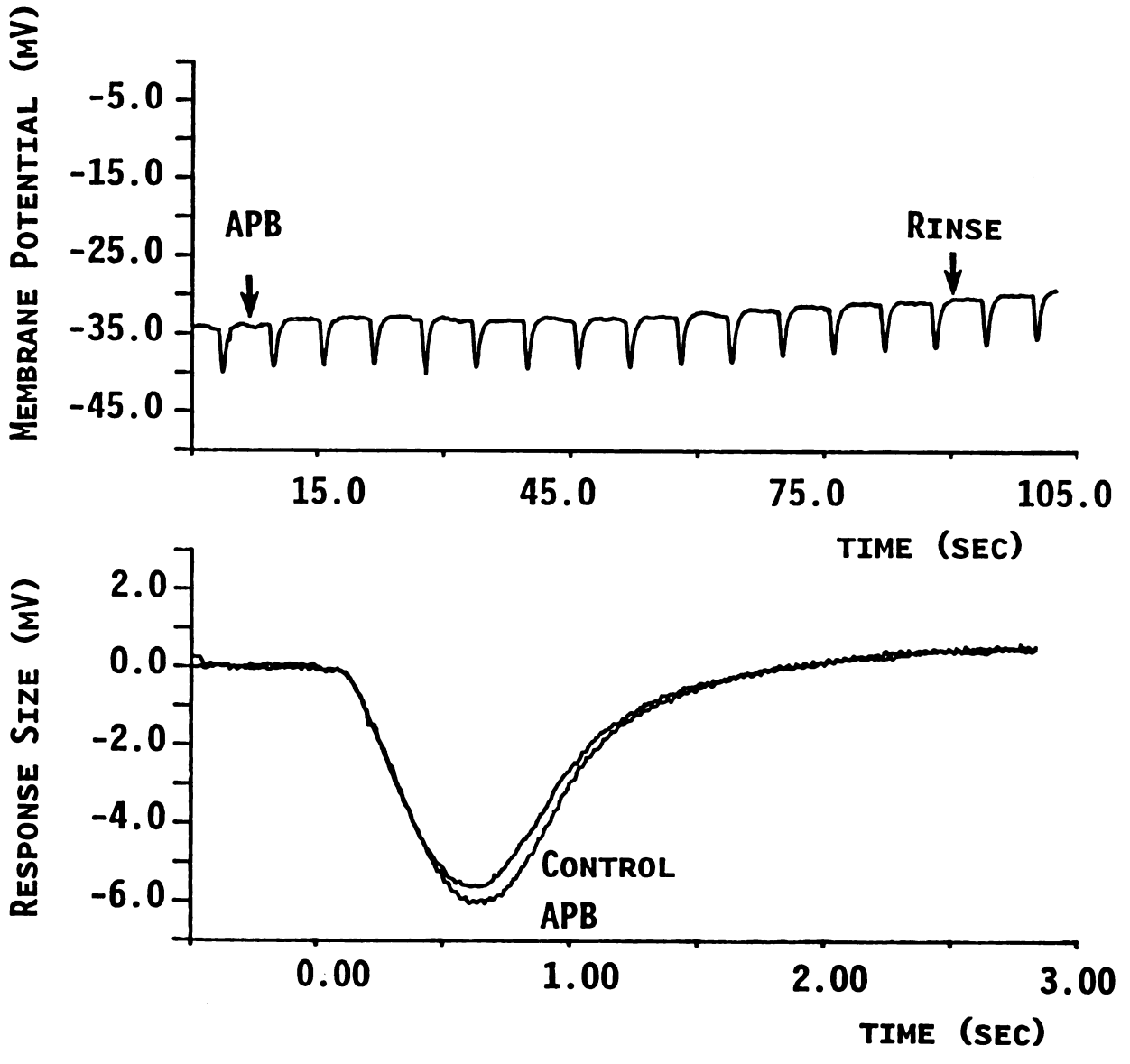
Membrane Potential (mV)
-5.0
-15.0
-25.0
-35.0
-45.0
APB
Rinse
15.0
45.0
75.0
105.0
Time (sec)
Response Size (mV)
2.0
0.0
-2.0
-4.0
-6.0
Control
APB
0.00
1.00
2.00
3.00
Time (sec)

Figure 19. APB has no effect on rod horizontal cells

A: Intracellular recording of a RHC. The downward deflections are responses to a 10 msec flash 550 nm light containing 3.7 photons/μm^2, delivered every 6 seconds. The control solution was switched to one containing 10 μM APB at the time indicated by the first arrow, and then back again at the second arrow. B: The averaged light response during superfusion of control solution is shown on a magnified gain and expanded time base. Average of 5 responses. C: Responses to the same stimulus as in (A) and (B) during superfusion of 10 μM APB. Average of 6 responses. APB had no substantial effect on either light response or membrane potential.

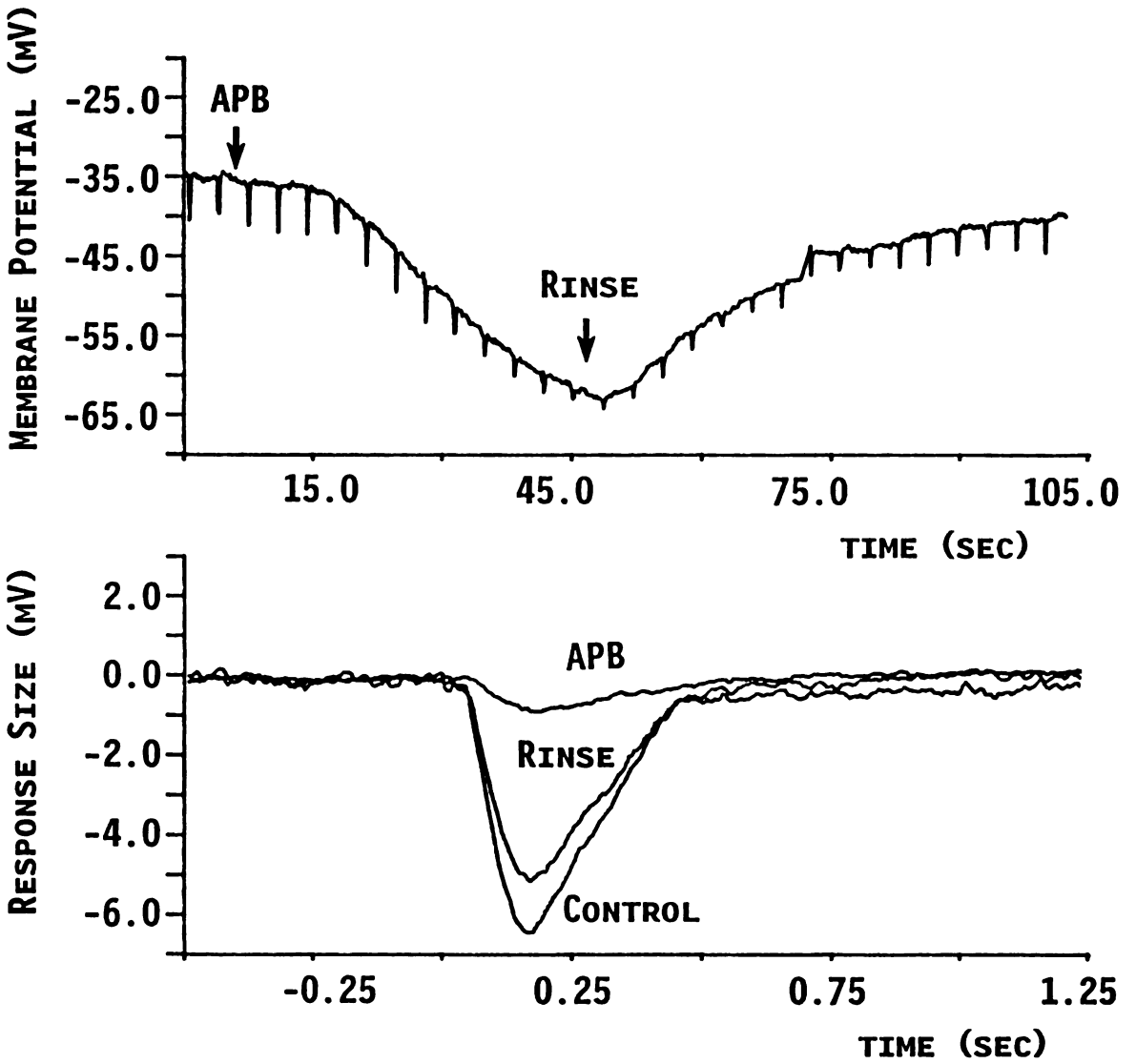
MEMBRANE POTENTIAL (MV)
-25.0
-35.0
-45.0
-55.0
-65.0
APB
RINSE
15.0
45.0
75.0
105.0
TIME (SEC)
RESPONSE SIZE (MV)
2.0
0.0
-2.0
-4.0
-6.0
APB
RINSE
CONTROL
-0.25
0.25
0.75
1.25
TIME (SEC)

Figure 20: Responses of cone-driven horizontal cell are blocked by APB

A: The same experiment as in fig. 2 except that the recording was from a green-sensitive cone-driven horizontal cell obtained from a light-adapted retina. The cell responded to application of 10 μM APB with a hyperpolarization and a reduction in the light response. The effects were reversed upon rinse out of APB.

B: Control responses, both before and after application of APB as indicated. The stimulus was a 10 msec flash of 650 nm light delivering 17,040 photons per μm^2.

C: Response to the same stimulus during application of APB.

that the light response was reduced to one-third of its control amplitude by 10 μM APB. Note that, following rinse-out, the light response did not reach its previous amplitude. Partial recovery such as this was often observed, and might be due to a residual action of APB. The loss of light responses was probably not due to an injury to the cell during superfusion changes since total recovery of the light response was usually seen following application of other drugs such as Co^{2+}. APB had profound effects on synaptic transmission from cones to all of the classes of horizontal cells which we studied.

The light response might have been blocked indirectly as a consequence of some nonsynaptic hyperpolarization of APB, such as through a voltage-dependent channel. Since the light response is thought to have a reversal potential of about 0 mV (Murakami and Takahashi, 1987), the hyperpolarization should increase the driving force for the light response. It seems more likely that the hyperpolarization is due to a block of synaptic transmission. To test this idea, we compared the effects of Co^{2+} and APB on a red-sensitive horizontal cell (figure 21) . After switching to a solution containing 1 mM Co^{2+}, the cell rapidly hyperpolarized and the light response was blocked. Following rinse-out, the solution was switched to one containing 10 μM APB. The cell hyperpolarized to nearly the same potential with a similar time course as in the presence of cobalt, suggesting that APB, like Co^{2+}, blocked synaptic transmission.

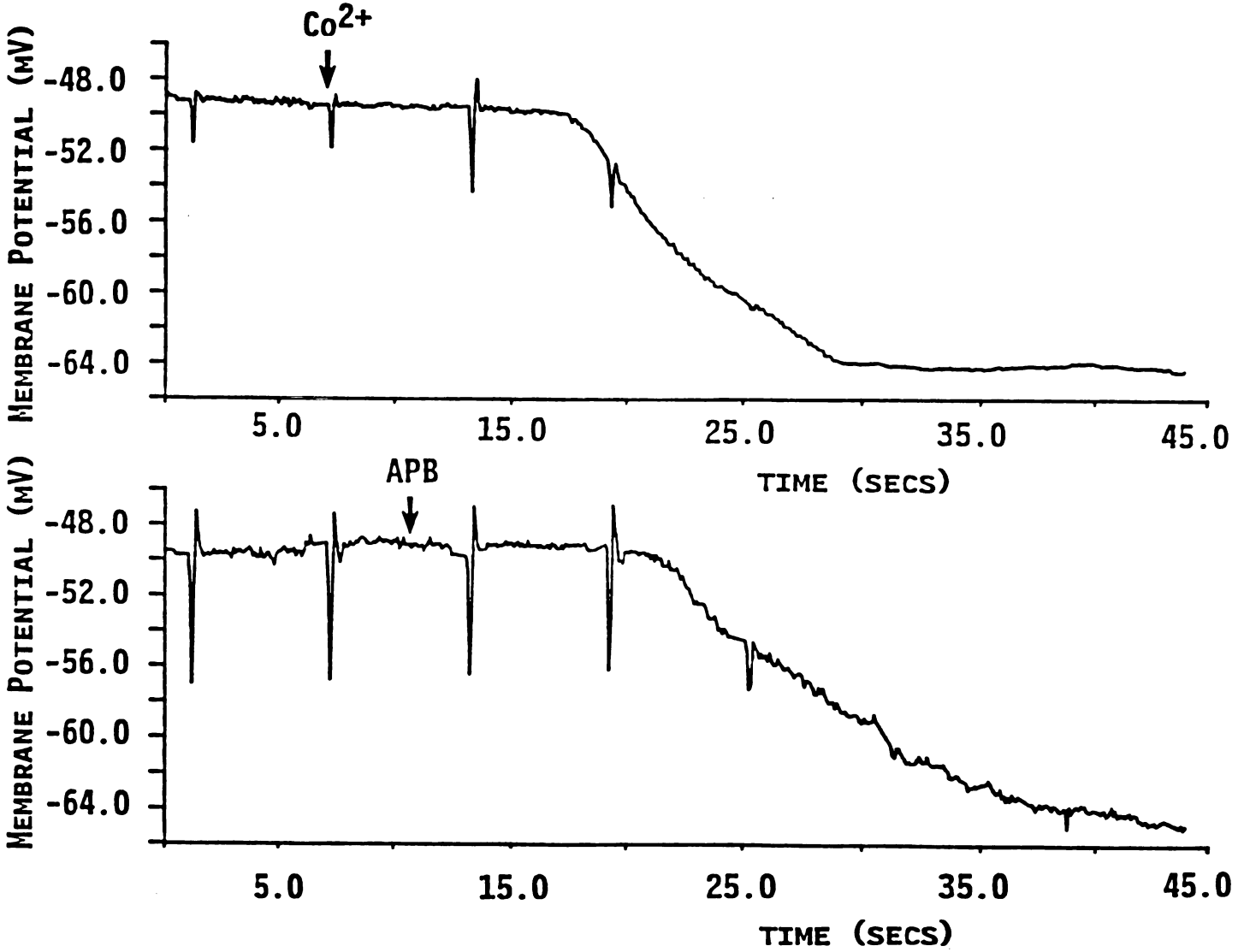
Co2+
-48.0
-52.0
-56.0
-60.0
-64.0
MEMBRANE POTENTIAL (mV)
5.0
15.0
25.0
35.0
45.0
TIME (SECS)
APB
-48.0
-52.0
-56.0
-60.0
-64.0
MEMBRANE POTENTIAL (mV)
5.0
15.0
25.0
35.0
45.0
TIME (SECS)

Figure 21: Cobalt and APB have similar effects

A: Recording from a red-sensitive cone-driven horizontal cell from a light-adapted retina. At the arrow, 10 μM APB was applied. The cell hyperpolarized and the light response was completely blocked. The cell membrane potential and light response recovered following rinse out (not shown). Stimulus was a 10 msec flash of 650 nm light containing 15,207 photons/μm^2.

B: Response of the same cell to application of 1 mM Co^{2+} (arrow) following rinse out of APB. The light response immediately prior to hyperpolarization and thereafter was to a 50 msec flash containing 38,017 photons/μm^2. Following rinse out, the cell recovered once again.

The effects of APB were variable. In some cells, such as the one illustrated in figure 20, APB produced only a partial blockade of the light response. In many cells, as with the one in figure 21, the light response was blocked completely. In several cells, there was no observable effect of APB on the light response, although there was still a reversible hyperpolarization associated with APB. The reason for this variable action of APB is unclear, and did not seem to be correlated with horizontal cell type.

The antagonistic effects produced by NMDA and APB on the cone horizontal cell were similar in appearance, suggesting that they acted through the same mechanism. However, the inability of APB to block rod horizontal cells, in contrast to NMDA, suggested that they may act at different locations. A previous study has demonstrated that NMDA, like other EAA antagonist, can block the actions of exogenously applied kainate as well as the native transmitter (Bloomfield and Dowling, 1985). The ability of APB to block the effects of kainate was therefore tested. Figure 22A illustrates the effect of 7 μM KA on a green cone-driven horizontal cell. Following a slight hyperpolarization, the cell depolarized to about 0 mV, as was demonstrated in figure 17. Following rinse-out, KA was reapplied, along with 10 μM APB, as shown in figure 22B. The action of KA was completely unaffected by APB, depolarizing the cell to the same potential and with a similar time course in the presence and absence of APB. This result strongly suggests that the action of APB is mediated presynaptically.

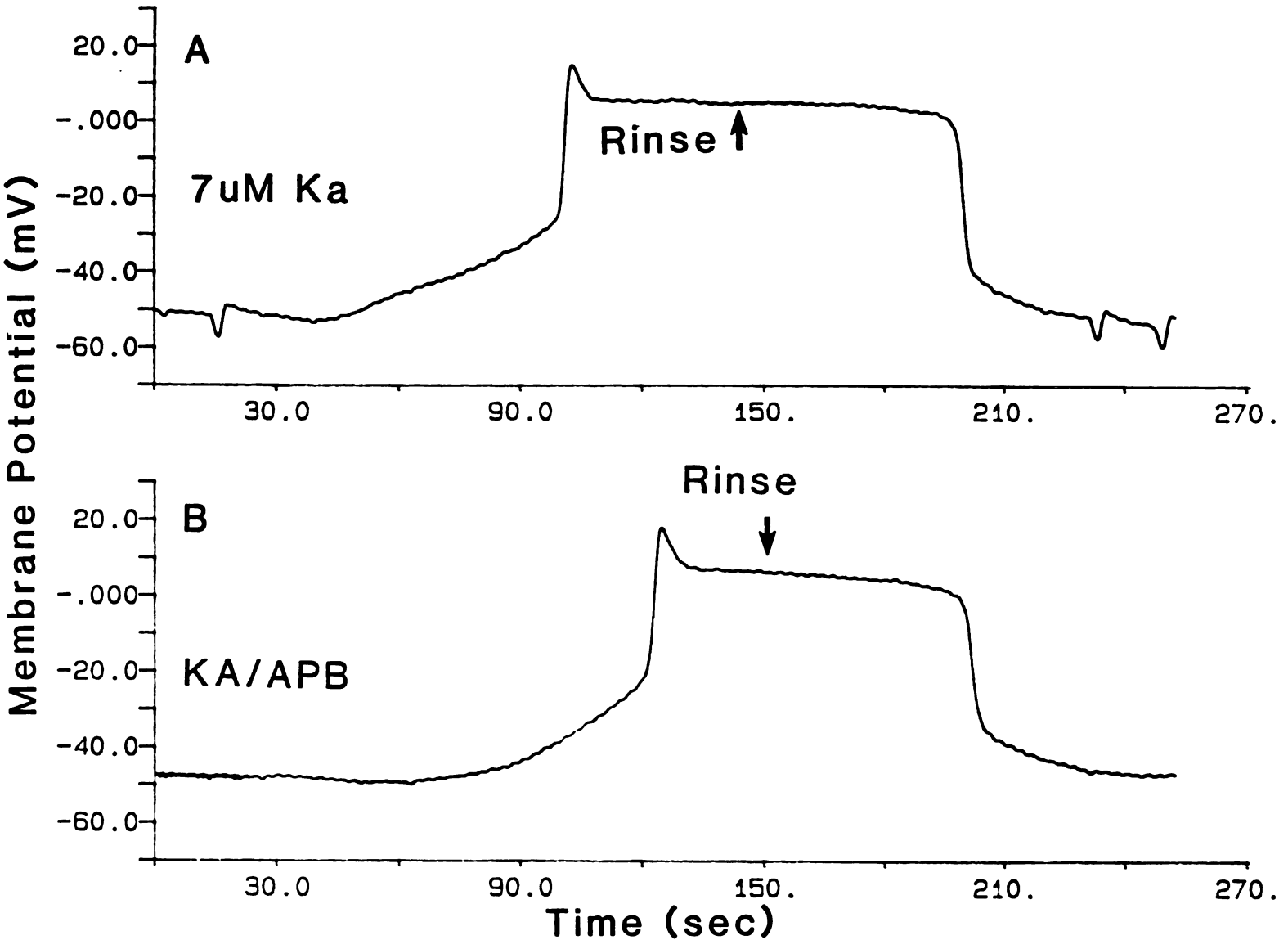
A
7uM Ka
Rinse
B
KA/APB
Rinse
20.0
-.000
-20.0
-40.0
-60.0
30.0
90.0
150.
210.
270.
Membrane Potential (mV)
Time (sec)

Figure 22: APB does not block the effect of KA

A: Response of a red-sensitive horizontal cell. At first arrow, the superfusion solution was switched to 7 μM KA. the cell depolarized slowly and then more rapidly. During this time the light response was nearly blocked (not shown). At the second arrow, the superfusion was switched back to control. Both fig 5A and 5B were constructed using the low-gain recording, since the large changes in membrane potential saturated the high gain records. The records were passed through a 2.5 Hz low-pass filter to remove tape recorder noise. As a result, only several responses in (A) to a 1 second stimulus are visible.
B: Same experiment as in (A), with 10 μM APB added with the KA. Note that the cell is driven to nearly the same potential with nearly the same timecourse in the presence and absence of APB, suggesting that APB has little or no effect on the action of KA.

In order to rule out the possibility that kainate was present in sufficient amounts to saturate the receptors and competitively inhibit the APB, we attempted to repeat the experiments with lower concentrations of KA. Between 1 and 5 μM, KA had little effect on the light response, and often produced a hyperpolarization. This effect of KA has been reported previously (Hankins and Ruddock, 1984), and is thought to be an indirect effect, perhaps mediated through the horizontal cell pathway. Higher concentrations of APB were also used. At a concentration of 100 μM, 50-fold higher than necessary to block the light response and hyperpolarize the CHC membrane, APB did not block the kainate-induced depolarization.

As a further control, we examined the ability of the excitatory amino acid antagonist, kynurenic acid (KYN), to block the response to KA. Fig 23B shows the effect of both APB and KYN on KA, applied in the same cell. At the time indicated by the first arrow, the control solution was switched to one containing both KA and KYN. As expected, KYN hyperpolarized the membrane even in the presence of KA. Following rinse back to control as indicated by the second arrow, the effect was reversed.

One model for a presynaptic action of APB requires only that it hyperpolarize the cone synaptic terminal, thus reducing the rate of transmitter release. The only direct way of testing this hypothesis is to record from the cones. This experiment proved to be technically difficult, as most of the intracellular recordings were lost during the

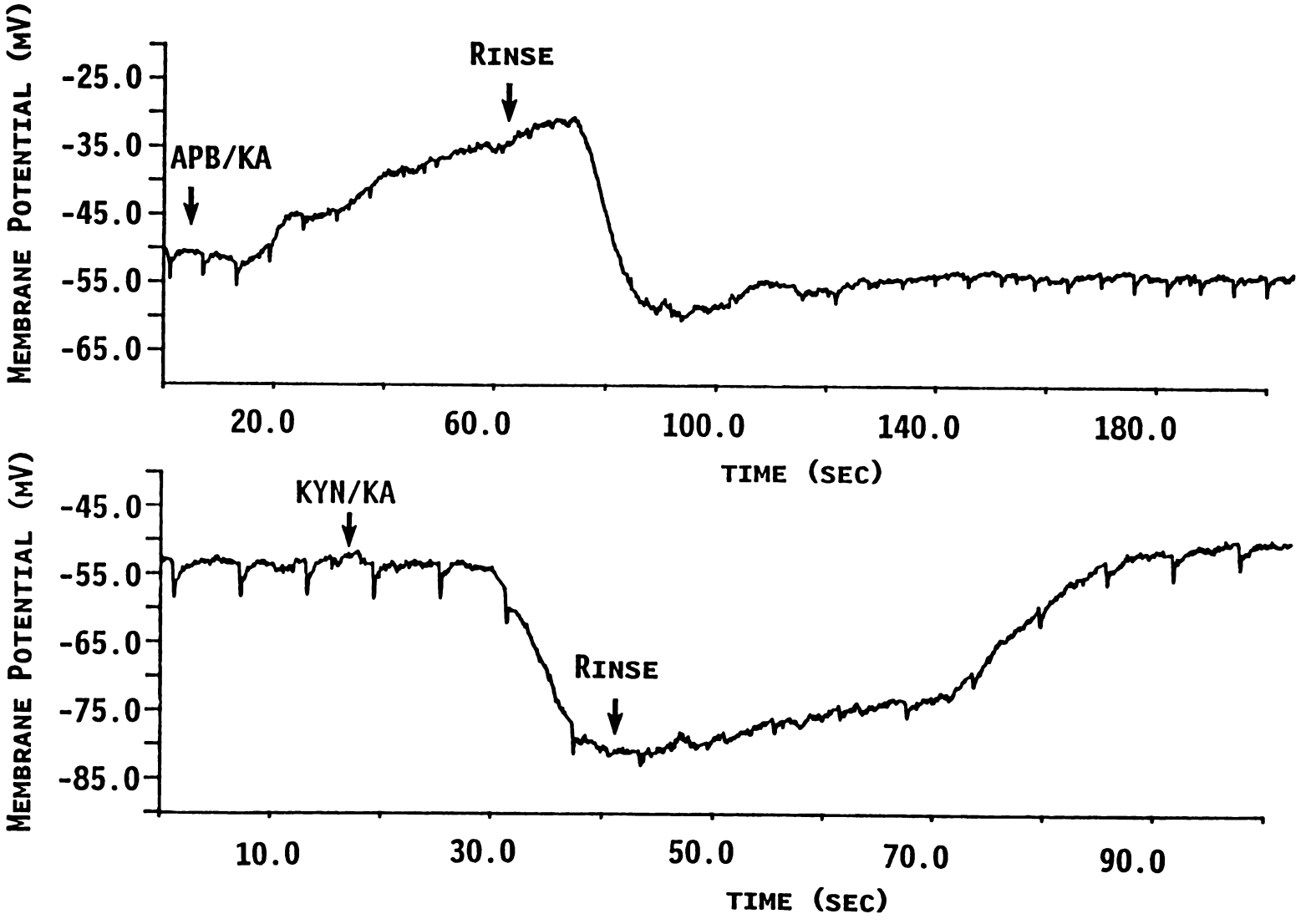
MEMBRANE POTENTIAL (mV)
-25.0
-35.0
-45.0
-55.0
-65.0
APB/KA
RINSE
20.0
60.0
100.0
140.0
180.0
TIME (SEC)
MEMBRANE POTENTIAL (mV)
-45.0
-55.0
-65.0
-75.0
-85.0
KYN/KA
RINSE
10.0
30.0
50.0
70.0
90.0
TIME (SEC)

Figure 23: Kynurenic acid blocks the action of KA

A: Experiment in a horizontal cell which received input primarily from green-sensitive cones. At the first arrow, the superfusion was switched to one containing 10 μM APB along with 10 μM KA. The depolarizing action of KA was unaffected by the addition of APB, as in the previous figure.

B: Response of the same cell to application of kynurenic acid (KYN; 2 mM) along with the kainate. The depolarizing action of kainate is now effectively blocked. Light stimulus for (A) and (B) was a 10 msec 550 nm flash containing 980 photons/μm^2.

switch to the solution containing APB. Therefore, the effect of APB was examined in only 1 cone. Unfortunately, a recording of the cone prior to APB application was not made, although the cell was seen to hyperpolarize in response to APB. Figure 24 shows the effect of APB rinse-out. The cone depolarized, and the light response grew in amplitude, as can be seen by comparing the responses indicated by the arrows. Although results from only 1 cell have been obtained, it is consistent with the proposed of mechanism for the action of APB.

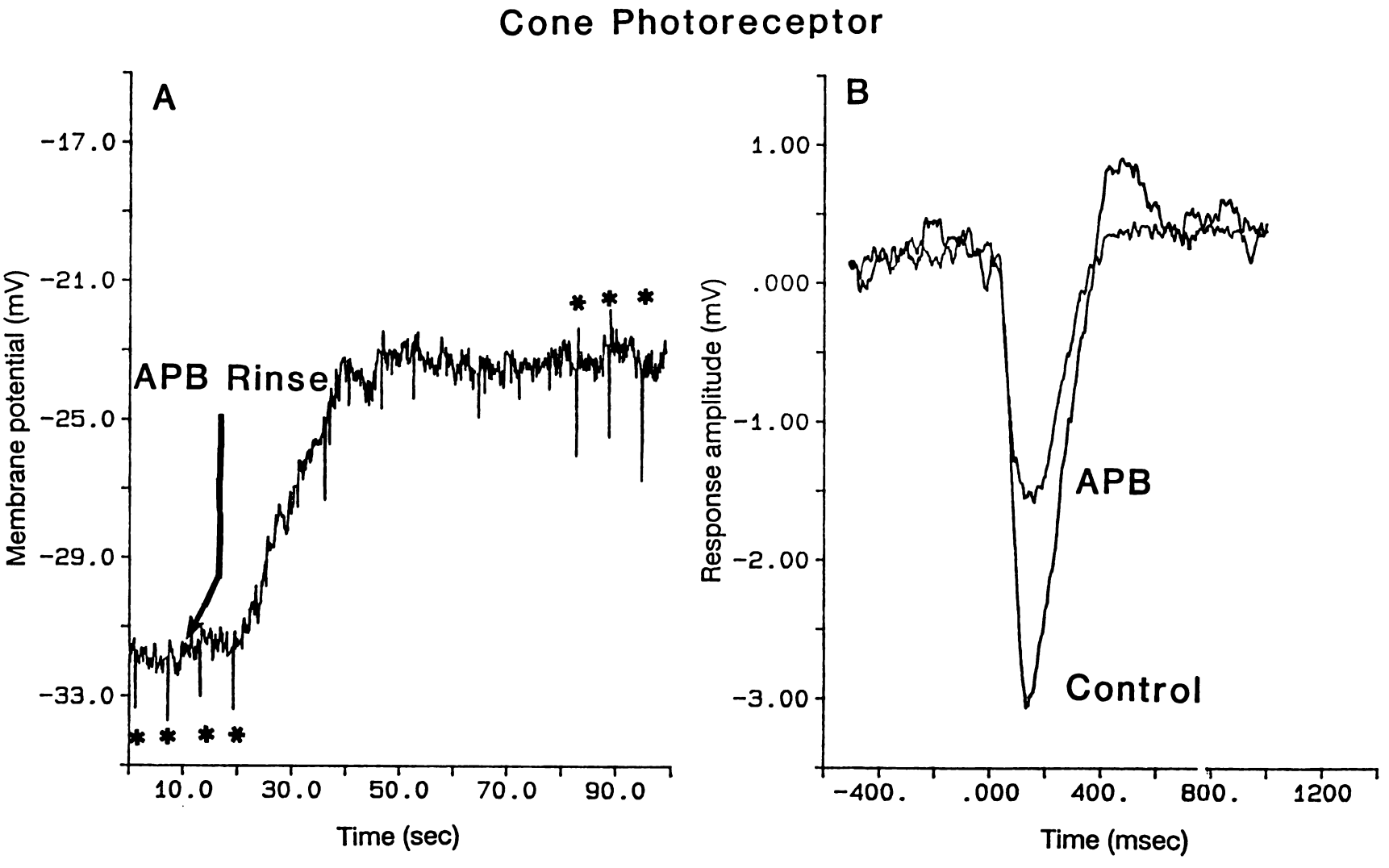
Cone Photoreceptor
A
B
-17.0
-21.0
-25.0
-29.0
-33.0
Membrane potential (mV)
APB Rinse
10.0
30.0
50.0
70.0
90.0
Time (sec)
1.00
.000
-1.00
-2.00
-3.00
Response amplitude (mV)
APB
Control
-400.
.000
400.
800.
1200
Time (msec)

Figure 24: APB acts directly on cone photoreceptors

A: Action of APB on a red-sensitive cone. The cell was identified by its proximity to the surface of the retina, and by its small receptive field. The tape recording was not operating during the onset of the APB effect, so that only the APB rinse-out is shown. The downward deflections are light responses to stimuli of varying wavelength and intensity. Those responses marked by asterisks are to the same stimulus, a 110 msec 650 nm flash containing $7.46X10^4$ photons/μm^2. B: The same responses, averaged and shown at a higher gain.

Cone input to other types of cells

Inhibition of cone transmitter release by APB should result in a loss of cone input to cone depolarizing bipolar cells (CDBCs) as well as horizontal cells. An example of the effect of APB on a CDBC was shown in figure 14 of chapter 2. Although APB blocked the light response in this cell, an indirect mechanism of blockade cannot be ruled out. For example, since the cone transmitter opens channels with a negative reversal potential, the level of hyperpolarization in this cell was great enough to reduce substantially the driving force for the light response, complicating the interpretation of the light response blockade. Figure 25 illustrates the application of 1 μM APB to another CDBC. In this cell, APB did not produce a significant hyperpolarization. It can be seen that APB blocked the light response in this cell as well, as the model put forth in this section would predict. It should be emphasized that the effect of APB on the cone light response is related to the postulated presynaptic effects on cones; mechanistically, it is a separate phenomenon from the postsynaptic effects of APB on the DBC receptor mediating rod input.

The effects of APB on cone-driven ganglion and amacrine cells was also examined. Emphasis was placed on cells which displayed responses at light-off as well as light-on, since these responses are thought to be driven by depolarizing and hyperpolarizing bipolar cells, respectively (Dachaux and Miller, 1976; Thibos and Werblin, 1977). Figure 26 illustrates the action of 4 μM APB on an unidentified cell

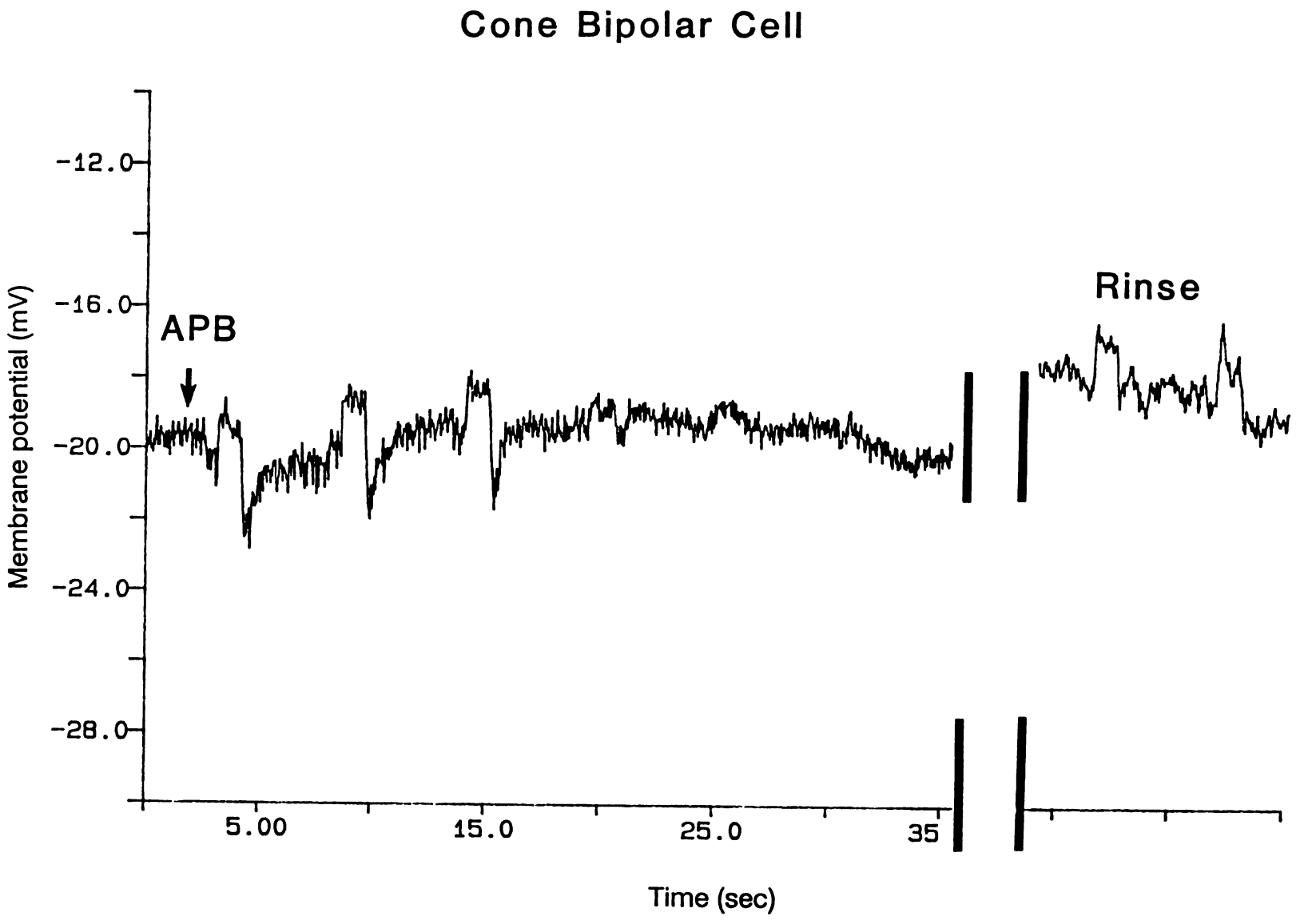
Cone Bipolar Cell
-12.0
-16.0
-20.0
-24.0
-28.0
Membrane potential (mV)
APB
Rinse
5.00
15.0
25.0
35
Time (sec)

Figure 25: APB blocks cone light responses in DBCs, independent of membrane potential.

Response of a CDBC to application of 1 μM APB. The stimulus was a 1 second "flash" of 650 nm light containing $6.73X10^3$ photons/μm^2. The break in the record represents about 2 minutes, during which the APB was rinsed out. Note that APB blocked the light response without hyperpolarizing the cell, demonstrating that the blockade is not due to a removal of the driving force for the synaptic current.

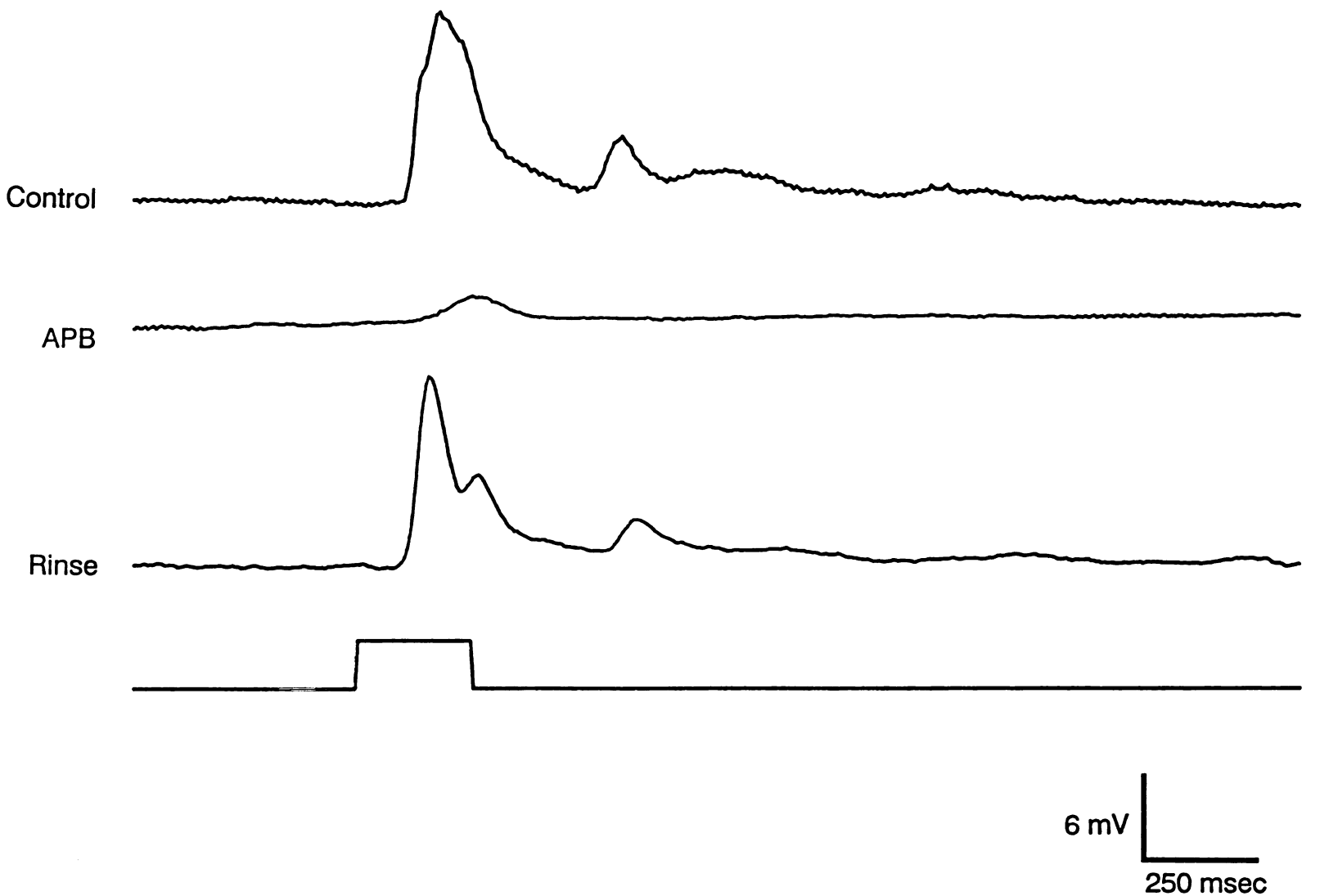
Control
APB
Rinse
6 mV
250 msec

Figure 26: APB blocks the ON and OFF responses of cells in the IPL

A: Response of an unidentified cell type to superfusion of 4 μM APB. The asterisks indicates where the stimulus of 550 nm was increased from $3.57X10^3$ photons/μm^2 to $3.57X10^4$, accounting for the sudden appearance of a light response in the presence of APB. The depolarization associated with APB was probably artifactual, induced by the movement of the electrode in the cell. B,C,D: Average of the light response in (A), shown at higher gain before, during and after application of APB. The light was turned on at 0 seconds on the X-axis, and remained on for 250 msec. Although the OFF response in this cell was not large, it was clearly and reversibly reduced even further in the presence of APB, suggesting that in the light-adapted retina goldfish retina, APB can effect OFF as well as ON pathways.

type in the inner plexiform layer. Application of APB at the time indicated by the arrow produced a depolarization and a reduction in both the on-and off-response to light. The depolarization was not reversible, and most likely was due to movement of the electrode during the solution change.

According to the existing model of APB action, only on-responses are blocked by APB application (Slaughter and Miller, 1981). This was observed in the present study as well, provided that the retina was dark-adapted. In the light-adapted retina, 4 of the 6 cells examined showed a reduction in both components of the light response, while in a single case, only the on response was blocked, and in the sixth cell, there was no clear effect of APB at all. While a precise interpretation of this data is difficult and highly model-dependent, it implies that, in the light-adapted retina, APB can act on the OFF as well as the ON pathway.

Discussion

Specificity of Action

This paper examines the light and pharmacological responses of 2 general classes of horizontal cells in the goldfish retina, one receiving synaptic input from rods and the other from cones. The type of cells yielding light responses in a given retina depended critically on the adaptation state of the retina at the time of isolation: Virtually all of the horizontal cells recorded in the dark-adapted retina were identified by several physiological criteria as belonging to the intermediate horizontal cell thought to be driven exclusively by rods (Stell, 1967; Kaneko and Yamada, 1972), while the majority (but not all) of those cells recorded in the light-adapted retina were believed to be the cone-driven internal and external horizontal cells, first described by Kaneko (1970). In many cases, stable potentials (between -40 mV and -60 mV) were encountered during a pass through the retina. These may have resulted when the electrode entered a cell whose input was rendered inoperative by the adaptation procedure.

The actions of 2 widely used EEA agonists, kainate and NMDA, on both classes of horizontal cells appeared to be identical to their actions in retinae of other species, as kainate depolarized and NMDA hyperpolarized all of the cells tested. While only one previous study has compared the actions of EEAs on both classes of horizontal cell (Massey and Miller, 1987), many studies have demonstrated the agonistic

properties of kainate on either rod- (Shiells et al., 1981; Shiells et al., 1985) or cone-driven (Rowe and Ruddock, 1982; Lasater and Dowling, 1982; Slaughter and Miller, 1983; Bloomfield and Dowling, 1984) horizontal cells. The presence of a kainate-sensitive receptor on both classes of horizontal cell seems clear, and is further supported by the present study.

The action of NMDA is not so clear. Its ability to hyperpolarize horizontal cells and block the light response, as well as its previously reported ability to block the effects of applied kainate (Bloomfield and Dowling, 1984) suggest that it is a postsynaptic antagonist at the kainate receptor. No such inhibition of the kainate/quisqualate receptor by NMDA has been reported elsewhere in the CNS. The disparate actions of NMDA on that receptor, and the one residing on horizontal cells suggests that there may be differences in their basic structure. Such differences might be more easily revealed with the use of patch clamp techniques on isolated cells.

The mechanism of NMDA block seems quite different than that of APB. The action of APB on CHCs but not RHCs might suggest a binding site separate from NMDA, possibly on the postsynaptic receptor. However, since APB cannot block the action of applied kainate, this seems unlikely. A scheme to explain all of the above results in terms of a postsynaptic APB action would require that APB acts at a site which does not bind NMDA or kynurenic acid, and can antagonize the action of

the native transmitter, but not glutamate or kainate. A more parsimonious explanation is that APB acts presynaptically on cones.

The results reported here appear to contradict earlier findings in amphibian (Slaughter and Miller, 1981) and rabbit (Bloomfield and Dowling, 1985; Massey and Miller, 1986) retina, where APB was found to be without effect on all types of horizontal cells. It is not clear if these conflicting results are due to species differences, or perhaps a difference in the experimental procedure, such as the state of adaptation. A few of the cells we tested did not respond significantly to APB, often in retinas which were exceptionally light-adapted. Why adaptation state effects responses to APB, and whether it can account for the results in previous studies is not clear.

APB and presynaptic inhibition

The proposed locations of two APB-preferring receptors in the outer plexiform layer of the goldfish retina is shown schematically in figure 27. One receptor has been shown previously to mediate synaptic transmission from rods to DBC's (Nawy and Copenhagen, 1987), underlying the sign-inverting synapse which forms the on-pathway. The action of APB in the retina was thought to be confined to this synapse. Results in this study describing the antagonistic effect of APB on CHCs has lead us to propose the presence of a second APB-preferring receptor, this one in the cone pathway. Previous studies estimate that a 2-4 mV hyperpolarization in photoreceptors can produce an e-fold decrease in

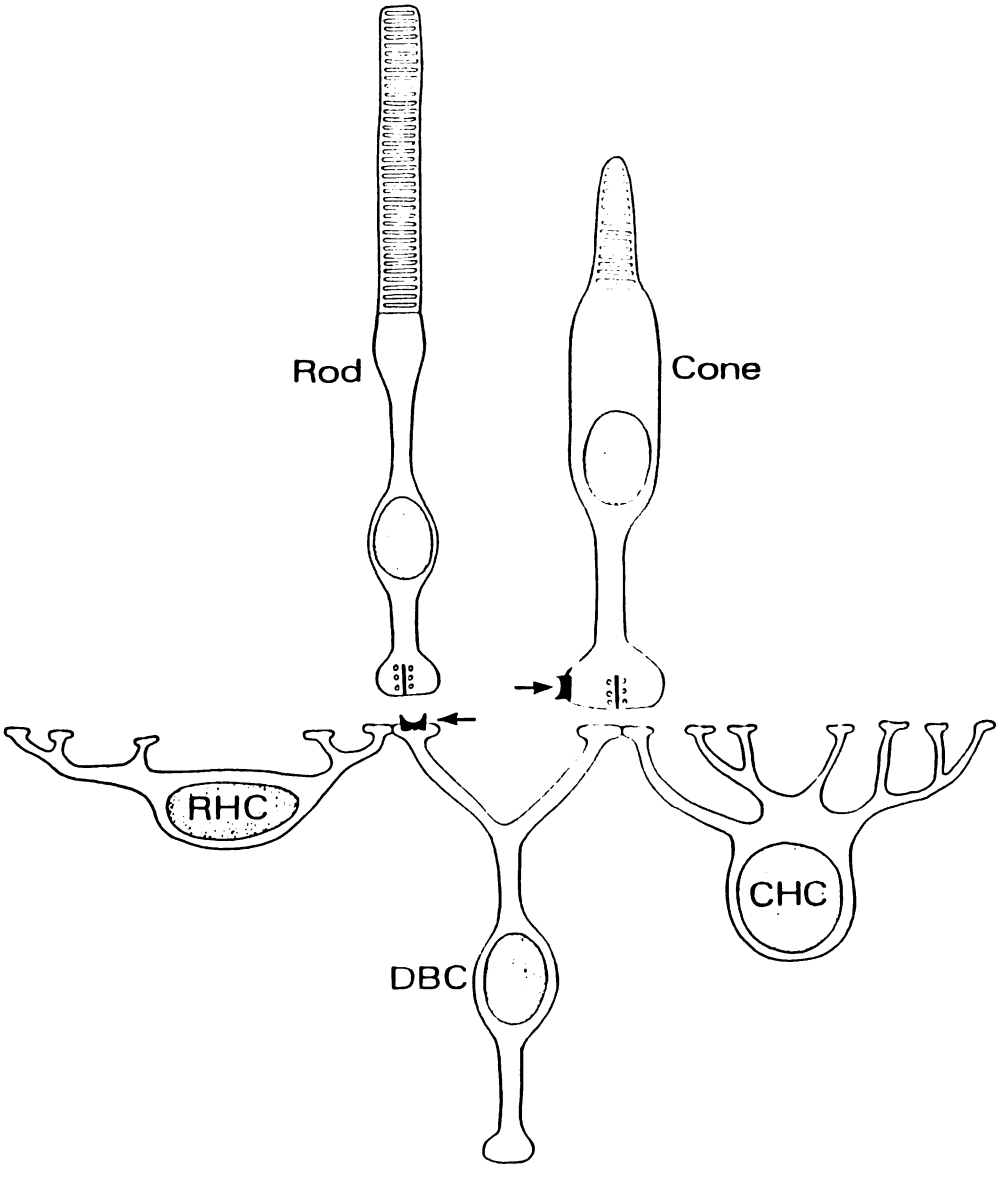
Rod
Cone
RHC
CHC
DBC

Figure 27: Summary of the actions of APB in the goldfish retina

The proposed sites of APB action are illustrated in this schematic representation of the goldfish outer retina. An APB-preferring receptor is located on cones (C) and on depolarizing bipolar cells (DBC) mediating input from rods (R). Both types of horizontal cells are shown as well (CHC, RHC).

transmitter release (Thibos and Werblin, 1977; Belgum and Copenhagen, 1988). Results from one cone presented here show that APB can hyperpolarize the cone membrane by this amount. The location of the electrode, although not precisely known, was probably far from the cone synaptic terminal. It is therefore not known if the membrane near the synaptic terminal was polarized by APB to the same extent (but see Normann and Lasater, 1987).

In DBC's, activation of the APB receptor leads to the closure of channels with a positive reversal potential and thus a membrane hyperpolarization. A model for the inhibition of cone transmitter release therefore does not require any difference in the properties of the two APB receptors, and would predict that they be blocked by the same APB antagonist and gate channels with the same ion selectivity. Both predictions must await further experimentation, particularly in light of the fact that an APB antagonist has yet to be developed.

An antagonistic action of APB in many regions of the CNS has been reported (see Mayer and Westbrook, 1987 for review), including the spinal cord (Davies and Watkins, 1982; Evans et al., 1982) olfactory cortex (Hori et al., 1982; Ffrench-Mullen et al., 1986) and hippocampus (Dunwiddie et al., 1978; Koerner and Cotman, 1981; Harris and Cotman, 1983). Several of these studies addressed the issue of pre vs. postsynaptic inhibition. Using the isolated frog and rat spinal cord, Evans et al. (1982) found that APB blocked the response of dorsal horn neurons to stimulation of the dorsal root, but did not block the effects

of applied NMDA, kainate or quisqualate, suggesting that the action of APB was presynaptic. In the hippocampal slice, Harris and Cotman (1983) used a much different technique, comparing the effect of APB and KYN on paired pulse potentiation, to reach the same conclusion. Other studies are less clear-cut: In olfactory cortex, APB blocked the monosynaptic activation of pyramidal cells, as well as the responses to applied NMDA and KA, but not glutamate or aspartate (Hori et al., 1982). Ffrench-Mullen et al. similarly suggest that APB acts postsynaptically since the field potential they recorded contained a presynaptic component following postsynaptic blockade with APB. Such inconsistencies between studies may reflect the inherent difficulty of interpreting results without benefit of intracellular recordings, or the ability to stimulate individual presynaptic pathways.

The mechanism of presynaptic action of APB proposed here for the retina (i.e., hyperpolarization of the presynaptic cell) is also consistent with the effects of APB reported elsewhere in the CNS. While future experiments may uncover regional differences in receptor function, a single conductance change seems able to account for the known effects of APB in the vertebrate CNS, including its agonist action on DBCs, bringing the retina closer in line with other regions of the brain by eliminating the need for postulating a unique type of APB receptor in the retina.

Chapter 4

ANALYSIS OF VOLTAGE FLUCTUATIONS IN THE MEMBRANE OF ROD-DRIVEN DBCS

Introduction

A knowledge of conductance changes produced by the native photoreceptor transmitters and glutamate was a crucial step in sorting out the actions of glutamate on goldfish DBCs. Two other useful parameters for describing the action of a transmitter are lifetime and conductance of the channels gated by the transmitter. Once obtained, these values would provide an additional basis for the comparison of rod and cone pathways as well as the actions of putative transmitters such as glutamate. The only direct way of obtaining this information is by recording the transmitter-evoked single channel currents with the cell-attached mode of the patch clamp on DBCs in a retinal slice, a difficult and perhaps unfeasible technique for the goldfish retina. An indirect approach is to analyze small fluctuations in membrane voltage produced by the activation of a population of transmitter-gated channels, a technique pioneered at the neuromuscular junction (Katz and Miledi, 1972; Anderson and Stevens, 1973). Kinetic analysis of fluctuations in membrane voltage (noise) has also been used in bipolar cells of the turtle (Ashmore and Copenhagen, 1980; 1983) and dogfish (Ashmore and Falk, 1982) to make estimates of the lifetime of channels gated by the photoreceptor transmitter, and to calculate the size of the event produced by the arrival of a quantum of transmitter.

I initially proposed to analyze membrane noise in the dark-adapted (rod-driven) and light-adapted (cone-driven) DBC in order to estimate the kinetics and conductance of channels gated by both the rod and cone transmitter within a single cell. I also proposed to examine the fluctuations produce by application of putative transmitters, analogous to the conductance experiments described earlier. Calculation of transmitter-gated channel parameters based upon analysis of voltage noise is dependent upon a number of assumptions, one of which is that the noise power is a function of transmitter concentration, and that changes in membrane voltage do not alter the noise (other than by changing the driving force of ions which flow through the transmitter-gated channel). A second assumption is that the rate-limiting step of ligand-induced changes in membrane potential is the lifetime of the ligand-sensitive channel, and that the lifetime is longer than the membrane time constant. Evidence presented in this section suggests that both assumptions are incorrect: voltage noise in goldfish DBCs is controlled by and membrane potential rather than transmitter concentration. Furthermore, application of putative transmitter and transmitter analogs does not produce any direct change in voltage noise, suggesting that the rod transmitter-gated channel kinetics are too rapid to be resolved with microelectrodes in a non-voltage-clamped cell.

Results

The membrane potential of rod-driven DBCs often fluctuated spontaneously at the dark resting potential. The fluctuations were reduced during presentation of a steady light background, and were often completely absent at saturating intensities, generally above 100 photons/$\mu m^2 \cdot$sec. The fluctuations were also eliminated by application of 1 mM Co^{2+}, a concentration which was sufficient to block light responses in both bipolar and horizontal cells, presumably by suppressing transmitter release from photoreceptors. These results are illustrated in figure 28, which shows a series of voltage records from one cell, the first in darkness, the next two during the presentation of steady backgrounds, and the last in the presence of 1mM Co^{2+}. Since transmitter release from rods is maximal in the dark, and minimal during application of bright backgrounds and cobalt, the data would suggest that the amplitude of the noise is loosely correlated with transmitter concentration.

The fluctuations could also originate in the rods and be faithfully transmitted through the synapse to the DBC. Although this possibility could be tested directly by recording from the rods, this is not possible in the goldfish retina because of the rod's small size. However, studies of membrane fluctuations in rods of the toad (Baylor et al., 1980) reveal two types of fluctuations which are both suppressed during the response to bright light. One type of fluctuation is a discrete event occurring approximately once every 50 seconds and is

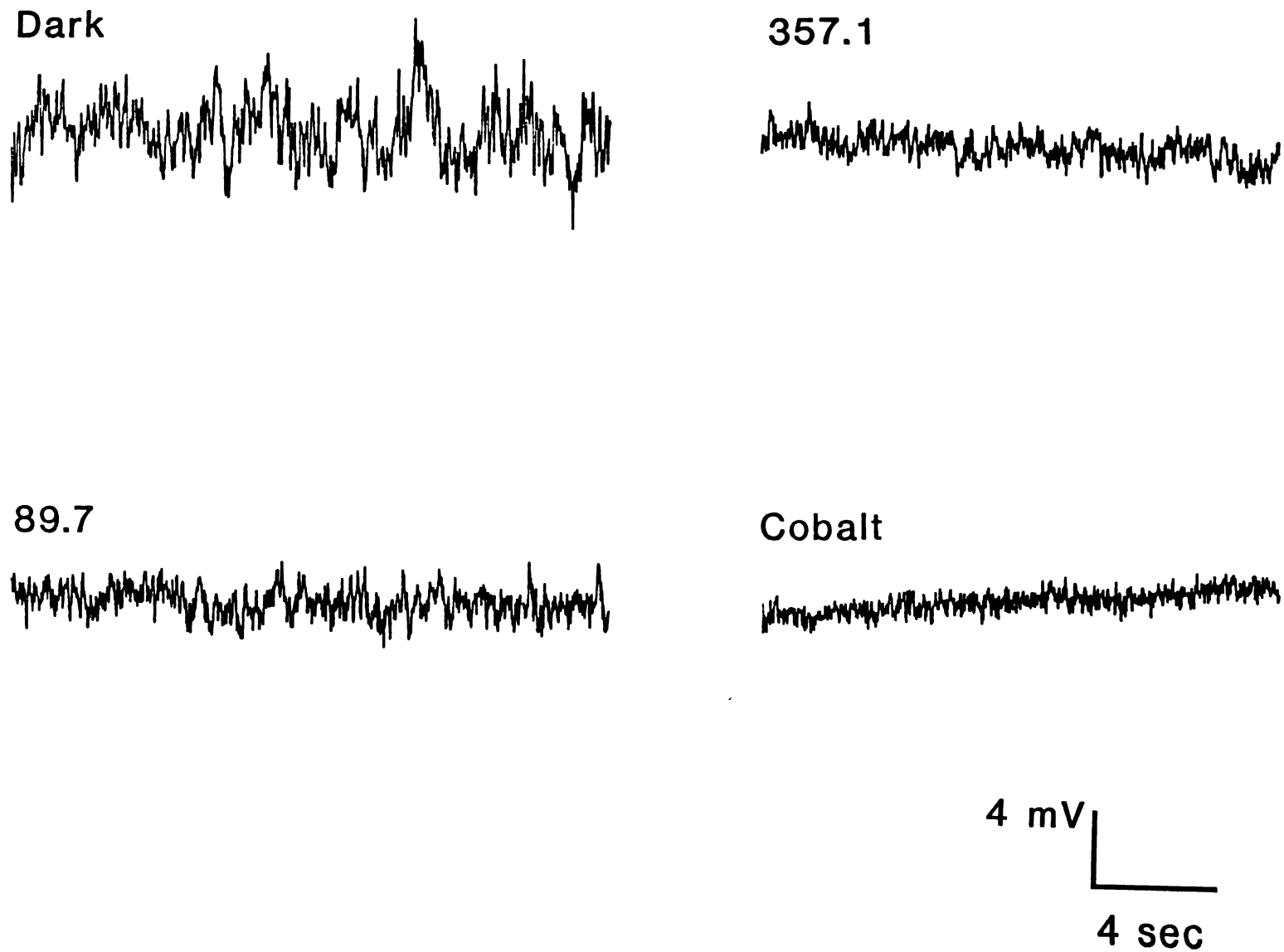
Dark
357.1
89.7
Cobalt
4 mV
4 sec

Figure 28: Voltage noise vs light intensity.
Continuous 20 second records of the same cell in darkness, in the presence of 2 steady backgrounds, and with 1 mM cobalt. Numbers refer to the photon flux (photons/$\mu m^2 \cdot$sec) of wavelength 550 nM. Noise is suppressed with increasingly bright backgrounds, and is completely abolished by cobalt.

clearly not seen here. Figure 29 compares the spectrum of the second noise component seen in toad rods with the difference spectrum of the light-suppressed noise in DBCs. The latter spectrum was obtained by subtracting the Fourier transform of continuous records obtained during presentation of bright backgrounds from the Fourier transform of records obtained in the dark. Comparison of the toad rod and goldfish DBC spectra demonstrate that the fluctuations in rods are much too slow to account for the noise seen in DBCs. Both spectra can be modeled as the product of lorentzians (low-pass filters), but the time constant of the rod lorenztian is on the order of 1 second, versus about 30-50 msec for the DBC. While it is possible that these data reflect differences in kinetics of toad and goldfish rod noise this seems unlikely, since, as will be demonstrated next, the fluctuations in the DBC can be altered directly, without acting through the rods.

Interpretations of the effects of light on voltage noise are complicated by changes in DBC membrane potential as well as transmitter concentration. In order to control for effects of membrane potential changes, it would be desirable to voltage-clamp the cell during the light response. However, the small diameter of DBCs (_8μm) required that high resistance microelectrodes be used in this study, preventing the use of single electrode voltage clamp. Instead, steady current was passed across the electrode and cell membrane in the current clamp mode during presentation of continuous light in order to repolarize the cell back to the dark potential. If the amplitude of the noise is governed by changes in transmitter levels alone, repolarization of the cell

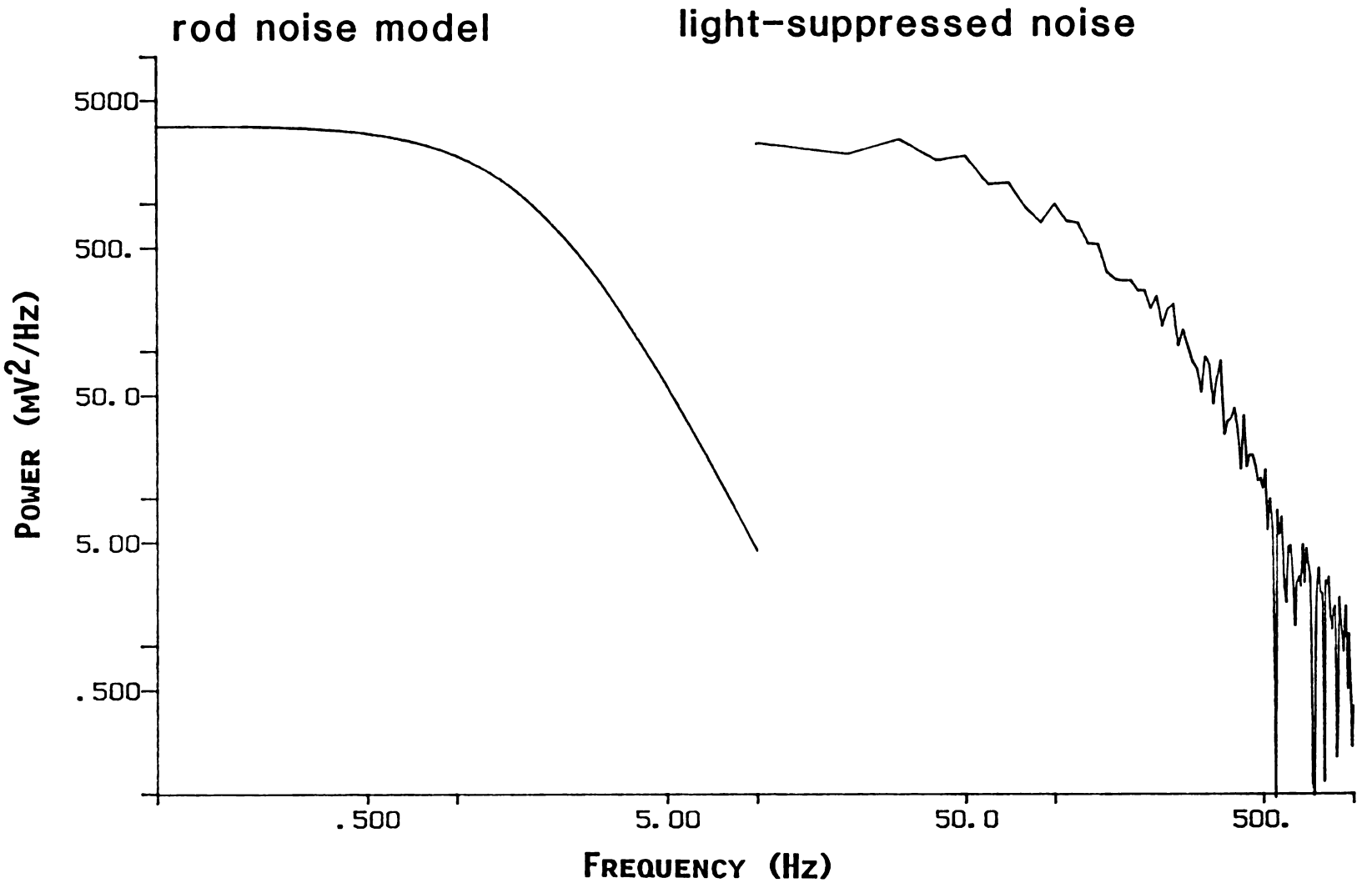
rod noise model
light-suppressed noise
5000
500.
50.0
5.00
.500
POWER (MV2/HZ)
.500
5.00
50.0
500.
FREQUENCY (HZ)

Figure 29: Power spectra of pre- and postsynaptic noise.

The power spectrum of the noise removed by bright steady backgrounds is plotted on the right. Records from the cell in figure 28 were filtered with an 8-pole Butterworth filter at 200 Hz and digitized at a sampling rate of 2 msec. Fast Fourier transforms of 1024 point records were performed and the resulting power spectra averaged. The averaged (at least 20) spectra of recordings obtained in light were subtracted from spectra of recordings obtained in darkness to yield the difference spectrum shown here. Left side: Model of the "continuous noise" observed by Baylor et al. in toad rods is plotted on the left according to the following equation: $S(f)=S(0)/(1+(2\pi f/\alpha)^2)^2$, $\psi\theta\epsilon\sigma\epsilon$ α is equal to 1.22 sec^{-1} and S(0) is the zero frequency asymptote. Note that the events depicted in the rod spectrum are about 100 times slower (i.e., roll off at lower frequencies) than the DBC events, suggesting that the DBC events originate postsynaptically.

membrane should have little effect. Figure 30 demonstrates an example of this experiment. The cell was initially depolarized with a steady background, and the noise was suppressed. While the light remained on, the membrane was repolarized towards the dark potential with extrinsic current. The current was able to restore the noise even in the presence of steady backgrounds. While a small amount of the noise increase was contributed by the electrode, it possessed different kinetics than the biological noise, and was too small to account for the large overall increase. This experiment demonstrates that the voltage noise is dependent upon DBC membrane voltage rather than amount of transmitter released by the rods.

In an effort to determine the type of voltage-dependent channel(s) that created the noise, the variance of the noise as a function of membrane potential was measured. This information would be useful for determining the potential at which the channel is activated, thus providing a clue to its identity. Technical limitations restricted the range over which the cell could be polarized. The high electrode resistance (usually between 700 MΩ and 1000 MΩ) limited the amount of steady current which could be passed through the electrode without introducing extraneous noise to about 0.15 nA. For a cell with an input resistance of 100 MΩ, this would correspond to a 15 mV polarization from rest. In order to obtain as wide a range as possible, cells were hyperpolarized from rest with as large an amount of current as possible, then depolarized with non-saturating (see below) intensities of light and then depolarized even further with current. This procedure yielded

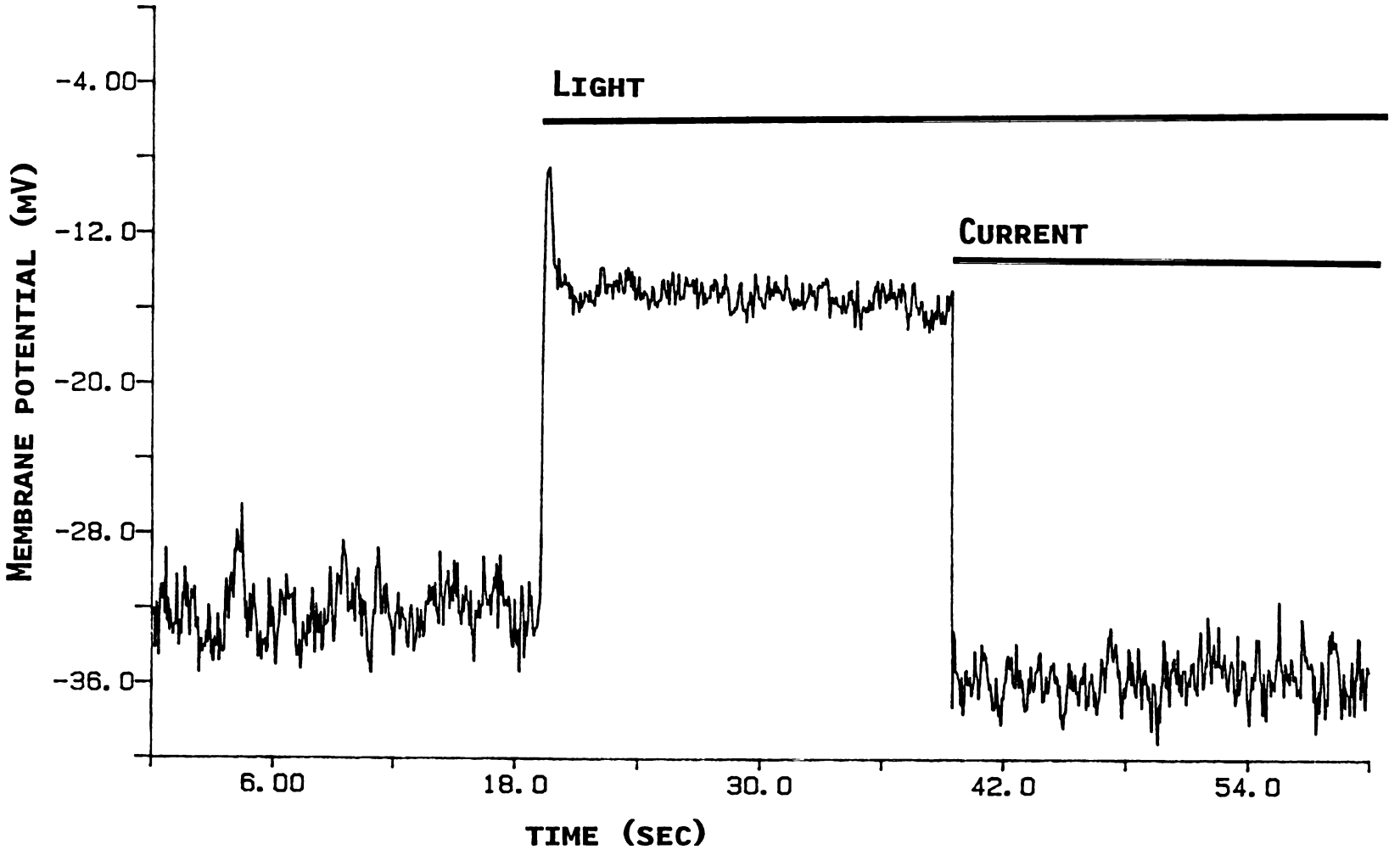
LIGHT
CURRENT
-4.00
-12.0
-20.0
-28.0
-36.0
MEMBRANE POTENTIAL (mV)
6.00
18.0
30.0
42.0
54.0
TIME (SEC)

Figure 30: Light-suppressed noise is restored with current.
The solid line at the top indicates the time at which a steady 550 nM light of about 900 photons/$\mu m^2 \cdot$sec was turned on. Note the decrease in noise. The lower solid line indicates the time during which a steady current of -0.1nA was injected into the cell. Although the record indicates that the cell was polarized past the original dark potential, this is probably an overestimate as the bridge was slightly underbalanced. Given an input resistance of 110 Mohms, estimated from the light current voltage relations, the true membrane potential during current injection was about -28 mV.

a range of about 40 mV over which the variance could be measured . Figure 31 shows an example of the result from one cell. The variance reached a maximum near -40 mV (near the dark potential) and then declined, reaching a variance minimum which was just above the variance of the electrode alone at -25 mV. Although this cell could not be hyperpolarized past -45 mV, results from other cells show that the variance also reaches a minimum at about -55 mV. According to the simplest interpretation of these results, the channels would be open about one-half of the time at the variance maximum. The variance minima at -55 mV and -25 mV would result either from the channels being continuously open or closed, or as the reversal potential for the permeant ions is approached.

Additional information about the identity of the channel came from pharmacological experiments with tetraethylammonium (TEA^+), which blocks K^+ channels, and Co^{2+}, which blocks Ca^{2+} channels. TEA^+ reversibly blocked the noise at concentrations as low as 200 μM. There was little or no change in the resting conductance or membrane potential associated with the action of TEA^+, suggesting that the channels producing the noise may have relatively little effect on the electrical properties of the cell at rest (i.e., in the dark). Results with Co^{2+} have already been illustrated in figure 28. Although part of cobalt's action is to block transmitter release presynaptically and depolarize the DBC, a postsynaptic action is indicated by experiments using current to repolarize the membrane back to the dark potential. Unlike experiments with steady backgrounds described earlier, current was unable to restore

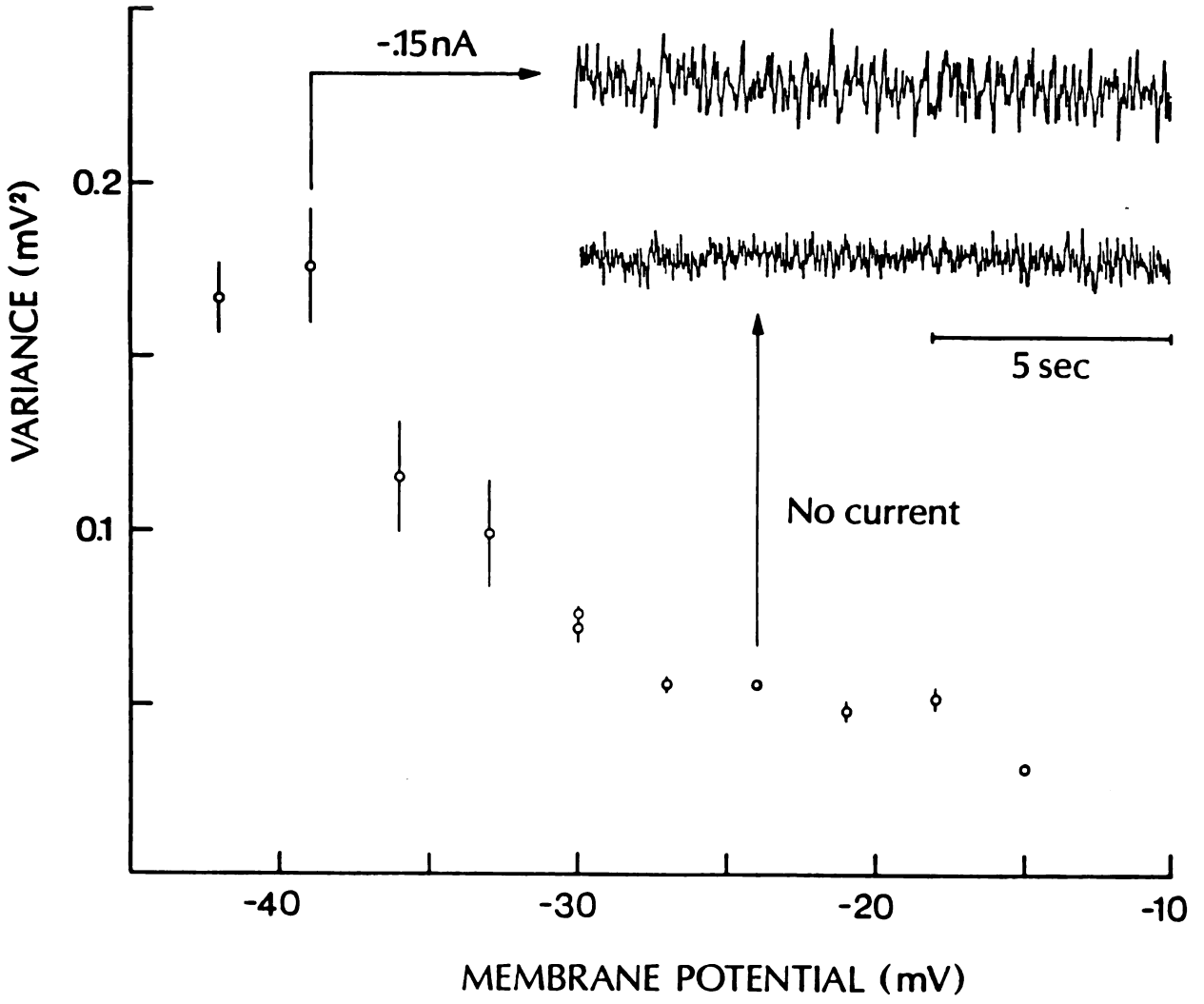
-.15nA
0.2
0.1
VARIANCE (mV²)
5 sec
No current
-40
-30
-20
-10
MEMBRANE POTENTIAL (mV)

Figure 31: Voltage variance as a function of membrane potential.
The cell was depolarized and hyperpolarized from rest with varying amounts current for approximately one minute. Data was filtered and digitized as in fig. 29 and displayed on an oscilloscope along with two vertical cursors set 128 points apart. The cursors were moved along the record and the variance of the noise between them was measured and stored, along with the average membrane potential. The variance as a function of membrane potential was than plotted. Vertical lines on dots indicate standard deviation. Cell could not be hyperpolarized further without introducing significant electrode noise. Inset: Sections of the raw records of the cell at rest and during injection of steady -0.15 nA current which were used to construct two of the data points.

any of the voltage noise which was blocked by Co^{2+}. The ability of both TEA^+ and Co^{2+} to block the noise suggests that the channel which produces the fluctuations may be a calcium-activated potassium channel (K^+_{Ca}). In several experiments apamin and charybdotoxin, specific blockers of different types of K^+_{Ca} conductances, had no effect on the voltage noise. The pharmacological data, together with the maximal variance data suggest that the voltage-sensitive noise may arise from a K^+_{Ca} channel which begins to activate at about -55 mV and is fully activated by about -30 mV. Furthermore, the stability of the noise over time predicts that the channel does not inactivate substantially at the membrane potentials examined here.

The noise-producing channel might play a role in shaping the time course of the light response. In order to test this possibility the response in control solution and solution containing 500 μM TEA^+ were compared. Figure 32 shows that in the presence of TEA^+, the flash response was delayed by about 100 msec, but was otherwise unchanged. Since TEA^+ was added from the outside, a change in the shape of the flash response might result from a direct action of TEA^+ on rods. Although TEA^+ does act on rods, blocking a potassium and producing spontaneous calcium-dependent action potentials (Fain et al., 1977), it is not reported to have any direct action on the rod light response (Fain and Quandt, 1980). Never-the-less, a presynaptic action cannot be ruled out.

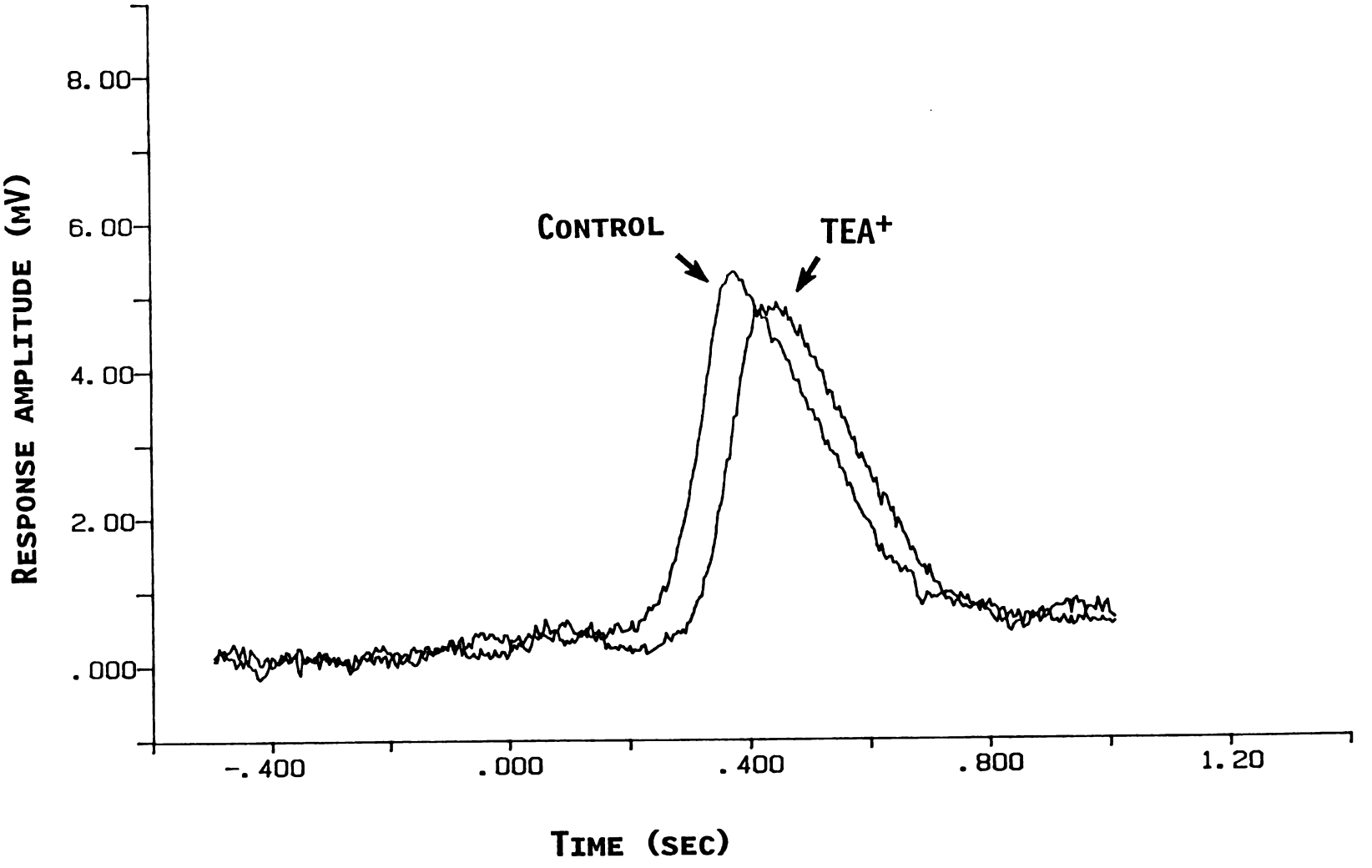
8.00
6.00
4.00
2.00
.000
RESPONSE AMPLITUDE (MV)
CONTROL
TEA+
-.400
.000
.400
.800
1.20
TIME (SEC)

Figure 32: Effects of TEA+ on flash response.

Response of a DBC to a 10 msec flash of 550 nM light containing 0.90 photons/μm^2 in control solution and solution containing 500 μM TEA. The flash was presented at time 0. Control is the average of 9 responses, while TEA^+ is the average of 4 responses. The effect was reversible. The time course of the response under both conditions are similar, with the response in TEA^+ shifted to the right.

These experiments do not rule out the possibility that there is a ligand-sensitive noise source which is swamped by larger voltage-dependent noise. This noise might be revealed if the voltage-dependent channel is blocked and glutamate, or a glutamate analog is applied to the cell. Unfortunately, glutamate, kainate, NMDA and APB produced no noise increase when applied in the presence of cobalt. These ligands were therefore added in the absence of cobalt to determine if they had any effect on the existing noise. Under these conditions, two general results were obtained. At concentrations below saturation (<2μm for APB, <2mM for glutamate, every concentration used for NMDA and kainate) the effects on noise seemed minimal: The existing noise was unaffected, and no new component was seen. With concentrations of APB and glutamate which were high enough to block the light response, the noise was completely blocked, an effect which was not due to the hyperpolarized membrane potential, since the noise could not be restored with depolarizing current.

Discussion

Rod-driven bipolar cells exhibit fluctuations in membrane voltage at their resting potential in the dark. Results described in this chapter demonstrate that these fluctuations can be reduced or completely blocked with a number of procedures, such as presenting a bright background, changing the membrane potential with extrinsic current, or adding TEA^+ or cobalt to the superfusion medium.

While all of these results are consistent with the idea that the fluctuations arise from the activity of voltage-dependent channels, they do not positively identify the type of channel(s). The simplest hypothesis, based upon the blocking action of cobalt and TEA^+, is for a Ca^{2+}-activated K^+ channel. However, the plots of variance vs mean, which were used to estimate the fraction of open channels as a function of voltage, are inconsistent with estimates of the voltage dependence of Ca^{2+}-activated K^+ channels in several previous studies. On the basis of these plots one might predict that the channels begin to open between -55 mV and -60 mV, and are fully activated by about -25 mV, with one-half of the channels being open at about -40 mV. A calcium-activated potassium conductance measured with whole-cell patch-clamp in isolated bipolar cells (Kaneko and Tachibana, 1985) was not observed until the membrane was depolarized to -10 mV. In a detailed study of K^+_{Ca} channels in excised patches of rat muscle (Barrett et al., 1982), the authors varied both intracellular Ca^{2+} and membrane potential and measured the percentage of time which the channels were open. Taking

into account the voltage at which the channels begin to open and are open one-half of the time, no concentration of Ca^{2+} gives an adequate fit to the present data. For example, they found that an intracellular Ca^{2+} concentration of about 10μm was required to open a significant fraction of channels at -50 mV, but at such high Ca^{2+} levels, the percent of open channels as a function of membrane potential is very shallow, such that the channels are not open 50% of the time until about 0 mV. At a lower concentration (1μm) of inside Ca^{2+}, the function is steeper, as required by the present model, an e-fold increase in the amount of open channel time produced by a 15 mV depolarization. Unfortunately, at this concentration, the channels do not begin to open until about 0 mV.

There are several possible explanation for these discrepancies. The absence of cytosolic compounds in the study of Barret et al. may change the behavior of the K^+_{Ca} channel. However, similar results in intact-cell preparations of *Aplysia* (Gorman and Thomas, 1980) and goldfish bipolar cells (Kaneko and Tachibana, 1985), make this unlikely. Measurement of K^+ tail currents in hair cells suggest that the K^+_{Ca} channel begins to open at about -50 mV, and is fully opened at about -30 mV (William Roberts, personal communication), in agreement with the present results. The measured voltage dependence of K^+_{Ca} may be more a function of the voltage-dependence of calcium entry than of the K^+_{Ca} channel itself. In order to unambiguously determine the noise source, whole-cell patch clamp recordings in the slice preparation would be required. In this configuration, current fluctuations could be analyzed

as a function of membrane potential while the cell is internally perfused with channel blockers such as TEA^+ and cesium.

The only argument against a purely voltage-dependent noise source is the observation that saturating levels of APB and glutamate block the noise in a voltage-independent manner. One interpretation of these results is as follows: If the APB-gated channels are permeable to Ca^{2+}, as the NMDA channel is (MacDermott et al., 1986; Mayer et al., 1987), then a substantial component of the Ca^{2+} current flowing into the cell and activating the K^+_{Ca} channels would enter through the APB channel. High levels of APB or glutamate would close all of the channels, reducing the Ca^{2+} current, and turning off the K^+_{Ca} channel.

Whatever the source of the noise, it clearly is not useful for defining parameters of synaptic transmission such as transmitter-gated channel conductance or lifetime. APB and glutamate, although clearly having a postsynaptic action, did not contribute any noise which could be resolved by the recording system, regardless of concentration. In retrospect, single-channel studies of glutamate-gated currents have demonstrated that the complexity of gating is well beyond the scope of noise analysis, perhaps even with the benefit of voltage-clamp, and certainly without it. An answer to detailed questions regarding the kinetics of the APB-preferring receptor/channel complex awaits the resolution afforded by single channel recordings.

CONCLUSIONS

This dissertation examines the postsynaptic action of the rod and cone transmitter on DBCs and horizontal cells of the goldfish retina using postsynaptic conductance-measuring and noise analysis techniques. The first two chapters measure conductance changes produced by APB and glutamate as well as the rod and cone transmitter, and show that two subtypes of EAA receptor are present on DBCs, an APB-sensitive receptor which mediates rod responses, and an APB-insensitive receptor which most likely mediates cone responses. The results demonstrate that rod and cone pathways in the retina can be separated pharmacologically, and provide an example of the segregation of multiple glutamate receptors onto different regions of a single cell. The third chapter demonstrates another difference in the pharmacology of the rod and cone pathways. Initially, APB was found to be a transmitter antagonist on cone driven horizontal cells, while having no effect on the rod pathway. Further experiments revealed APB-induced effects on a variety of cells in the cone-driven retina, including a possible effect on the cones themselves. Results from this chapter suggest that APB may act directly on cones.

The proposed sites of APB action on DBCs and cones in the outer plexiform layer of the goldfish retina are summarized in figure 32. Note that the APB acts "cleanly" in the rod-dominated retina, interfering only with synaptic transmission from rods to DBCs, while leaving the other pathways unaffected. In the light-adapted retina, the effects of APB are more extensive. Application of APB to a cone-

dominated retina can potentially affect every cone-driven cell in the retina, including bipolar cells. APB clearly blocks both rod and cone input onto mixed DBCs in the goldfish retina, but according to the model presented here, its site and mechanism of action is quite different in each case.

Chapter 4 describes experiments, using noise analysis, that were intended to reveal more about the gating mechanism of the glutamate receptors. However, the source of this noise continues to be elusive; the evidence suggests that it may not arise from transmitter-gated channels at all, but from voltage-dependent channels.

The observation that APB can block cone-driven OFF responses in the goldfish retina (chapt. 3) has important implications for the use of APB as a pharmacological tool in the study of higher order visual systems. Since APB was first shown to block the light response of DBCs in the mudpuppy (Slaughter and Miller, 1981) and dogfish retinas (Shiells et al., 1981), a number of studies have examined the effects of APB on higher order pathways of the visual system in mammals, including monkey (Schiller, 1982; 1984), cat (Horton and Sherk, 1984; Boltz et al., 1984) and rabbit (Knapp and Mistler, 1983; Sherk and Horton, 1984). The main finding in many of these studies is that intraoccullarly injected APB reversibly blocks both the center and surround responses of ON-center cells in the LGN, while having minimal effects on OFF-center cells. A wiring diagram of the synaptic inputs to ganglion cells has been proposed, based largely on the APB results. In this model,

ganglion cells are driven by only one type of bipolar cell (i.e., ON-center ganglion cell driven by DBC), and the center-surround channels are created from the receptive field of the bipolar cell driving it, rather than from the converging inputs of both classes of bipolar cell. However, detailed models of retinal wiring diagrams based upon the pharmacological actions of one compound seem premature, particularly if, as the present study indicates, the actions of this compound may be more widespread in the retina than previously thought.

The inhibitory action of APB may have implications in retinal function as well. Prolonged darkness has been reported to inhibit the responses of cone-driven horizontal cells in the retinae of several types of fish (Yang et al., 1986). Presentation of a steady background increases the amplitude of the CHC response from 4 mV to as much as 30 mV. One possible explanation for these results is an inhibition of the cone pathway by the rods in the dark-adapted retina, when the rod system is functioning. Inhibitory interactions between the rod and cone systems have been hypothesized previously on the basis of psychophysical (Mackous and Boothe, 1974), and electrophysiological (Shefner and Levine, 1977) experiments. The release of an APB-like transmitter from rods onto cones as well as DBCs would produce such as inhibition. Although tight junctions between rods and cones have been observed in the fish (Scholes, 1975), there is no evidence for an inhibitory chemical synapse between photoreceptor types. On the other hand, such a connection has never been looked for, and would probably require

reconstructions of serially-sectioned cones whose processes have been filled with an intracellular dye; a difficult and laborious task.

Active inhibition of cone transmitter release would be an elegant way of regulating membrane conductance on the DBC. In the dark-adapted retina, transmitter released from rods would close channels on the DBC membrane, and inhibit the release of channel-opening transmitter from cones, thus closing a second set of channels on the DBC. The resulting high membrane impedance would allow the DBC to produce the maximum voltage response to a small change in synaptic current, a useful mechanism for detecting dim stimuli. Under light-adapted conditions, transmitter release from rods would presumably be reduced, allowing not only the rod transmitter gated channels on the DBC to open, but the channels gated by the now-released cone transmitter as well. The decrease in input impedance would effectively decrease the gain of the cone-DBC synapse and increase the operating range of the DBC in brighter light.

REFERENCES

Altmann, H., Ten Bruggencate, G., Pickelmann, P. and Steinberg, R. (1976). Effects of glutamate, aspartate, and two presumed antagonists on feline rubrospinal neurones. Pflugers Archiv. 364, 249-255.

Anderson, C.R. and Stevens, C.F. (1973) Voltage clamp analysis of acetylcholine produced end-plate current fluctuations at frog neuromuscular junction. J. Physiol. 235, 665-692,

Ashmore, J.F. and Copenhagen, D.R. (1980) Different postsynaptic events in two types of retinal bipolar cell. Nature. 287, 84-86.

Ashmore, J.F. and Copenhagen, D.R. (1983). An analysis of transmission from cones to hyperpolarizing bipolar cells in the retina of the turtle. J. Physiol. 340, 569-597.

Ashmore, J.F. and Falk, G. (1980). Responses of rod bipolar cells in the dark adapted retina of the dogfish, Scyliorhinus canicula. J. Physiol. 300, 115-150.

Ashmore, J.F. and Falk, G. (1982). An analysis of voltage noise in rod bipolar cells of the dogfish retina. J. Physiol. 332, 273-297.

Atwell, D., Mobbs, P., Tessier-Lavigne, M. and Wilson, M. (1987) Neurotransmitter-induced currents in retinal bipolar cells of the Axolotl, *Ambystoma mexicanum*. J. Physiol. 387, 125-161.

Barrett, J.N., Magleby, K.L. and Pallotta, B.S. (1982) Properties of single calcium-activated potassium channels in cultured rat muscle. J. Physiol. 331, 211-230.

Baylor, D.A., Matthews, G. and Yau. K.-W. (1980) Two components of electrical dark noise in toad retinal rod outer segments. J. Physiol. 309, 591-621.

Belgum, J.H. and Copenhagen, D.R. (in press) Synaptic transfer of rod signals to horizontal and bipolar cells in the retina of the toad (*Bufo Marinus*). J. Physiol.

Belgum, J.H., Dvorak, D.R. and McReynolds, J.S. (1982). Sustained synaptic input to ganglion cells of mudpuppy retina. J. Physiol. 326, 91-108.

Bloomfield, S.A. and Dowling, J.E. (1985). Roles of aspartate and glutamate in synaptic transmission in rabbit retina. I. outer plexiform layer. J Neurophys 53, 699-713.

Bloomfield, S.A. and Miller, R.F. (1982) A physiological and morphological study of the horizontal cell types of the rabbit retina. J. Comp. Neurol. 208, 288-303.

Bolz J., Wässle, H. and Thier, P. (1984) Pharmacological modulation of ON and OFF ganglion cells in the cat retina. J. Neurosci. 3, 875-885.

Brown, T.H. and Johnston, D. (1983). Voltage-Clamp Analysis of Mossy Fiber Synaptic Input to Hippocampal Neurons. J Neurophys. 50, 487-507.

Cervetto, L and Piccolino, M. (1974) Synaptic transmission between photoreceptors and horizontal cells in the turtle retina. Science 183, 417-419.

Cervetto, L. and MacNichol, E.F. (1972). Inactivation of horizontal cells in turtle retina by glutamate and aspartate. Science 178, 767-768.

Collingridge, G.L., Kehl, S.J. and McLennan, H. (1983) The antagonism of amino acid-induced excitations of rat hippocampal CA1 neurones *in vitro*. J. Physiol. 314, 19-31.

Crunelli, V., Forda., S., Collingridge, G.S., and Kelly, J.S. (1984) The reversal potential of excitatory amino acid action on granule cells of the rat dentate gyrus. J. Physiol. 351, 327-342.

Cull-Candy, S.G. and Usowicz, M.M. (1987) Multiple-conductance channels activated by excitatory amino acids in cerebellar neurons. Nature 325, 525-528

Cull-Candy, S.G., Donnellan, J.F., James, R.W. and Lunt G.G. (1976) 2-amino-4-phosphonobutyric acid as a glutamate antagonist on locust muscle. Nature 262, 408-409.

Curtis, D.R., Phillis, J.W. and Watkins, J.C. (1960) The excitation of spinal neurons by certain acidic amino acids. J. Physiol. 150, 656-682.

Dacheux, R.F. and Raviola, E. (1982) Horizontal cells in the retina of the rabbit. J. Neurosci. 2, 1486-1493.

Dale, N. and Grillner, S. (1986) Dual-component synaptic potentials in the Lamprey mediated by excitatory amino acid receptors. J. Neurosci. 6, 2653-2661.

Dale, N. and Roberts, A. (1985) Dual-component amino-acid-mediated synaptic potentials: Excitatory drive for swimming in Xenopus embryos. J. Physiol. 363, 35-59.

Davies, J. and Watkins, J.C. (1982). Actions of D and L forms of 2-amino-5-phosphonovalerate and 2-amino-4-phosphonobutyrate in the cat spinal cord. Brain Res. 235, 378-386.

Dawis, S.M. (1981). Polynomial expressions of pigment nomograms. Vis. Res. 21, 1422-1430.

Dowling, J.E. and Ripps, H. (1973) Effect of Magnesium on horizontal cell activity in the skate retina. Nature. 242, 101-103.

Dunwiddie, T., Madison, D. and Lynch, G. (1978). Synaptic transmission is required for initiation of long-term potentiation. Brain Res. 150, 413-417.

Dvorak, D. (1984) Off-pathway synaptic transmission in the outer retina of the axolotl is mediated by a kainic acid-preferring receptor. Neurosci. Letts. 50, 7-11.

Engberg, I., Flatman, J.A. and Lambert, J.D.C. (1979) The actions of excitatory amino acids on motoneurones in the feline spinal cord. J. Physiol. 288, 227-261.

Evans, R.H., Francis, A.A., Jones, A.W., Smith, D.A.S. and Watkins, J.C. (1982). The effects of a series of w-phosphonic -carboxylic amino acids on electrically evoked and excitant amino acid-induced responses in isolated spinal cord preparations. Br. J. Pharmac. 75, 65-75.

Ffrench-Mullen, J.M.H., Hori, N. and Carpenter, D.O. (1986) Receptors for excitatory amino acids on neurons of the rat pyriform cortex. J. Neurophys. 55, 1283-1294.

Foster, A.C. and Fagg, G.E. (1984) Acidic amino acid binding sites in mammalian neuronal membranes: Their characteristics and relationship to synaptic receptors. Brain Res. Rev. 7, 103-164.

Hablitz, J.J. and Langmoen, I.A.(1982). Excitation of hippocampal pyramidal cells by glutamate in the guinea pig and rat. J. Physiol. 325, 317-331.

Hals, G., Christensen, B.N., O'Dell, T., Christensen, M. and Shingai, R. (1986) Voltage-clamp analysis of currents produced by glutamate and some glutamate analogues on horizontal cells isolated from the catfish retina. J. Neurophys. 56, 19-31.

Hankins, M.W. and Ruddock, K.H. (1984). Hyperpolarization of fish retinal horizontal cells by kainate and quisqualate. Nature 308, 360-363.

Harris, E.W. and Cotman, C.W. (1983). Effects of acidic amino acid antagonists on paired-pulse potentiation at the lateral perforant path. Ex. Brain Res. 52, 455-460.

Hayashi, T. (1954) Effects of Sodium glutamate on the nervous system Keio J. Med. 3, 183-192.

Hori, N., Auker, C.R., Braitman, D.J. and Carpenter, D.O. (1982). Pharmacologic sensitivity of amino acid responses and synaptic activation of in vitro prepyriform neurons. J. Neurophys. 48, 1289-1301.

Horton, J. C. and Sherk, H. (1984) Receptive field properties in the cat's lateral geniculate nucleus in the absence of on-center retinal input. J. Neurosci. 4, 374-380.

Ishida, A.T. (1984) Responses of solitary retinal horizontal cells to L-glutamate and kainic acid are antagonized by D-aspartate. Brain Res. 298, 25-32.

Ishida, A.T. and Fain, G.L.(1981) D-Aspartate potentiates the effects of L-glutamate on horizontal cells in goldfish retina. Proc. Natl. Acad. Sci., USA, 78, 5890-5894.

Ishida, A.T. and Neyton, J. (1985) Quisqualate and L-glutamate inhibit retinal horizontal-cell responses to kainate. Proc. Natl. Acad. Sci. USA. 82, 1837-1841.

Ishida, A.T., Stell, W.K. and Lightfoot, D.O. (1980). Rod and Cone Inputs to Bipolar Cells in the Goldfish Retina. J. Comp. Neurol. 191, 315- 335.

Jahr, C.E. and Jessell T.M. (1985) Synaptic transmission between dorsal root ganglion and dorsal horn neurons in culture: antagonism of monosynaptic excitatory synaptic potentials and glutamate excitation by kynurenate. J. Neurosci. 5, 2281-2289.

Jahr, C.E. and Stevens, C.F. (1987) Glutamate activates multiple single channel conductances in hippocampal neurons. Nature 325, 522-525.

Kaneko, A and Tachibana, M. (1985). A voltage-clamp analysis of membrane currents in solitary bipolar cells dissociated from *Carassius auratus*. J. Physiol. 358, 131-152.

Kaneko, A. (1970). Physiological and morphological identification of horizontal, bipolar and amacrine cells in goldfish retina. J. Physiol. 207, 623-633.

Kaneko, A. and Shimazaki, H. (1976) Synaptic transmission from photoreceptors to bipolar and horizontal cells in the carp retina. Cold Spring Harb. Symp. Quant. Biol. 40, 537-546.

Kaneko, A. and Tachibana, M. (1978). Convergence of Rod and Cone Signals to Single Bipolar Cells in the Carp Retina. Sensory Proc. 2, 383-387.

Kaneko, A. and Yamada, M. (1972). S-potentials in the dark-adapted retina of the carp. J. Physiol. 227, 261-273.

Katz, B. and Miledi, R. (1972) The statistical nature of the acetylcholine potential and its molecular components. J. Physiol. 224, 665-699.

Knapp, A.G. and Mistler, L.A. (1983) Response properties of cells in rabbit's lateral geniculate nucleus during reversible blockade of retinal On-center channel. J. Neurophys. 5, 1236-1245.

Koerner, J.F. and Cotman, C.W. (1981). Micromolar L-2-amino-4-phosphonobutyric acid selectively inhibits perforant path synapses from lateral entorhinal cortex. Brain Res. 216, 192-198.

Lasater, E.M and Dowling, J.E. (1982) Carp horizontal cells in culture respond selectively to L-glutamate and its agonists. Proc. Natl. Acad. Sci. USA 79, 936-940.

Leeper, H.F. and Copenhagen, D.R. (1979). Mixed rod-cone responses in horizontal cells of snapping turtle retina. Vis. Res. 19, 407-412.

Liebman, P.A. and Entine, G. (1964) Sensitive low-light level microspectrophotometer: Detection of photosensitive pigments of retinal cones. J. Opt. Soc. Am., 54, 1451-1459.

MacDermott, A.B., Mayer, M.L., Westbrook, G.L., Smith, S.J. and Barker, J.L. (1986) NMDA-receptor activation increases cytoplasmic calcium concentration in cultured spinal cord neurones. Nature 321, 519-522.

Makous, W. and Boothe, R. (1974) Vision Res. 14, 285.

Malchow, R.P. and Yazulla, S. (1986) Separation and light adaptation of rod and cone signals in the retina of the goldfish. Vision Res. 26, 1655-1666.

Marc, R. and Lam, D.M.K. (1981) Uptake of aspartic and glutamic acid by photoreceptors in goldfish retina. Proc. Natl. Acad. Sci. USA. 78, 7185-7189.

Marks, W.B.(1965) Visual pigments of single goldfish cones. J. Physiol. 178, 14-32.

Marshall, L.M. and Werblin, F.S (1978) Synaptic transmission to the horizontal cells in the retina of the larval tiger salamander. J. Physiol. 279, 321-346.

Massey, S.C. and Miller, R.F. (1987) Excitatory amino acid receptors of rod- and cone-driven horizontal cells in the rabbit retina. J. Neurophys. 57, 645-659.

Massey, S.C. and Redburn, D.A. (1987) Transmitter circuits in the vertebrate retina. Prog. in Neurobiol. 28, 55-96.

Mayer, M.L. and Westbrook, G.L. (1984). Mixed-Agonist Action of Excitatory Amino Acids on Mouse Spinal Cord Neurones Under Voltage Clamp. J. Physiol. 354, 29-53.

Mayer, M.L. and Westbrook, G.L. (1985). The Action of N-Methyl-D-Aspartic Acid on Mouse Spinal Neurones in Culture. J. Physiol. 361, 65-90.

Mayer, M.L. and Westbrook, G.L. (1987). The physiology of excitatory amino acids in the vertebrate contral nervous system. Prog. Neuro. 28, 197-276.

Mayer, M.L., Westbrook, G.L. and Guthrie, P.B. (1984). Voltage-dependent block by Mg^{2+} of NMDA responses in spinal cord neurons. Nature 309, 261-263.

Merigan, W.H. (1984) APB effects on the primate ERG. Invest. Ophthalmol. (suppl.) 25, 259

Miller, A.M. and Schwartz, E.A. (1983) Evidence for the identification of synaptic transmitters released by photoreceptors of the toad retina. J. Physiol. 334, 325-349.

Miller, R.F. and Slaughter, M.M. (1985). Excitatory amino acid receptors in the vertebrate retina. In: *Retina Transmitters and Modulators: Models for the Brain*, Vol II., 123-160. Ed W.W. Morgan. CRC Press. Boca Raton.

Mosinger, J.L. and Altshuler, R.A. (1985) Aspartate aminotransfrease-like immunoreactivity in the guinea pig and monkey retina J. Comp. Neurol. 233, 255-268.

Munz, F.W. and Schwanzara, S.A. (1967). A nomogram for $Retinene_2$-based visual pigments. Vis. Res. 7, 111-120.

Murakami M. and Takahashi, K-I (1987) Calcium action potential and its use for measurement of reversal potentials of horizontal cell responses in carp retina. J. Physiol. 386, 165-180.

Nawy, S. and Copenhagen, D.R. (1987). Multiple Classes of Glutamate Receptor on Depolarizing Bipolar Cells in Retina. Nature 325, 56-58..

Nelson, P.G., Pun, R.Y.K. and Westbrook, G.L. (1986). Synaptic Excitation in Cultures of Mouse Spinal Cord Neurones: Receptor Pharmacology and Behaviour of Synaptic Currents. J. Physiol. 372, 169-190.

Nelson, R.H. (1973) A comparison of electrical properties of neurons in Necturus retina. J. Neurophys. 36, 519-535.

Normann, R.A. and Lasater, E. (1987) Propagation of signals from cell body to pedicle in turtle cones. Invest. Ophthal. and Vis. Sci. suppl. 402.

Nowak, L., Bregestovski, P., Ascher, P., Herbet, A. and Prochiantz, A. (1984). Magnesium Gates Glutamate-activated Channels in Mouse Central Neurones. Nature 307, 462-465.

O'Brien, R.J. and Fishbach, G.D. (1986a) Characterization of Excitatory Amino Acid Receptors Expressed by Embryonic Chick Motoneurons In Vitro. J. Neurosci. 6, 3275-3283.

O'Brien, R.J. and Fishbach, G.D. (1986b) Excitatory synaptic transmission between interneurons and motoneurons in chick spinal cord cell cultures. J. Neurosci. 6, 3284-3289.

Puil, E. and Werman, R. (1979). Intracellular cesium blocks various K^+ conductances in cat motoneurons. Can. Physiol. 10, 185-204.

Rowe, J.S. and Ruddock, K.H. (1982a). Hyperpolarization of retinal horizontal cells by excitatory amino acid neurotransmitter antagonists. Neurosci. Lett. 30, 251-256.

Rowe, J.S. and Ruddock, K.H. (1982b) Depolarization of retinal horizontal cells by excitatory amino acid neurotransmitter agonists. Neurosci. Lett. 30, 257-262.

Saito, T. and Kaneko, A. (1983) Ionic mechanisms underlying the responses of off-bipolar cells in the carp retina: I. Studies on responses evoked by light. J. Gen. Physol. 81, 589-601.

Saito, T., Kondo, H. and Toyoda, J. (1978). Rod and Cone Signals in the On-Center Bipolar Cell: Their Different Ionic Mechanisms. Vision Res. 18, 591-595.

Saito, T., Kondo, H. and Toyoda, J. (1979). Ionic Mechanisms of Two Types of On-Center Bipolar Cells in the Carp Retina I. The responses to Central Illumination. J. Gen. Physiol. 73, 73-90.

Saito, T., Kujiraoka, T. and Toyoda, J.-I. (1984) Electrical and morphological properties of off-center bipolar cells in the carp retina J. Comp. Neurol. 222, 200-208.

Schiller, P.H. (1984) The connections of the ON and OFF pathways to the lateral geniculate nucleus of the monkey. Vis. Res. 24, 923-932.

Schiller, P.H., Sandell, J.H. and Maunsell, J.H.R. (1986) Functions of the ON and OFF channels of the visual system. Nature, 322, 824-825.

Scholes, J.H. (1975) Philos. Trans. R. Soc. London Sec. B 270, 61-

Schnapf, J.L. and Copenhagen, D.R. (1982). Differences in the kinetics of rod and cone synaptic transmission. Nature, 296, 862-864.

Shefner, J.M. and Levine, M.W. (1977) Interactions between rod and cone systems in the goldfish retina. Science 198, 750-753.

Shiells, R.A., Falk, G. and Naghshineh, S. (1981). Action of glutamate and aspartate analogues on rod horizontal and bipolar cells. Nature 294, 592-594.

Shiells, R.A., Falk, G. and Naghshineh, S. (1986). Iontophoretic study of the action of excitatory amino acids on rod horizontal cells of the dogfish retina. Proc. R. Soc. Lond. B. 227, 121-135.

Slaughter, M.M. and Miller, R.F. (1981). 2-Amino-4-phosphonobutyric acid: a new pharmacological tool for retina research. Science 211, 182-185.

Slaughter, M.M. and Miller, R.F. (1983). The role of excitatory amino acid neurotransmitters in the retina: an analysis with kainic acid and N-methyl aspartate. J. Neursci. 3, 1701-1711.

Slaughter, M.M. and Miller, R.F. (1985). Characterization of an extended glutamate receptor of the ON bipolar neuron in the vertebrate retina. J. Neurosci. 5, 224-233.

Stell, W.K. (1967) The structure and relationships of horizontal cells and photoreceptor-bipolar synaptic complexes in goldfish retina. Am. J. Anat. 121, 401-424.

Tachibana, M. (1985) Permeability changes induced by L-glutamate in solitary retinal horizontal cells isolated from *Carassius Auratus*. J. Physiol. 358, 153-167.

Thibos, L.N. and Werblin, F.S. (1977). The response properties of the steady antagonistic surround in the mudpuppy retina. J. Physiol. 278, 79-99.

Tomita, T., Kaneko, A., Murakami and Pautler, E.L. (1967). Spectral response curves of the single cones in the carp. Vis. Res. 7, 519-531.

Toyoda, J. (1973). Membrane Resistance Changes Underlying the Bipolar Cell Response in the Carp Retina. Vision Res. 13, 283-294.

Watkins, J.C. and Evans, R.H. (1981) Excitatory amino acid transmitters. Ann Rev Pharmacol. Toxicol. 21, 165-204.

Witkowsy, P. Dowling, J.E. (1969) Synaptic relationships in the plexiform layers of carp retina. Z. Zellforsch. 100, 60-82.

Yamada, E. and Ishikawa, T. (1965) Fine structure of the horizontal cells in some vertebrate retinae. Cold Spr. Harb. Symp. Quant. Biol. 30, 383-392.

Yang, X.-L. and Dowling J.D. (1987) Modulation of cone inputs to horizontal cells in the tiger salamander retina. Soc Neurosci. Abst. 13, 25.

Zieglgansberger, W. and Puil, E.A. (1973) Action of glutamic acid on spinal neurones. Expl. Brain Res. 17, 35-49.